



LITHOGRAPHIC MICRO- AND NANOSTRUCTURING OF SU-8 FOR BIOTECHNOLOGICAL APPLICATIONS

Pinkie Jacob Eravuchira

Dipòsit Legal: T 773-2015

ADVERTIMENT. L'accés als continguts d'aquesta tesi doctoral i la seva utilització ha de respectar els drets de la persona autora. Pot ser utilitzada per a consulta o estudi personal, així com en activitats o materials d'investigació i docència en els termes establerts a l'art. 32 del Text Refós de la Llei de Propietat Intel·lectual (RDL 1/1996). Per altres utilitzacions es requereix l'autorització prèvia i expressa de la persona autora. En qualsevol cas, en la utilització dels seus continguts caldrà indicar de forma clara el nom i cognoms de la persona autora i el títol de la tesi doctoral. No s'autoritza la seva reproducció o altres formes d'explotació efectuades amb finalitats de lucre ni la seva comunicació pública des d'un lloc aliè al servei TDX. Tampoc s'autoritza la presentació del seu contingut en una finestra o marc aliè a TDX (framing). Aquesta reserva de drets afecta tant als continguts de la tesi com als seus resums i índexs.

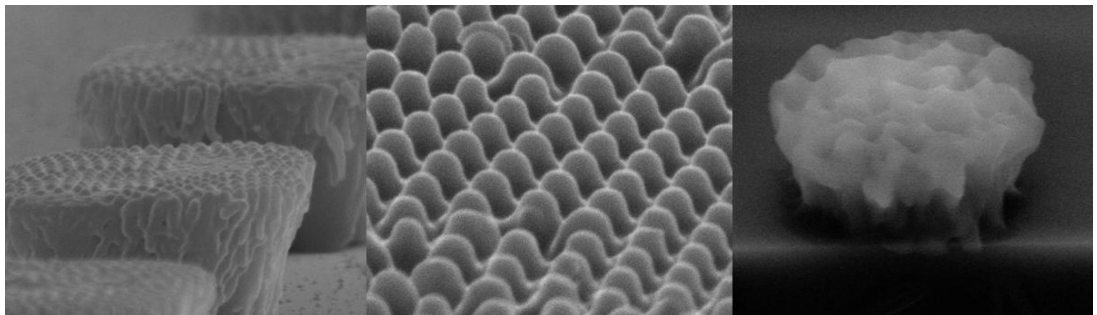
ADVERTENCIA. El acceso a los contenidos de esta tesis doctoral y su utilización debe respetar los derechos de la persona autora. Puede ser utilizada para consulta o estudio personal, así como en actividades o materiales de investigación y docencia en los términos establecidos en el art. 32 del Texto Refundido de la Ley de Propiedad Intelectual (RDL 1/1996). Para otros usos se requiere la autorización previa y expresa de la persona autora. En cualquier caso, en la utilización de sus contenidos se deberá indicar de forma clara el nombre y apellidos de la persona autora y el título de la tesis doctoral. No se autoriza su reproducción u otras formas de explotación efectuadas con fines lucrativos ni su comunicación pública desde un sitio ajeno al servicio TDR. Tampoco se autoriza la presentación de su contenido en una ventana o marco ajeno a TDR (framing). Esta reserva de derechos afecta tanto al contenido de la tesis como a sus resúmenes e índices.

WARNING. Access to the contents of this doctoral thesis and its use must respect the rights of the author. It can be used for reference or private study, as well as research and learning activities or materials in the terms established by the 32nd article of the Spanish Consolidated Copyright Act (RDL 1/1996). Express and previous authorization of the author is required for any other uses. In any case, when using its content, full name of the author and title of the thesis must be clearly indicated. Reproduction or other forms of for profit use or public communication from outside TDX service is not allowed. Presentation of its content in a window or frame external to TDX (framing) is not authorized either. These rights affect both the content of the thesis and its abstracts and indexes.



Department of Electronic, Electric and Automatic Control Engineering

Lithographic Micro- and Nanostructuring of SU-8 for Biotechnological Applications



Doctoral Thesis

Pinkie Jacob Eravuchira

Tarragona, 2015

UNIVERSITAT ROVIRA I VIRGILI

LITHOGRAPHIC MICRO- AND NANOSTRUCTURING OF SU-8 FOR BIOTECHNOLOGICAL APPLICATIONS

Pinkie Jacob Eravuchira

Dipòsit Legal: T 773-2015

Pinkie Jacob Eravuchira

Lithographic Micro- and Nanostructuring of SU-8 for Biotechnological Applications

DOCTORAL THESIS

Supervised by:

Prof. Josep Ferré-Borrull, Prof. Eduard Llobet Valero, and

Prof. Francesc Díaz

Department of Electronic, Electric and Automatic Control Engineering



UNIVERSITAT ROVIRA I VIRGILI

Tarragona

2015

UNIVERSITAT ROVIRA I VIRGILI

LITHOGRAPHIC MICRO- AND NANOSTRUCTURING OF SU-8 FOR BIOTECHNOLOGICAL APPLICATIONS

Pinkie Jacob Eravuchira

Dipòsit Legal: T 773-2015



UNIVERSITAT ROVIRA I VIRGILI
Departament d'Enginyeria Electrònica, Elèctrica I Automàtica
Escola Tècnica Superior d'Enginyeria
Campus Sescelades
Avda. Països Catalans 26
43007 Tarragona, Spain
Tel. +34 977 55 65 71

WE STATE that the present study, entitled “Lithographic Micro- and Nanostructuring of SU-8 for Biotechnological Applications”, presented by Pinkie Jacob Eravuchira for the award of the degree of Doctor, has been carried out under our supervision at the Department of Electrical, Electronic and Automatic Control Engineering of the University Rovira i Virgili, and that it fulfills all the requirements to be eligible for the Doctorate Award.

Tarragona, 3rd of February 2015

Doctoral Thesis Supervisors

A handwritten signature in blue ink, appearing to be 'J. Ferré-Borrull'.

Prof. Josep Ferré-Borrull

A handwritten signature in blue ink, appearing to be 'E. Llobet Valero'.

Prof. Eduard Llobet Valero

A handwritten signature in blue ink, appearing to be 'F. Díaz'.

Prof. Francesc Díaz

UNIVERSITAT ROVIRA I VIRGILI

LITHOGRAPHIC MICRO- AND NANOSTRUCTURING OF SU-8 FOR BIOTECHNOLOGICAL APPLICATIONS

Pinkie Jacob Eravuchira

Dipòsit Legal: T 773-2015

Acknowledgments

First of all I would like to express my deepest gratitude and appreciation to my supervisor, Prof. Josep Ferré-Borrull for his support, guidance, encouragement and advices all throughout the last four years of my Ph. D. I would also like to thank Prof. Eduard Llobet Valero and Prof. Francesc Díaz for their valuable suggestions and advice.

Financial support from Agaur-Generalitat de Catalunya is greatly acknowledged.

My heartfelt gratitude to Dr. Malgorzata Baranowska for all the support, help, and advices during my Ph.D. Special thanks to Agata Slota and Maria Alba for helping me with the laboratory works.

My sincere thanks to Mercé, Mariana, Lukas, Rita and Núria in Servi de Recursos Científics i Tècnics of the Universitat Rovira i Virgili, for their guidance and support. A special gratitude to Lukas for training and helping me with the clean techniques.

I would also like to express my gratitude to the members of Nephos and Minos groups: especially to Enrique for all his supports, advices and helps specially with the final preparation of this dissertation, and to Rosa, Sergio, Badia, Oriol, Elena, Pillar, Elizabeth, Pelin, Raul, and Pierrick, for their support, kindness, and collaboration.

Special thanks to Fatima for her friendship, and support during the last four years. I am grateful to Ximena, Padmja, Laxmi, Nuria, Rahama, and Sandra for giving me many memorable days in Tarragona.

I would like to express my deepest love to my parents, Achan and Amma, and my sister, Steffie for their unconditional love, encouragement, and support all through my life, and to Joseph for his love, and support, and for being there for me always.

UNIVERSITAT ROVIRA I VIRGILI

LITHOGRAPHIC MICRO- AND NANOSTRUCTURING OF SU-8 FOR BIOTECHNOLOGICAL APPLICATIONS

Pinkie Jacob Eravuchira

Dipòsit Legal: T 773-2015

Table of Contents

Introduction.....	1
1.1. Objectives	2
1.2. Document structure.....	3
State of the Art	5
2.1. SU-8: Composition and physical properties	6
2.2. Structuring of SU-8 using lithographic techniques.....	9
2.2.1. Photolithographic structuring of SU-8.....	10
2.2.2. Soft lithographic structuring of SU-8.....	21
2.3. Applications of SU-8 in biology and biotechnology.....	25
Micro- and Nanostructuring of SU-8 Surfaces Using Lithographic Techniques	33
3.1. Lithographic techniques for structuring surfaces.....	34
3.1.1. Photolithography.....	34
3.1.2. Laser lithography	44
3.1.3. Soft lithography	47
3.2. Experimental procedures to obtain photomasks and patterning SU-8 surfaces ...	50
3.2.1. Laser lithography for the patterning of photomask.....	51

X | Contents

3.2.2. Photolithography for the fabrication of SU-8 microstructures	57
3.2.3. Hierarchical structuring of SU-8 with soft lithography and hybrid lithography.....	68
Application of Micro- and Nanostructured SU-8 for Immunosensing	87
4.1. Surface modification of SU-8 surfaces.....	89
4.1.1. Functionalization of SU-8 surfaces with APTMS and GTA	91
4.1.2. Fourier transform infrared spectroscopy - Attenuated Total Reflectance	93
4.1.3. Immobilization of aIgG and IgG on surface-modified SU-8.....	95
4.1.4. Labelling of IgG with Rhodamine.....	97
4.2. Immunosensing by reduction of luminescence in SU-8 planar and macropillar surfaces.....	99
4.2.1. Photoluminescence reduction on planar and macropillar SU-8 surfaces after each surface treatment	100
4.2.2. Comparison of photoluminescence of SU-8 planar and macropillar surfaces	103
4.2.3. Sensing response with IgG concentration on SU-8 macropillar surfaces...	105
4.3. Immunosensing by reduction of photoluminescence in SU-8 hierarchical structures.	107

Laser Lithographic Patterning of Silicon Wafers	113
5.1. Fabrication of platinum interdigital electrodes and their application for gas sensing.	114
5.1.1. Fabrication of platinum interdigital electrodes	116
5.1.2. Deposition of WO ₃ nanoneedles	121
5.2. Fabrication of silicon inverted micropylamid arrays and their applications in biotechnology.....	123
5.2.1. Fabrication of silicon inverted micropylamid arrays	124
5.2.2. Inverted micropylamids as a template for the formation of macroscale plasmonic substrates for surface enhanced raman scattering.....	127
5.2.3. Fabrication of SiO ₂ hollow micropillar arrays and their application for dual-side functionalization.	130
Conclusions.....	135
References.....	139

UNIVERSITAT ROVIRA I VIRGILI

LITHOGRAPHIC MICRO- AND NANOSTRUCTURING OF SU-8 FOR BIOTECHNOLOGICAL APPLICATIONS

Pinkie Jacob Eravuchira

Dipòsit Legal: T 773-2015

Chapter 1

Introduction

Materials with improved characteristics such as non-toxicity, biocompatibility, stability under varying environmental conditions and the possibility of being patterned with simplicity and low-cost are of great value in the fields of biology and biotechnology. Wide range of both organic and inorganic materials such as silicon, porous silica, porous alumina, and various nanoparticles have proved to be biocompatible and they have been widely used for various biological and biotechnological applications. Similarly, lately, polymers have been gaining much interest as a valuable structural material in biotechnology due to their biocompatibility and ease of structuring with sizes down to few nanometers. Among various polymers, SU-8 is an epoxy based negative photoresist which has found a broad range of biomedical and biotechnological applications due to their biocompatibility and high thermal, mechanical, and chemical resistance [Voskerician 2003, Liu 2007]. Since its invention in the nineties, SU-8 has been extensively used in micro- and nanotechnologies and in microelectromechanical systems for fabricating scaled-down components and devices such as micro- and nanochannels, membranes, microfluidic devices, cantilevers, biosensors and more.

The fabrication of devices and components becomes challenging when the features are miniaturized. Ease of structuring into any desired shapes and dimensions using conventional lithographic techniques such as photolithography, laser lithography, or soft lithography is one of the advantages of using SU-8 for micro- and nanofabrication. Briefly, lithography is referred as a method for patterning planar or rough surfaces with geometrical shapes and patterns either by selective exposure of radiations (ex: UV light, X-ray, or e-beam) or using molds and stamps (ex: PDMS stamps, Si molds). SU-8 structures with dimensions down to few nanometers and high aspect ratio structures can be fabricated using these low-cost lithographic techniques.

1.1. Objectives

The main objectives of this Ph. D. dissertation are to develop new techniques to pattern SU-8 surfaces and to explore their possible biotechnological applications. Thus, different lithographic techniques such as photolithography, soft lithography, and hybrid lithography will be applied and combined to reach such objective.

Using photolithographic and soft lithographic techniques we aimed to produce three-dimensional SU-8 pillar and porous surfaces at the micro- and nano-scale. Furthermore, using hybrid lithographic technique, a newly developed lithographic technique where photolithographic and soft lithographic methods were combined, we intended to produce SU-8 macropillar surfaces decorated with micrometric and nanometric pores and pillars. All the produced SU-8 surfaces were then tested for immunosensing.

One of the factors that limit the use of SU-8 for biotechnological applications, mainly for fluorescence based biosensing, is the photoluminescence SU-8 has in the near UV and visible wavelength ranges. However, in this study we aimed to exploit the photoluminescence property of SU-8 to fabricate a cost-effective and reliable tool for immunosensing, where the reduction of photoluminescence of SU-8 with its surface modification functions as the sensing transduction parameter. The application of SU-8 for immunosensing is demonstrated by immobilizing a model antigen-antibody (aIgG-IgG) pair on to SU-8 surfaces.

1.2. Document structure

This Ph.D. dissertation is organized as follows:

Chapter 2 introduces the fundamentals of SU-8, and reviews the state-of-the-art on the photolithographic and soft lithographic structuring of SU-8. Finally, a survey on some of the biotechnological applications of SU-8 is presented.

Chapter 3 initially addresses the concepts on lithographic techniques, and instrumentations that were employed in our experimental work. Following this, a detailed description on the methods and parameters of photolithography, soft lithography and hybrid lithography, which were used for the SU-8 structuring, and obtained SU-8 structured are presented in this chapter.

Chapter 4 describes the experimental procedures followed to demonstrate the applicability of the structured SU-8 surfaces as an immunosensor on the basis of its

4 | Chapter 1

photoluminescence. The methodology followed to demonstrate such applicability, the results of the experiments and the discussion on the results are presented here.

Chapter 5 is devoted to introduce other works related to lithographic patterning that has been carried out in the framework of this Ph. D. The laser lithographic structuring of silicon wafer to produce interdigital electrodes for gas sensing application, and inverted micropylramid arrays for biotechnological applications, are presented in this chapter. The works discussed in this chapter were done in collaboration with two of the research groups (Minos and Nephos) among EMaS.

Finally, chapter 6 presents the major conclusions obtained from this Ph.D. work.

Chapter 2

State of the Art

Lithography is a process of patterning geometrical shapes of desired dimensions and patterns on substrate surfaces such as silicon, crystals, glass, and more. It is one of the conventional modes of creating structures and patterns in micro- and nanofabrication technology. Photolithography, electron beam lithography, direct laser lithography, X-ray lithography, and interference lithography are some examples of the lithographic techniques for patterning substrate surfaces. Referring to the optical lithography, the custom shapes are initially transferred to a thin film of light-sensitive material called photoresist, which is covered over the substrate surface. During optical lithography, a selective irradiation of the photoresist with a light beam activates the photochemical reactions in the irradiated region of the resist. This photochemical reaction in turn changes chemical and physical properties of the irradiated region of the photoresist. A series of chemical treatments and etching following this irradiation helps to transfer the patterns on to the material underneath the photoresist.

Briefly, a photoresist is light-sensitive material which is mainly composed of three main components such as, resin, photosensitizer, and the solvent. The resin is a synthetic polymer that provides the mechanical characteristics such as adhesion and strength, thermal stability and chemical resistance to the photoresist. When exposed to light, depending on the type of resin, they get either polymerized or photo-solubilized. This polymer reaction in a photoresist is controlled by the component called the photosensitizer. This sensitizer is the photoactive compound in the resist, and it alters its chemical properties upon light absorption. And finally the chemical solution called solvent helps to have a liquid texture for the photoresist, which is required for a photoresist so that it can be spun coated on to the substrates.

Although since its discovery, the term photoresist has been referred as a material that helps to transfer pattern on to the substrates during lithography, studies show the possibility to use certain resists as a valuable structural material in micro- and nanotechnology. SU-8, an epoxy based negative photoresist is a typical example of one of such photoresists which has been widely used as a structural material in semiconductor industry and microelectromechanical system [Conradie 2002, Padgen 2009, Ribeiro 2005].

2.1. SU-8: Composition and physical properties

SU-8 (glycidyl ether of bisphenol A) is an acid-catalyzed, near-UV photoresist based on EPON SU-8 epoxy resin which was developed and patented by IBM in 1989 (US Patent 4882245). The first commercial SU-8 products were introduced in 1996 by MicroChem

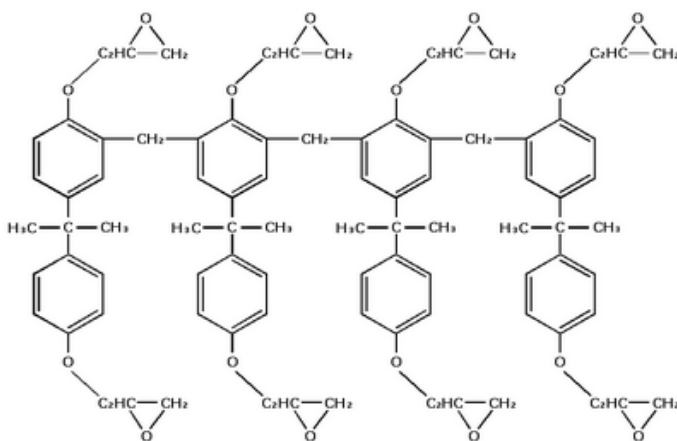


Figure 2.1: Molecular structure of SU-8 [Genolet 2001].

(Westborough, MA). SU-8 is produced by dissolving the EPON SU-8 resin in an organic solvent (cyclopentanone or gamma-butyrolactone), and triarylsulfonium-hexafluoroantimonate is the photosensitizer used in SU-8 resist. SU-8 dissolved in cyclopentanone and gamma-butyrolactone solvents are classified as SU-8 2000 and SU-8 3000 series respectively. SU-8 has eight epoxy groups per monomer and the number eight in SU-8 refers to the eight epoxy sites present in each monomer. The molecular structure of SU-8 is shown in figure 2.1.

Referring to the physical texture of SU-8, it is a highly viscous liquid and the viscosity is determined by the ratio of solvent to EPON resin mixed. The viscosity influences the thickness of the resist film when spun coated on a substrate. A broad range of thickness ranging from 200 nm to 350 μ m can be achieved by single spin coating of SU-8 [Liu 2004]. Upon the radiation exposure (UV, e-beam or X-ray), SU-8 gets cross-linked and

becomes insoluble to the developer solution. The physical properties of SU-8 are listed here [Ghodssi 2010, Campo 2007, The 2005]. The cross-linked SU-8 structures exhibit exemplary thermal resistance, mechanical and chemical properties and they are resistant to most of the acids and bases such as NaOH, nitric acid, or acetone. The mechanical properties such as the tensile strength and the thermal conductivity of the cross-linked SU-8 ranges from 70 to 60 Mpa, and 0.2 to 0.3 W/mK for SU-8 3000 and SU-8 2000 series respectively. SU-8 has a poisson coefficient of 0.22 and a friction coefficient of 0.19. This epoxy resist has a high degradation temperature ($\sim 380^{\circ}\text{C}$) and a coefficient of thermal expansion of 52 ppm/ $^{\circ}\text{C}$. The cross-linked resist is highly stable at elevated temperatures and resistance to moisture and most of the solvents, and therefore the resist does not get dissolved and degrades in solvent exposing environments. The unexposed resin has a glass transition temperature of $\sim 50^{\circ}\text{C}$ and after the cross-linking the transition temperature increases to $>200^{\circ}\text{C}$. SU-8 has a refractive index of 1.67 ($\lambda=365\text{nm}$) and 1.650 ($\lambda=405\text{nm}$). The density of the raw SU-8 is 997.8 kg/m^3 and it gets elevated to 1200 kg/m^3 with the cross-linking. The electrical properties such as the dielectric constant and the dielectric strength of the cross-linked SU-8 varies from 3.2 to 4.1 (1GHz) and 112-115 (V/ μm) respectively. It has a volume resistivity of $1.8\text{-}2.8 \times 10^{16}\ \Omega\text{cm}$ and a surface resistivity of $1.8\text{-}5.1 \times 10^{16}\ \Omega\text{cm}$. SU-8 possesses a young's modulus of 4 GPa, and it has excellent adhesion ability on various substrates like Si, SiN, glass, Al_2O_3 , Cu, Au, and GaAs.

2.2. Structuring of SU-8 using lithographic techniques

After the invention of SU-8, for a while its applications were limited only to the fabrication of printed circuit boards. However, due to its exemplary chemical, mechanical and physical properties it soon became a promising structural material in microelectromechanical system (MEMS) [Zhang 2001, Tuomikoski 2005, Lopez 2006, Esquivé 2010, Duarte 2011], and biological microelectromechanical system (BioMEMS) [Lee 1995, Vernekar 2008, Patel 2008]. The first SU-8 microchannel model was produced in 1997 by Guerin and coworkers at the Institute of microsystem, Lausanne, Switzerland [Guerin 1997]. Afterwards SU-8 was extensively used in microfluidics since thick layers of this resist can be patterned precisely and rapidly on different substrates using lithographic techniques. However, the application of SU-8 mostly confined to define only channel walls or larger fluidic areas then. Later researches proposed a vast range of models based on SU-8, such as SU-8 cantilevers, interferometer, ring resonators and optical filters and thus soon SU-8 became one of the prominent materials in many research fields.

When it comes to the structuring of SU-8 surfaces, this polymeric resist exhibits high material and process flexibility and so the structuring of this resist does not require high-cost and tedious dry etching techniques as those used for inorganic materials. Lithographic techniques such as photolithography, soft lithography, e-beam lithography and x-ray lithography are the most widely used SU-8 structuring methods. SU-8 structures with diverse designs and dimensions (micrometric and nanometric) can be produced by selectively exposing the resist to a polymerization precursor (ex: e-beam,

x-ray or proton beam, or UV light) followed by the chemical development of the exposed region. Among all the above mentioned methods, due to its advantages such as low cost, ease of patterning, and good spatial resolution, photolithographic patterning of SU-8 is the most common lithographic method used.

2.2.1. Photolithographic structuring of SU-8

Photolithography is referred as a method that transfers patterns on a photomask to a resist surface. From the early stages onwards, UV photolithographic structuring has been one of the promising and efficient structuring techniques in IC fabrication, semiconductor industry, and MEMS. Photolithography is one of the widely used SU-8 patterning. A schematic of photolithographic patterning of SU-8 is shown in figure 2.2.

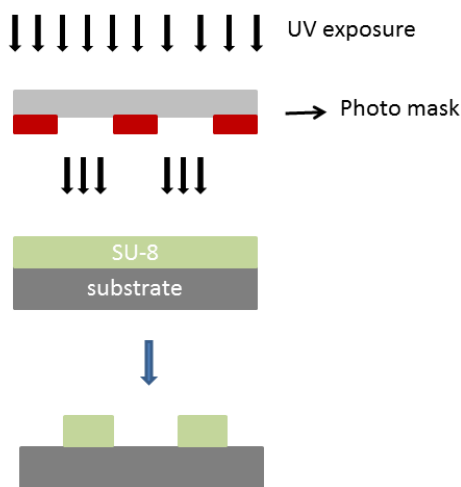


Figure 2.2: Schematic representation of photolithographic patterning of SU-8.

The basic process for the patterning of SU-8 using photolithography includes i) substrate preparation, ii) spin coating of the resist on to the substrate, iii) soft baking of the spin coated resist, iv) UV exposure of the soft baked resist film, v) post exposure bake of the exposed surface, and vi) finally the development of the baked surface. During photolithography the cross-linking of the exposed SU-8 takes places in two steps: 1) initially, upon the exposure, the photochemical reaction gets initiated by the photosensitizer and produces an acid which opens the epoxide rings of the resin, following this 2) the acid generated by the exposure in turn acts as the catalyst to promote the cross-linking of the resist during the post exposure bake. Thus, the cross-linking renders the exposed region of this resist insoluble to the developer.

To obtain desired SU-8 structures with maximum resolution and definition, the optimization of the photolithographic parameters such as baking time and temperature, exposure conditions, developing time and proper substrate preparation are necessary. Studies show that the lack of proper substrate preparation prior to the resist deposition is one of the major reasons for the instability (removal) of the resist from the substrates [Barber 2007, Zhang 2011]. Due to the highly hydrophobic nature (contact angle about 73° [Zhang 2005]) of SU-8, prior to the spin coating the substrates have to be modified to obtain a homogeneous and stable SU-8 film. Literature review shows that SU-8 has poor adhesion to most of the substrate such as SiO_2 , TiO_2 , Al, Ni, glass, Au or Ni, and certain surface pre-treatments are required to improve the adhesion of SU-8 on the substrates [Dai 2005, Barber 2007, Zhang 2011, Liu 2014]. Different research groups such as that of Wouters at KULeuven and Morikaku at the University of Hyogo proved that coating the substrate with chromium or primers helps to increase the adhesion of SU-8 on silicon and SiO_2 substrates [Wouters 2012, Morikaku 2013]. Similarly, studies

have carried out to investigate the change in adhesion ability of SU-8 on glass substrates by surface pretreatment with RCA, Acetone or Isopropyl alcohol rinse, oxygen plasma treatment, and the results show that such surface pretreatment offers improved adhesion of SU-8 on substrates [Grist 2010, Serra 2007]. Similarly, MicroChem [www.microchem.com] has suggested that cleaning of the substrates with piranha, or with RIE can significantly improve the adhesion of SU-8 due to the increased hydrophilicity of the substrates. Therefore, a proper substrate pre-treatment is always required for better adhesion of SU-8 on to the substrates.

Apart from the substrate pre-treatment, the non-optimization of structuring parameters, especially the baking and exposure conditions are one of the major reasons that produce deformed or undesired SU-8 structures. Significant works have been carried out to study the effects and to find the optimized lithographic conditions to obtain SU-8 structures with maximum resolution and definition. Referring to the baking conditions, the baking time and temperature are two of the critical parameters that define the produced SU-8 structures, and therefore they have to be optimized to achieve high defined SU-8 structures. The physical and mechanical properties of the cured SU-8 highly depend on the soft baking and post exposure bake (PEB) conditions and so researches have been conducted to study the effect of each process for SU-8 structuring [William 2004, Chung 2013, Johari 2014]. In optical lithography, the soft baking step is intended to remove the solvent and thus to improve the SU-8 adhesion on substrates, and PEB is performed to thermally cross-link the exposed region of the resist. A higher soft baking temperature ($T > 137$ °C) might initiate the cross-linking of the resist even if the photosensitization is not carried out. Also, a shorter soft bake will not be enough to remove the solvent. Similarly at a lower PEB temperature the cross-linking will not

occur and higher PEB causes film stress. Therefore optimization of both soft baking and PEB conditions is necessary for the structuring of SU-8. Williams and co-workers at Louisiana State University recommended that a progressive increase in the baking (soft baking and PEB) temperature up to 95°C can produce SU-8 structures without cracks due to reduced residual film stress [Williams 2004]. They have investigated on the influence of thermal and mechanical properties of SU-8 at different baking temperatures. Their study shows that a PEB temperature above 100 °C changes the tensile strength of the cured SU-8. Further studies recommended a two-step baking process where the temperature slowly increases from 65 to 95 °C for SU-8 structuring, especially for the fabrication of high aspect ratio structures [Chung 2013, Nguyen 2002]. The gradual increase of temperature helps to avoid a drastic temperature change and to achieve a more controlled solvent evaporation from the resist film.

Thus, the various studies show that by applying the optimized conditions, a range of 2D and 3D SU-8 structures such as microfluidic systems, micropillars, or microneedles can be fabricated by photolithography. However, while patterning SU-8 films, the thickness of the resist film has to be considered as the structuring parameters (especially the baking conditions and exposure time) depend on the thickness of the SU-8 resist film. Table 2.1 represents the soft bake and PEB conditions for various SU-8 types.

SU-8 type	Thickness (μm)	Soft bake (min) at 65°C	Soft bake (min) at 95°C	PEB (min) at 65°C	PEB (min) at 95°C
SU-8 2	1.5-5	1	1-3	1	1
SU-8 5	5-15	1	3-5	1	1-2
SU-8 25	15-40	3-5	5-15	1	2-4
SU-8 2002	2-5	1	2	1	1
SU-8 2007	8.5-10	1	2	1	1-2
SU-8 2025	41-75	1-3	3-9	1	3-7
SU-8 2050	50-165	3-5	6-30	1	5-12
SU-8 2100	100-260	5-7	20-60	1	10-15

Table 2.1: Table represents the processing time of SU-8 of different thicknesses [Campo 2007].

When it comes to SU-8 structures produced using photolithography, so far many works have been reported on the photolithographic fabrication of SU-8 microfluidics [Guerin 1997, Chuang 2003, Svasek 2004, Abgrall 2006, Stanciu 2012]. The applications of those produced structures vary from enzymatic microreactors [Hostis 2000] to separation devices like dielectrophoresis [Cui 2000, Cui 2002]. In 2005 Tuomikoski and team at Helsinki University of Technology demonstrated the fabrication of electrospray tip with SU-8 for electrospray ionization-mass spectrometry, and in 2012 Stanciu at IMT, Bucharest shows the fabrication of electrokinetic microfluidic structures using SU-8 to study the electro-osmotic (EO) mobility [Tuomikoski 2005b, Stanciu 2012].

A three-layer process was demonstrated for the fabrication of free-standing SU-8 microfluidic chips with enclosed microchannels and high density of fluidic inlets where

photolithography combined with an adhesive bonding and etching technique was used [Tuomikoski 2005a]. Using this method they have fabricated microchannels with a channel width ranging from 10 to 2000 μm , depths from 10 to 500 μm , and lengths up to 6 cm. Similarly, in 2006 Lopez at MEMS/MST Department, Arrasate reported on the use SU-8 as a lab-on a chip device by integrating low-cost optical sensors and microfluidic structures using photolithographic steps accompanied with a bonding technique [Lopez 2006]. In 2004 Carlier at IEMN, Villeneuve d'Ascq Cedex shows the fabrication of an integrated lab-on-a chip microsystem with SU-8 microchannels on silicon wafers using for protein analysis by mass spectrometry (figure 2.3a) [Carlier 2004]. Besides, various studies proved that SU-8 is an ideal structural material for the fabrication of microfluidic devices [Zhang 2001, Duarte 2011]. In 2009 Saha at IIT, Mumbai has reported on the fabrication of SU-8 microfluidic channels with integrated pillars using lithography to understand the capillary flow, surface tension and viscosity of the working fluid (ethanol) with the surface texture of microfluidic channels (figure 2.3b) [Saha 2009]. To study the influence of the pillar sizes (diameter, pitch, height) on the capillary flow they have fabricated pillars with varying size, and the results show that the geometry of the pillar was observed to significantly influence the capillary flow in the micro channels. Furthermore, the fabrication of multilevel microchannels using two-step photolithography and they have produced microchannels with different widths (20-600 μm) and height (20-30 μm) was also reported [Choi 2010].

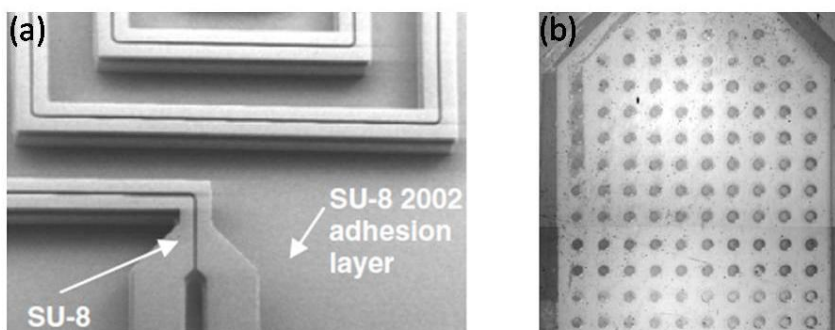


Figure 2.3: SU-8 a) microchannels and b) microfluidic channels with integrated pillars. [Figures reproduced from Carlier 2004 and Saha 2009 respectively].

Apart from microfluidic devices, successful photolithographic fabrication of SU-8 cantilevers, interferometers, ring resonators and more are reported. In 2010 Keller at the Technical University of Denmark reported on the photolithographic fabrication of SU-8 cantilevers having a thickness of $2\mu\text{m}$ and length of $100\mu\text{m}$ using dry release method and two-step photolithography figure (2.4a) [Keller 2010]. Similarly, the fabrication of SU-8 cantilevers for various bio-chemical applications was also reported [Nordstrom 2008].

The relatively high refractive index of SU-8 makes it suitable for evanescent-wave optical sensors methods such as interferometry [Shew 2008, Beche 2010], planar waveguides [Lee 2003, Nordstrom 2007], Y-splitters [Shew 2005, Parida 2009], and ring and resonators [Leinse 2004, Yanga 2010, Salleh 2013]. Shew and team at NSRRC, Hsinchu reported on the photolithographic fabrication of SU-8 MZI and Y-splitters where SU-8 is the core material [Shew 2005]. The produced devices were then

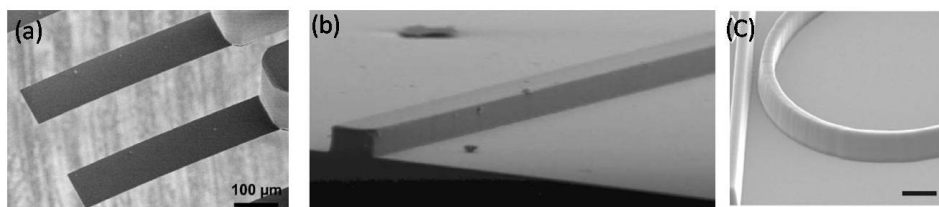


Figure 2.4: SU-8 a) cantilevers, b) waveguide and c) ring resonator. [Figures reproduced from Keller 2010, Nordstrom 2007 and Salleh 2003 respectively].

used for biochemical detection where they have shown detection of NaCl solution down to a concentration of 10^{-9} g/l. Apart from this, studies show the possibility of applying photolithographically patterned SU-8 MZI as ammonia sensors [Bednorz 2006] and as micro-sensors for gage pressure measurements [Pelletier 2007]. In 2007 Nordstrom and co-workers at the Technical University of Denmark showed the possibility of fabrication of single-mode SU-8 waveguide using UV lithography for micro-opto-electromechanical system applications (figure 2.4b) [Nordstrom 2007]. The fabricated waveguides had a height and width of 4.5 and $5\mu\text{m}$ respectively. Additionally, Boiragi at IIT, Mumbai presents both theoretical and experimental studies on single mode SU-8 based MZI for bio-sensing and they have studied the effect of sensitivity of the sensor by varying the length of sensing window [Boiragi 2011]. Apart from SU-8 MZI, studies are presented on the fabrication of single-mode rib optical waveguides composed of SU-8 with low optical losses using photolithography [Beche 2004, Pelletier 2006].

In 2003, Salleh at University of Glasgow reported on SU-8 based dual disk ring resonator integrated with microfluidic device for high sensitive label-free optical

biosensing, where the SU-8 structures were produced using photolithography (figure 2.4c) [Salleh 2003]. Similarly, studies have demonstrated on the photolithographic fabrication of SU-8 micro-ring resonators [Yanga 2010]. The produced structure was then used as an optofluidic ring resonator switch for optical particle transport.

Additionally, SU-8 is also one of the favorable materials to fabricate high aspect ratio (HAR) structures due to the excellent mechanical properties it offers. Range of HAR SU-8 structures can be made by controlling the lithographic conditions [O'Brien 2001, Zhang 2001, Lin 2002, Abgrall 2007]. Studies show that optimized photolithographic conditions produce SU-8 structures having aspect ratios up to 20 [Dentinger 2002, Loechel 2000, Campo 2007, O'Brien 2001, Lin 2002]. In 2005 Yang and Wang from Louisiana State University reported on the capability of SU-8 to produce structures with HAR around 191. The produced structures have a height of 1150 μm and a thickness of 6 μm . By optimizing the lithographic conditions, mainly the baking temperatures, fabrication of HAR SU-8 micropillars with aspect ratio up to 8 is shown to be possible by Amato and co-workers from Technical University of Denmark [Amato 2012]. The fabricated micropillars showed pillar heights bigger than 20 μm and a diameter smaller than 2.5 μm .

Besides, an approach for the fabrication of inclined three-dimensional SU-8 structures by inclined photolithography was demonstrated by Sato at Waseda University and Han at Pohang University of Science and Technology [Sato 2004, Han 2004]. In a conventional lithographic system the mask and the resist coated substrate are aligned perpendicularly to the light source and as a result vertical structures are produced. However, in an inclined lithographic method, with the help of a tilting stage the mask

and the resist film are aligned at an inclined angle with respect to the light source resulting in the formation of inclined structures. The shapes of the microstructure are defined by the UV irradiation angles and the number of exposures. In 2004 Han demonstrated the fabrication of SU-8 cylinders, bridges, embedded channels, V-grooves and truncated cones with aspect ratios higher than 4 using 100 μm thick SU-8 layers by an inclined photolithographic method using a conventional mask aligner (figure 2.5) [Han 2004]. Moreover, they have produced tapered structures with non-vertical sidewalls by tilted and simultaneously rotating the photomask and photoresist coated substrates during the light exposure.

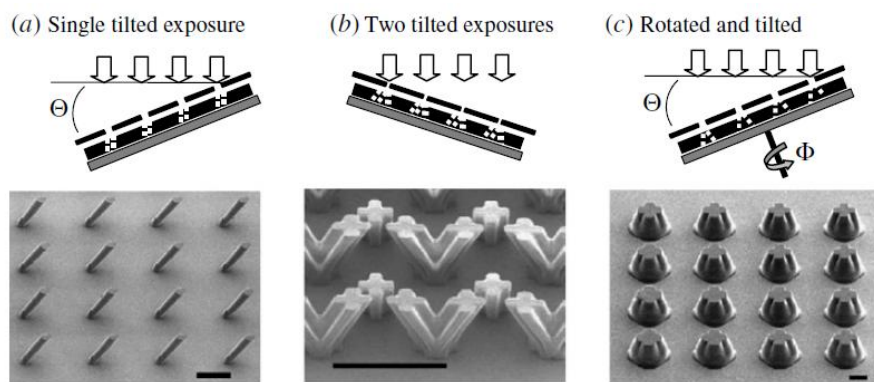


Figure 2.5: a) Tilted SU-8 pillars obtained by tilted UV single exposure (scale bar 100 μm), b) SU-8 structures obtained by double exposure (scale bar 200 μm), and c) tapered structures obtained by tilted and rotated UV exposure (scale bar 50 μm). [Figures reproduced from Han 2004].

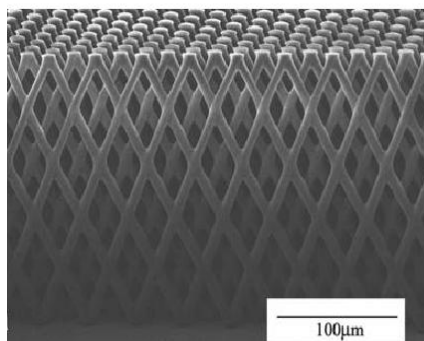


Figure 2.6: SU-8 micromesh obtained with multiple UV exposures [Figure reproduced from Sato 2004].

Similarly, complex three-dimensional structures can be produced by multiple exposures of the resist film at different inclined angles [Sato 2004]. They have fabricated HAR (aspect ratio 20) SU-8 three-dimensional micromesh by multiple backside exposure and by tilting the substrate and the mask at different angles (figure 2.6).

Apart from using SU-8 as a permanent structural material, the high chemical and thermal resistance, and mechanical strength it offers makes SU-8 one of the most suitable material for creating master mold for the soft lithographic production of various polydimethylsiloxane (PDMS) based MEMS and lab-on-a-chip structures and devices. The required pattern is initially transferred on to SU-8 by lithography and then PDMS structures/devices are replicated from SU-8 structure using soft lithography. The soft lithographic replication of PDMS microfluidic devices using SU-8 molds fabricated using photolithography was demonstrated by Natarajan at University of Utah, and Jenkins at Nanjing University [Natarajan 2008, Jenkins 2013]. Using SU-8 as a mold allows rapid replication of PDMS microfluidic structures.

2.2.2. Soft lithographic structuring of SU-8

Soft lithography comprises a set of techniques for replication and pattern transfer of micrometer and nanometer scale structures and devices on planar or, flexible substrates using elastomeric stamps, and molds [Scott 1998, Xia 1998]. In soft lithography initially the master mold has to be produced and then the structure on the master mold is transferred on to stamps or molds. Figure 2.7 presents the schematic representation of fabrication of PDMS stamp.

The stamps are usually produced by cast molding in which the polymer is poured over a master template having a relief structure on its surface. This is followed by curing the polymer over the master template either thermally, or by light exposure. The curing mode depends on the properties of the polymer used for stamp. Then using tweezers the cured polymer is peeled off from the master and thus forms the stamps with relief pattern. The stamps create an inverse pattern of the master template pattern, and so the final structure will contain the pattern on the master templates. Following this, the patterns are then transferred on to the sample surface by pressing the stamp against the sample surface.

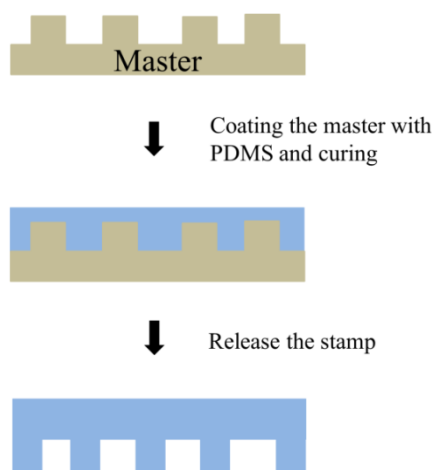


Figure 2.7: Figure represents four main soft lithographic approaches for structuring surface.

Soft lithography includes a board range of techniques and depending on the basic principle of pattern transfer, all the method are grouped into three general categories such as replica molding, embossing, and printing [Gates 2004].

Replica molding is a method in which the master mold itself acts as the stamp for the pattern transfer (figure 2.8a). Here the patterns are transferred by solidifying a liquid pre-polymer mixture which is in contact with the master by thermal or UV radiation curing.

Embossing, also known as imprinting is a method in which the pattern is imprinted on to a flat solid surface by pressing the stamp or mold against a soft surface such as photoresist accompanied by thermal or UV curing (figure 2.8b). The stamp or mold is embossed with pressure, thermally, or with solvent assisted method.

Finally, printing also known as microcontact printing is a technique in which a patterned elastomeric stamp transfers the surface pattern on to the sample surface (figure 2.8c). In this method initially a thin layer of alkanethiol "ink" is spread on to the elastomeric stamp. By using this inking method the molecules to be transferred are immobilized on to the stamp surface and subsequently they are transferred to the substrates by printing.

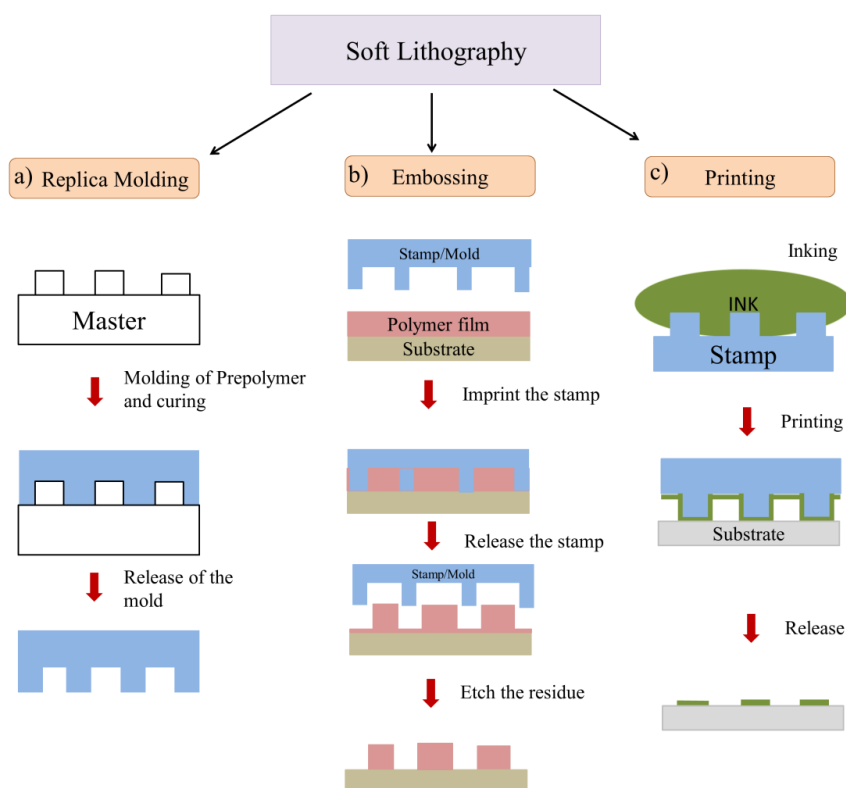


Figure 2.8: Figure represents four main soft lithographic approaches for structuring surface.

Referring to the soft lithographic structuring of SU-8, studies have reported on the fabrication of SU-8 structures in both micrometric and nanometric scale using various soft lithographic techniques. The applications of the soft lithographically patterned SU-8 structures range from micro-electronic and micro-optics to biotechnology. Microstructuring of SU-8 by UV assisted imprinting with a non-transparent mold (Ni mold) was demonstrated by Youn at AIST, Ibaraki [Youn 2008]. Using this process they fabricated arrays of 1 mm long SU-8 lines having a width of 10 μm and a 10 μm spacing between the adjacent lines. Additionally, the fabrication of SU-8 microring resonator filters using soft lithographic method was demonstrated by Poon and co-workers at, California Institute of Technology, where PDMS stamps were used for the pattern transfer to the SU-8 film [Poon 2004]. Further, in 2005 Moona and team at KAIST, Daejeon demonstrated the fabrication of patterned polymer photonic crystals using a hybrid combination of holographic lithography and soft lithography [Moona 2005].

Various works has been performed by a hybrid combination of soft lithographic and photolithographic techniques to create various 2D and 3D periodic structures [Nordstrom 2006, Hu 2006, Jeon 2007, Cannistra 2010]. In 2006 Hu and co-workers at University of Michigan successfully produced 3D SU-8 micro- and nanostructures using reversal UV imprint process where the SU-8 was initially coated on a patterned glass mold and then transferred on to various substrates by reversal UV imprint at an ambient temperature and pressure [Hu 2006]. Using this method they have produced 100 nm to 1 μm wide SU-8 gratings, multiple-level nanochannels, cavities, and air-bridging polymer structures having a width ranging from 400 nm to 10 μm on flat or patterned substrates (figure 2.9).

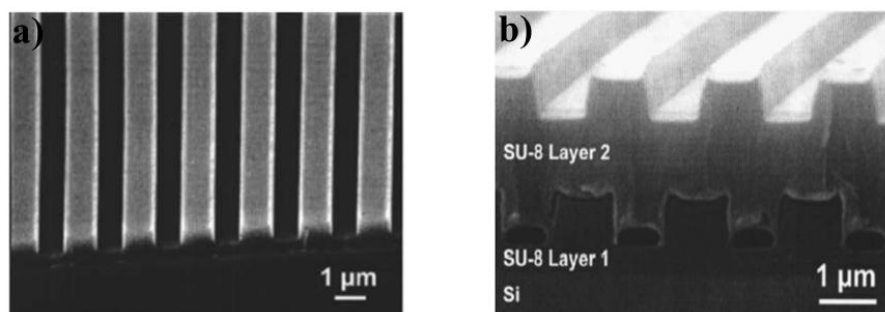


Figure 2.9: SEM images of SU-8 structures produced by reversal UV imprinting: a) SU-8 gratings having a depth of 650nm and width of 1 μm on Si substrate, and b) sealed SU-8 channels.

Similarly, a work was demonstrated on a method for the fabrication of sloped-side walled (54.7°) SU-8 structures using a combination of hot embossing and UV exposure, where electrochemically etched silicon wafers served as the master molds [Nordstrom 2006]. Likewise, later in 2010 Cannistra and co-workers at University of North Carolina reported on the fabrication of complex 3D micro-optical components such as spherical and cylindrical refractive microlens array of SU-8 using a combination of micro-molding and photolithography [Cannistra 2010]. Micro-optical components sized down to 100 nm fabricated by this method.

2.3. Applications of SU-8 in biology and biotechnology

For many years' inorganic materials such as silicon, silicon dioxide and silicon nitride have been the most prominent structural materials used in biotechnology and BioMEMS. Miniaturized biosensors and devices of such inorganic materials can be

fabricated by various micro- and nanofabrication techniques such as physical and chemical vapor deposition, or chemical and reactive ion etching. However, these fabrication techniques can be time consuming and involves high production costs, which is one of the drawbacks of using an inorganic material. Studies show that the polymers such as PDMS and SU-8 can be equally valuable materials as that of inorganic materials for biological studies as are biocompatible and they can be patterned with any required designs using low-cost and rapid lithographic techniques [Holgado 2010, Fernandez 2007, Walther 2007]. Although for many years SU-8 was considered as a structural material in MEMS, studies found SU-8 can be an promising material for biosensors [Holgado 2010], drug delivery [Fernandez 2007, Pramanick2013, Altuna 2013], and cell culture [Matschegewski 2010, Walther 2007]. The characteristics such as biocompatibility, nonirritant, and non-toxicity attribute SU-8 a valuable material in biological research.

In 2002 kotzar and co-workers at BIOMECH, Cleveland studied on the biocompatibility of some of the commonly used BioMEMS materials such as silicon nitride, silicon dioxide, single-crystal silicon, titanium and SU-8 [Kotzar 2002]. They have carried out five of the ISO 10993 physiochemical and biocompatibility tests and the results show that except silicon nitride and SU-8 all other materials fell below the detectable limits in four test categories (residue on ignition, nonvolatile residues, UV absorption and turbidity). Similarly, in 2002 Weisenberg at University of Minnesota showed that the biocompatibility and good chemical compatibility SU-8 offers makes it a potential material for microfluidic applications [Weisenberg 2002].

Successful fabrication and application of various biosensor devices such as include SU-8 optical waveguides [Lee 2002], cantilevers [Johansson 2006, Nordstrom 2008], interferometers [Shew 2005, Esinenco 2005], and ring resonators [Salleh 2013] using SU-8 has been reported so far. In reference to the analytes, studies show different methods of immobilization of DNA [Marie 2006, Wang 2011], and protein [Blagoi 2008, Shew 2006] on to SU-8 surfaces. Studies have reported on a successful perfusion of brain tissue cells using microfluidic chamber patterned with SU-8 micropillars of different arrangements [Passaeraub 2003]. A rapid and one-step procedure for the immobilization of cholesteryl-tetraethyleneglycolmodified oligonucleotides (chol-DNA) on SU-8 surfaces was reported and the results showed that a robust and efficient attachment of DNA was achieved on SU-8 surfaces (figure 2.10) [Erkan2007].

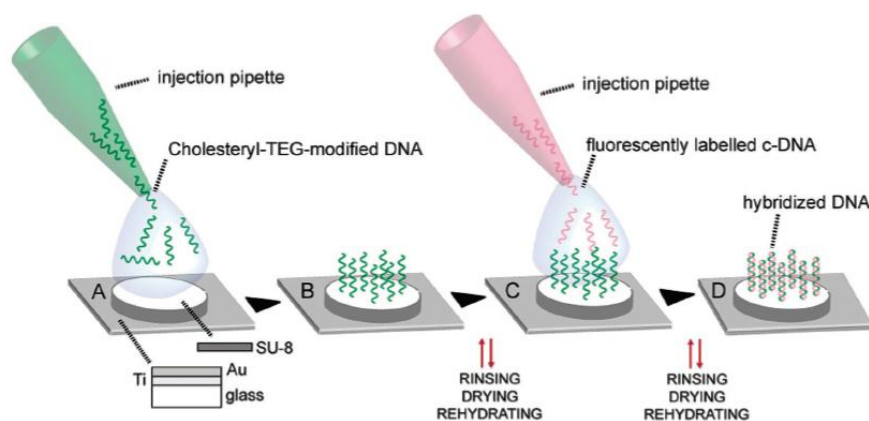


Figure 2.10: Schematic diagram of chol-DNA immobilization and the hybridization procedure on SU-8 surfaces.

The devices used for biological applications always require the immobilization of biomolecules on the device surface. Some of the different methods for immobilization of biomolecules on to device surface are encapsulation, adsorption, or covalent bonding. Since a covalent bonding results in a better biomolecule activity, greater stability and reduced non-specific adsorption, a covalent immobilization of biomolecules is preferred for those molecules that do not adsorb, adsorb very weakly or adsorb with improper orientation and conformation to polymer surfaces [Wei 2000, Parl 2002, Tatte 2003]. Many studies have been conducted to develop a highly functionalized SU-8 surface with a high immobilization efficiency and good accessibility to target biomolecules [Tao 2006, Sethi 2010]. Target molecules such as nucleic acids, antigens or antibodies can be immobilized on SU-8 by physical adsorption [Marie 2006, Erkan 2007, Blagoi 2008, Holgado 2010], but the instability and higher non-specific adsorption makes this method less favorable for biosensing purposes. By modifying the polymer surface to have at least one of the functional group such as amine, thiol, aldehyde, or carboxyl helps to achieve a strong covalent bonding between the biomolecules and SU-8. Studies shows different wet (ex: silanization) and dry (ex: plasma treatment) methods for the SU-8 surface functionalization [Wang 2006, Joshi 2007a, Joshi 2007b, Tao 2008, Blagoi 2008, Deepu 2009].

Wet functionalization of SU-8 surfaces with sulphochromic solution followed by [3-(2-aminoethyl) aminopropyl]-trimethoxysilane (AEAPS) and glutaraldehyde was demonstrated by Joshi at IIT, Mumbai [Joshi 2007a]. Following this, human immunoglobulin (HIgG) was then immobilized on to the functionalized SU-8 surfaces. Similarly, in 2009 Deepu and co-worker at IIT, Mumbai have presented a wet functionalization method using two cross-linkers, glycine and 11-mercapto undecanoic

acid [Deepu 2009]. Initially the SU-8 surfaces were hydrolyzed using NaOH and HCl and the hydrolyzed surfaces were treated with the crosslinkers to produce amine or thiol group on the SU-8 surfaces and then the functionalized surfaces were then treated with EDC:NHS mixture. Also, a dry method for the functionalization of SU-8 with amine group as achieved using pyrolytic dissociation of ammonia in a hotwire CVD setup [Joshi 2007b]. IgG was then successfully immobilized on to the functionalized SU-8 cantilevers surfaces.

The functionalized nano- and microfabricated SU-8 surfaces find application in various fields of biomedicine and biotechnology. In 2010 Holgado at Universidad Politécnica de Madrid presented label-free optical biosensors made of SU-8 planar and nanopillars surfaces for the detection of bovine serum albumin (BSA) antigen and anti-BSA antibody (aBSA) [Holgado 2010]. The detection measurements were performed using UV spectrophotometer and the results showed increased detection sensitivity with the structuring of sensing surfaces (figure 2.11).

An optical biosensor based on SU-8 MZI for the detection of antibody was shown by Shew at NSRRC, Hsinchu [Shew 2008]. IgG was allowed to interact with the antigen immobilized on SU-8 surface and results showed that the SU-8 MZI achieves a maximum sensitivity of 10^{-9} g/ml ($\sim 6.7 \times 10^{-12}$ M). Besides, they have used SU-8 MZI chip to detect the refractive index change in the enzyme-linked immunosorbent assay (ELISA) process. In 2009 Boiragi at IIT, Mumbai has reported on the fabrication of integrated optical biosensor with SU-8 multimode waveguides (Y-splitters) for the detection of IgG of different concentrations

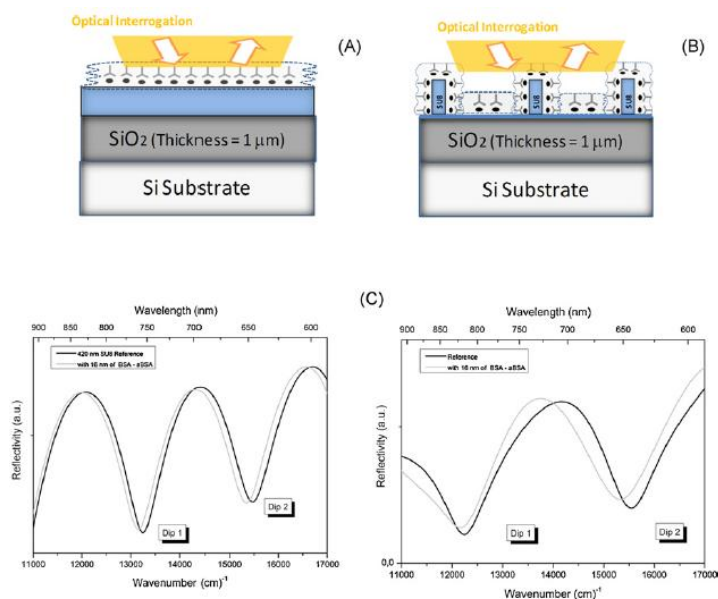


Figure 2.11: Schematic representation: A) BSA-aBSA on planar SU-8 surface, B) BSA-aBSA on SU-8 nanopillar surfaces, C) optical response of each structure with the antigen-antibody interaction on planar and structures SU-8 surfaces.

(down to 0.0125mg/ml) [Boiragi 2009]. In this study the SU-8 surfaces were initially hydrolyzed and treated with EDC:NHS solution to achieve a covalent bonding of the biomolecules to the SU-8 surfaces. Similarly, using photolithography, Shameli and team have fabricated a hybrid chip of quartz-SU-8-PDMS produced for the rapid simple isoelectric focusing for proteins [Shameli 2011]. The microchip helps for the separation and detection of proteins and PI markers with UV absorbance-based whole-channel imaging detection method. Furthermore, Walther at Technical University Munich showed a study on the enhancement of cell growth on O₂ plasma activated SU-8 surfaces [Walther 2007]. The results showed that the cell proliferation increases

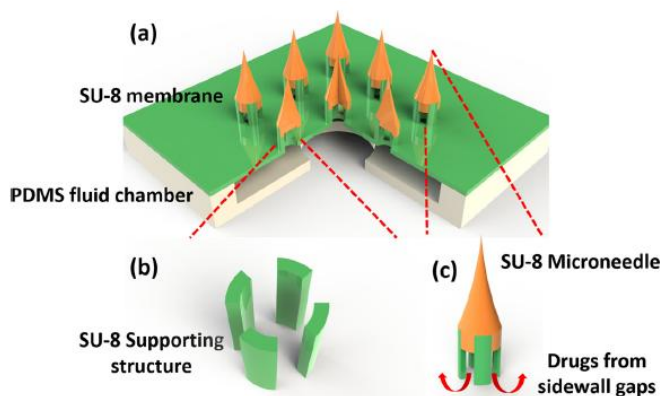


Figure 2.12: Schematic picture of the SU-8 nanoneedles. a) Overview of the whole device, b) SU-8 supporting structures made of SU-8 pillars, and c) SU-8 nanoneedle.

significantly with the plasma activation of SU-8 surfaces. Moreover, Xiang and team have successfully demonstrated the possibility of SU-8 microneedles for transdermal drug delivery (figure 2.12) [Xiang 2013]. The produced SU-8 nanoneedles were tested by penetrating it into the pig skin to delivered drugs. The study shows that the SU-8 needles are strong enough to stand forces during its penetration to the skin for drug delivery.

Despite the fact SU-8 is a valuable material for biosensing and biotechnological applications, the photoluminescence in the visible wavelengths [Marie 2006, Sikanen 2006] limits the uses of it in many applications, especially for the detection of fluorescence tagged analytes or when fluorescence is used as the predominant detection mode. So far only few studies have been reported on the reduction of SU-8

luminescence to use it for biological applications [Cao 2012]. Cao and team at Technical University of Denmark presented a method for the reduction of SU-8 luminescence by coating the SU-8 surface with a thin gold nanoparticle layer. Significant reductions of SU-8 luminescence (up to 81% compared to bare SU-8) were observed after coating it with a gold film and improve the sensitivity of fluorescence-based detection (figure 2.13). DNA was then successfully immobilized on to the gold coated SU-8 surface facilitating sensitive bio-analytical applications, such as DNA hybridization and SP-PCR.






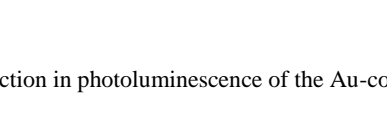
F	SU-8	AuNPs-coated SU-8	Autofluorescence reduction value
Cy5 channel			83.6%
Cy3 channel			81.8%
FITC channel			82.5%

Figure 2.13: The reduction in photoluminescence of the Au-coated SU-8 surface for the different wavelength ranges: Cy3, Cy5 and FITC.

Chapter 3

Micro- and Nanostructuring of SU-8 Surfaces Using Lithographic Techniques

Lithographic techniques such as photolithography, laser lithography and soft lithography are widely used as a tool for patterning and structuring devices in the field of microfabrication, nanotechnology and biotechnology [Stevenson 1986, Qin 1998, Cedeno 2002, Torres 2003, Lee 2005, Zaouk 2006, Lipomi 2012]. The advantages such as the ease of handling, rapid and low cost of structuring of surfaces make these lithographic techniques a key technique for the fabrication of micro- and nanostructures, especially in semiconductor industry.

This chapter is divided into two sections: i) first section gives an overall insight about the various steps and parameters involved in structuring of sample surfaces using any of these three lithographic techniques, and ii) the second section describes on the patterning of SU-8 surfaces using photolithography and soft lithography and the resulting SU-8 structures we have obtained. Besides, in the second section a detailed

description on laser lithography, which was the tool for the fabrication of photomask, is also presented.

3.1. Lithographic techniques for structuring surfaces

In this section, initially a general description of various steps and parameters involved in structuring of any sample surfaces using photolithography is given. This is followed by a descriptive note on parameters and methods of structuring sample surfaces by laser lithography. And finally, a description on soft lithographic technique for transferring patterns from a master template to sample surface is presented.

3.1.1. Photolithography

Photolithography is an optical means of transferring various geometrical patterns from a photomask on to sample substrates such as silicon, glass, GaAs, InP e.t.c. To achieve this transfer of patterns to the substrate, it is necessary to coat the substrate to be patterned with an intermediate material called the photoresist, which is a light-sensitive material. After coating the substrate with the photoresist, by light exposure followed by a cascade of surface treatments such as post bake, development and hard bake, the resist film can be patterned with the desired pattern. The patterns drawn on the imagable photoresist film is then transferred on to the substrate by various processes like etching, lift-off.

Figure 3.1 represents a typical photolithographic process. There are two types of photoresists and depending on the type of photoresist used, positive photoresist or negative photoresist, the steps involved in the photolithographic patterning process differ slightly. The patterning of a positive photoresist by photolithography involves five steps; i) substrate preparation (figure 3.1a), ii) spin coating of the photoresist on to the substrate (figure 3.1b), iii) soft baking of resist coated substrates (figure 3.1c), iv) light exposure of soft baked sample through the photomask (figure 3.1d), and v) finally, development of the exposed samples using a developer solution (figure 3.1e). However, in case of a negative photoresist an additional step called (vi) post exposure bake is required after the light exposure of the sample substrates (figure 3.1f). After the post exposure bake, the samples undergo development as in the case of a positive

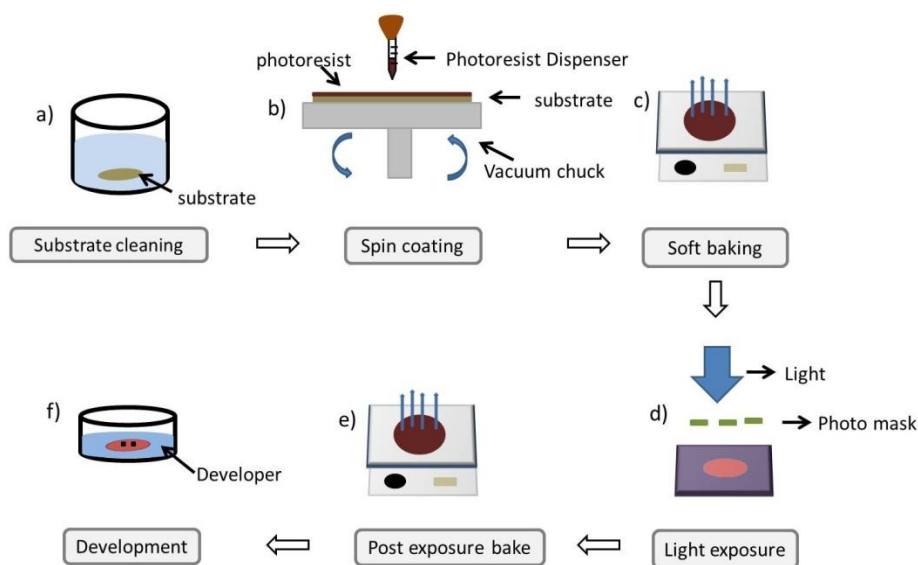


Figure 3.1: The schematic representation of various steps involved in the photolithographic patterning of any sample.

photoresist. A detailed description on each steps involved in photolithographic patterning is explained here.

i. Substrate preparation

The substrates preparation is achieved in two steps: cleaning of the substrates for the removal of contaminants presents on it, and followed by the dehydration of cleaned substrates to remove the water content. The substrate contaminants can be either in the form of particulates or in the form of any organic or inorganic layer. The presence of particulates causes defects in final photoresist pattern if they are not removed before spin coating, and the presence of organic or inorganic film on the substrate causes poor adhesion of resist on the substrates. Therefore the removal of the substrate contamination is important to improve the adhesion of the photoresist to the substrates and to obtain maximum process reliability.

The substrate cleaning can be accomplished by various methods such as wet chemical cleaning, ozone stripping or by plasma cleaning [Choi 2003a, Choi 2003b]. One of the widely used methods for substrate cleaning is the wet chemical cleaning. Cleaning with solutions such as piranha (a mixture of H_2SO_4 and H_2O_2), acetone, ethanol, water, or trichloroethylene is usually performed for the removal any organic and inorganic contaminants present on the substrates. If the substrates are not highly contaminated, simple degreasing can be achieved by ultra-sonication of the substrates in acetone, ethanol or methanol for 5-10 min.

Once the substrates are cleaned, they have to be baked at a set temperature. This baking helps to get rid of any water content present on the substrates, which otherwise would

cause poor adhesion of the photoresists on to the substrates. Depending on the types of substrates the temperature and time for baking varies from 150 to 200 °C for 10 to 15 min. respectively. After baking, the substrates are allowed to cool down, and as soon as after cooling it down, they can be coated with the photoresists.

ii. Spin coating

Photoresists are coated on to the substrates by spin coating using a spin coater. The spin coating helps to obtain a uniform thin film of photoresist on the substrates. Initially the substrate to be coated is held on a spinner having a vacuum chuck and then the liquid photoresist is dispensed on to that substrate. The substrate is then rotated at a controlled spinning speed and thus the resist gets spread over the substrate and form a thin film. The thickness of the resist film obtained by spin coating depends on many factors such as, the spinning speed, the properties of the solvent solution of photoresist (viscosity and surface tension), and the substrate material. A thinner resist film can be obtained when the spinning speed is high enough. However, a very high spinning speed might cause irregularities in the obtained resist film. Similarly, a highly viscous resist will have to be coated at a higher spinning speed to obtain a thin film, while the spinning speed can be reduced when using a resist which has less viscosity. Thus, to obtain a desired thickness for the resist film, calibration of the spinning parameters is required when different resists are used.

iii. Soft bake

After spin coating, 20-40% of the solvent still remains on the coated resist film. In order to remove these solvent present in the coated resist film, the substrates has to be

soft baked after the spin coating. This soft baking helps to evaporate out the solvent present in the resist film. The soft baking also helps to improve the adhesion of the resist on to the substrates and minimize the dark erosion during the development. Dark erosion is the removal of the undesired area of the photoresist from the substrate during development. Besides, the removal of the solvent prevents the photomasks from sticking on to the resist layer in the case of contact photolithographic exposure, which might otherwise contaminate the photomask.

A soft bake is usually done on a level hot plate to have a good thermal contact and heating uniformity. The rate of evaporation of the solvent depends on the rate of heat transfer and thus the soft baking time and temperature has to be adjusted depending on the thickness of the photoresist and the substrates. Excessive baking results in the degradation of photosensitivity of the resist by thermally decomposing the photoactive compound of the resist. On the other hand insufficient soft baking results in higher dark erosion during development of the UV exposed samples. After the soft bake, the substrates are allowed to cool down to room temperature and then they are ready for the light exposure.

iv. Light exposure

In photolithography, in order to transfer the patterns from the photomask on to the resist surface, the soft baked samples undergo a light exposure through the photomask. This light exposure is accomplished using a mask aligner. Figure 3.2 represents a contact mask aligner setup and following this a short general description on the working of mask aligner is given.

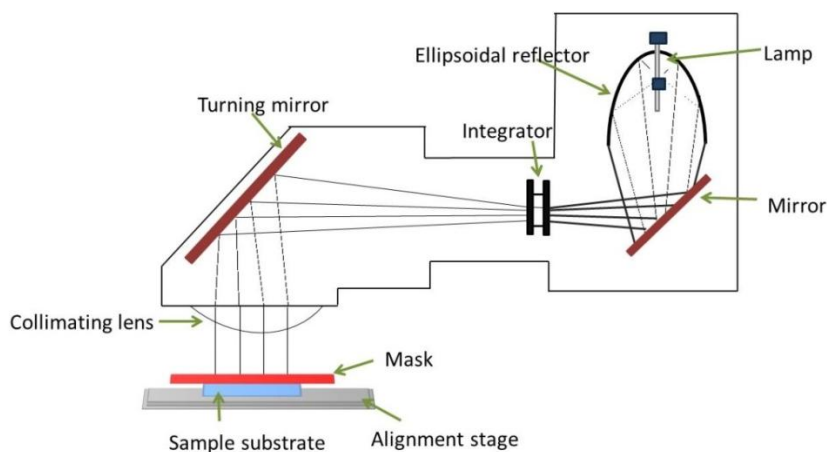


Figure 3.2: Schematic of a mask aligner.

A mask aligner consists of three main parts, a lamp house, a microscope, and an alignment stage. The lamp house of a mask aligner contains the source of light and the optical components such as the lenses and mirrors. A typical mask aligner uses gas discharging lamps such as mercury arc lamps. These lamps emit light in a broad spectrum in the DUV, UV and visible regions. During a light exposure, the absorption spectrum of the photoresist needs to be matched with the emission spectrum of the lamp in the aligner so that the photoactive compound in the resist becomes activated. A wavelength ranging from 365 to 440 nm can be produced with a mercury arc lamp. The sensitivity of almost all the photoresist lies in this range of the electromagnetic spectrum.

The lamp house has a second optical system called the integrator, which consists of a set of filters, lenses and mirrors. The filters help to select particular spectral lines of the Hg

emission, and the lenses and mirrors are employed in the path of light to collimate and reflect the light before it gets incident on the sample. Other than the lamp house, the alignment stage and the microscope in a mask aligner helps to hold and align the sample and the mask for the light exposure. The sample substrates are held on the XY alignment stage and the photomask is placed over the sample substrate. In order to enhance the contact between the sample substrate and the mask, the alignment chuck is equipped with a vacuum holder. The microscope helps to obtain a correct alignment between the photomask and the sample substrate.

Once the photomask is properly aligned with the sample substrate, the light is shined on to the photoresist. During this light exposure, the light from the lamp is allowed to pass through the photomask and then projected it on to the sample substrate. Upon the light exposure, the chemical properties of the resist gets modified thus in turn changes solubility of the resist in the developer solution. When a positive photoresist is used, the exposed regions get dissolved in the developer while the unexposed regions remain on the substrate. The opposite happens for a negative photoresist. In this case, during development the exposed region of photoresist is polymerized and it renders insoluble to the developer, while the unexposed parts get dissolved. Figure 4.3 shows the schematic on difference between patterning processing positive and negative resist. During a light exposure, the exposure time is a critical parameter to be considered in order to obtain structures with maximum resolution. In a positive resist a shorter exposure time is not enough to activate the photosolubilization of the resist, while in a negative resist the cross-linking of the sensitizer cannot occurs with a low exposure time. A longer exposure time causes undesired exposure by the scattering, reflection and

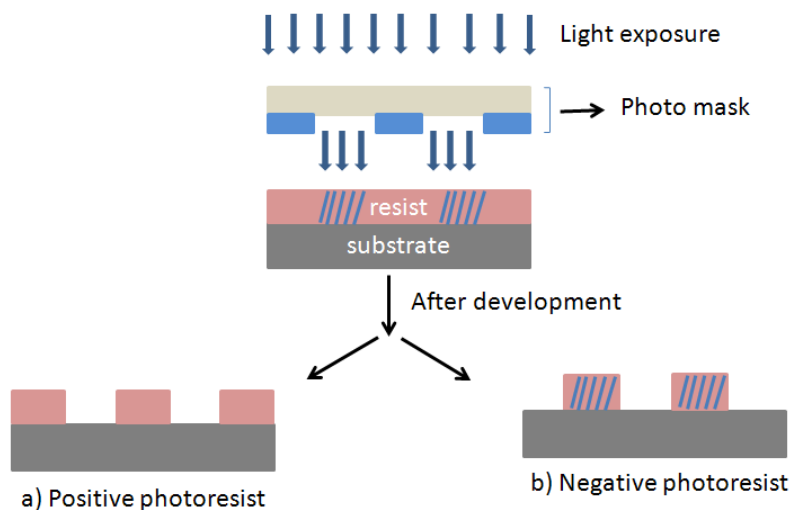


Figure 4.3: Schematic diagram of patterning of a positive and negative photoresists.

diffraction of light in the region on the photoresist layer which should not be exposed. Therefore the dimensions of pattern on the photomask are not precisely reproduced on the resist layer. On the other hand, a shorter exposure time can cause the formation of structures with very low dimension due to the insufficient exposure, and a too short exposure time is insufficient to activate the photoresist and causes dark erosion during development. A schematic of overexposed and underexposed patterns which are produced due to longer exposure time and shorter exposure respectively are shown in figure 3.4.

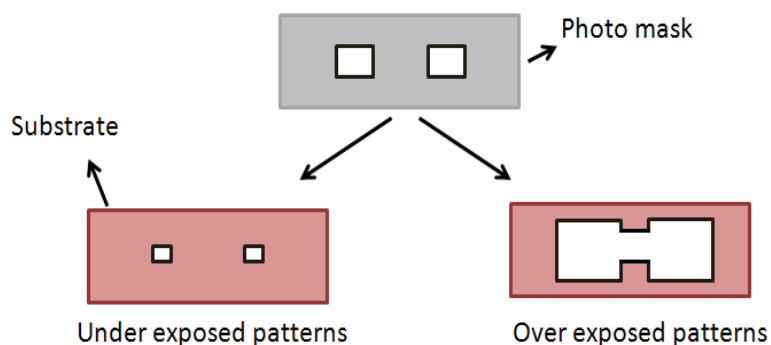


Figure 3.4: Schematic representation of overexposed and underexposed patterns on photoresist film.

The required exposure time to obtain structures with correct dimensions depends on various factors such as the power of the UV lamp in the mask aligner, the thickness of the photoresist and on the type of substrates used. The exposure time needed when using a lamp with high power is lower than one when a lamp with low power is used. For example, a light intensity of approximately $20\text{-}30\text{ mW/cm}^2$ can be achieved with a mask aligner equipped with a 350W Hg bulb. Thus, when using a 1000W Hg bulb, the exposure time should be reduced to approximately three times than the one with 350W bulb.

Apart from the power of the lamp, the exposure time has to be adjusted according with the thickness of the photoresist and the reflectivity of the substrates used. A thicker photoresist has to be exposed for longer time than a thinner layer of resist, because of the thickness of a thick-resist is higher than that of the penetration depth of the exposure light. Wherein, a short exposure dose is sufficient to make the thinner resist layer active.

Similarly, depending on whether the substrate using is highly reflective or transparent, the required exposure time varies. The exposure time needed to activate the photoresist is shorter for a highly reflecting sample substrate than that of a transparent substrate. Therefore, taking into account all these influencing factors, the calibration of the exposure time has to be done beforehand when using a photoresist.

v. Post exposure bake

After the light exposure, a positive photoresist can directly undergo development using a developer solution. But in case of a negative photoresist, to increase the chemical etch resistance of the exposed polymer for development an additional baking steps called a “post exposure bake” is required after the exposure and before the development. The post exposure bakes helps to thermally cross-link the exposed portion of the sample surface and thus in turn make the exposed portion inert to the developer. A post exposure bake is usually performed either on a hot plate and the time and temperature depends on the type of resist used. The exposed and baked resist are then ready for development.

vi. Development

Development is a wet chemical etching process performed using a solution known as the developer. A developer is an aqueous solution which is formulated either with an inorganic or with an organic compound. As explained above, for a positive resist the exposed parts get dissolved by the developer, while for a negative resist it is the unexposed parts that get removed. During development the parameters such as the developer concentration and the development time are important parts that have to be

considered in a photolithographic process. The developer concentration affects the development time of a resist, and thus a calibration between the concentration and time has to be performed initially. In some cases, a higher developer concentration causes higher dark erosion and therefore the developer has to be diluted with base solution (ex: water) during the developer preparation. A longer developing time will dissolve both the exposed and un-exposed resist and a shorter developing time will result only in a partial dissolution of the exposed or un-exposed region.

3.1.2. Laser lithography

Laser lithography, also known as direct laser lithography is a mask-less optical lithographic technique mainly used for patterning photomasks and for rapid prototyping. Three major steps involved in the structuring of a sample substrate using laser lithography are; i) sample preparation, ii) designing the pattern to be drawn and iii) laser exposure for transferring designs on to sample surface.

i. Sample preparation

The sample preparation for laser lithography is carried out in a similar fashion as that in photolithography. Initially the substrates are cleaned and dried to remove the contaminants and water present on the surface. This is followed by spin coating of the resist on to the substrate and then soft bake. Afterwards, instead of exposing the sample surface with lamps having a broad band of wavelength, the samples are exposed using a laser that emits a narrow band around a given single wavelength. The exposure is followed by the post exposure bake and development as explained in section 3.2.1.

ii. Pattern preparation

As in photolithography, in this technique the structuring is achieved by the exposure of light on to substrates coated with a photoresist, followed by the development of the exposed samples. But, unlike in photolithography where the light exposure is performed through a photomask, in laser lithography the exposure is performed by the raster scanning of a focused laser beam. The sample holder is a translation stage that can shift the sample in two dimensions in the plane of the sample by means of two precision servo motors controlled by a computer connected to the lasers lithographic unit. Therefore, prior to the fabrication, the desired design of the device has to be designed and modeled and then transferred to the photomask. The designing can be performed with the support of any computer-aided design or mathematical modeling tool (ex: Clewin or LASI). Afterwards, the computer that controls laser unit is loaded with the digital pattern desired to be drawn on the sample surface. Once the design is ready it is transferred to the computer that controls the laser lithographic unit. Thus, during the exposure the laser will be drawn only through these designed areas.

iii. Laser exposure

Once the system is ready with the designs to be patterned on to the sample surface, the next step is the laser exposure of the prepared samples. The exposure is performed by a beam of laser equipped in the laser lithographic unit. The three major parts of a laser lithographic unit are; a source of laser, filters and lenses, and a scanning stage. A general schematic representation of a laser lithographic unit is shown in figure 3.5.

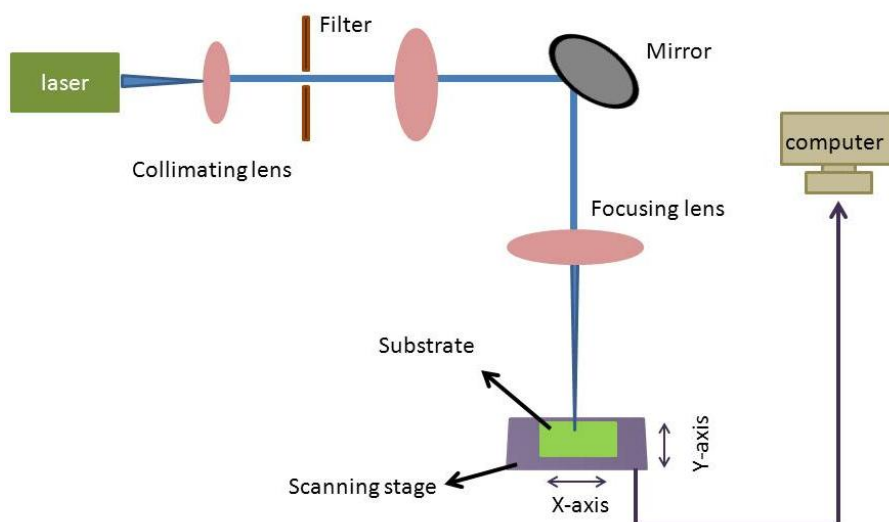


Figure 3.5: Schematic representation of a laser lithographic system.

The laser source can either be a high power pulsed or continuous wave laser. Some of the commonly used sources of laser in a laser lithographic unit are GaN laser (405nm), krypton fluoride laser (248nm), or argon fluoride laser (193nm). As mentioned in the section 3.2.1, the selection of the light (laser) source depends on the absorption spectrum of the photoresist.

During laser exposure, the laser power incident on the substrates is controlled by the use of neutral density filters (ex: 1%, 10% and 30% filters), which permits the transmission of a given amount of the beam power. The power of laser has to be optimized and by using neutral filters the laser power reaching the substrate can be controlled. For example use of 1% filter will let only 1 percentage of the total power of the laser to be incident on the sample surface. Similarly 10% and 30% will let only 10 and 30

percentage of the initial laser power to be used for the exposures respectively. The light that comes out through the filter is then reflected by a mirror and then finally focused on to the sample through a focusing lens.

In a laser lithographic system the substrates are loaded on an XY scanning stage equipped with a vacuum chuck. The vacuum helps to hold the substrate on the scanning stage. In order to eliminate external vibrations during exposure, all the components of a laser lithographic system are self-contained in an anti-vibrational unit. Besides, a temperature controlling and stabilization system is embedded in the unit to keep the internal temperature constant.

3.1.3. Soft lithography

Soft lithography is a collective term referring to various fabricating or structure replicating techniques using elastomeric stamps or rigid molds to pattern soft materials such as polymers and photoresists. Using this technique, both two-dimensional and three-dimensional structures can be easily achieved, which might be harder and tedious to obtain using photolithography [Xia 1998, Torres 2003, Wolfe 2010]. Compared to most of the lithographic techniques such as e-beam lithography, laser lithography, and nanosphere lithography that comprises high cost, time taking and tedious formulas, soft lithography is a rapid and cost effective technique for the structuring samples.

Figure 3.6 represents an overview on the structuring of any surfaces by soft lithography. The three major step involved in the structuring of a sample using soft lithography are; i) fabrication of a master template (figure 3.6.1), ii) transferring the patterns on the

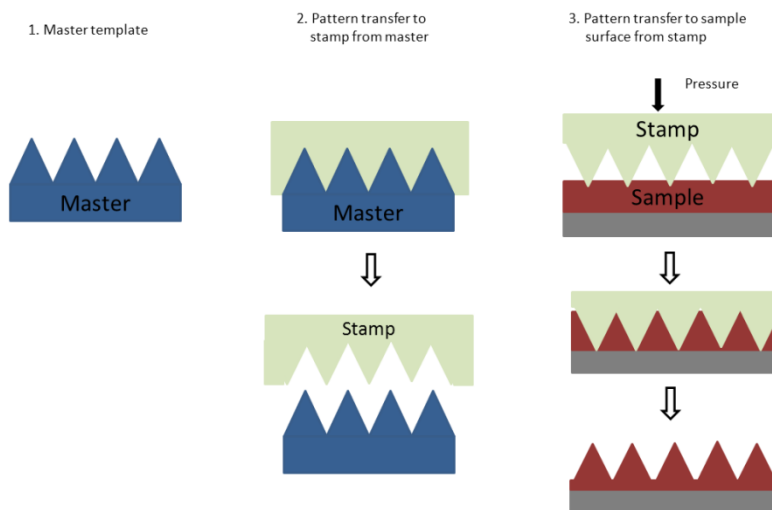


Figure 3.6: Schematic diagram of soft lithographic technique.

master to produce a stamp (figure 3.6.2), and finally iii) imprinting the patterns on the stamps on to the sample surface (figure 3.6.3).

i. Master templates

The first step in soft lithography is the fabrication of master templates. Silicon, metals, alumina, plastics, poly-(methyl methacrylate) (PMMA), or photoresists are some of the commonly used master template. One of the major requirements when choosing a master template is the rigidity of the template surface. The rigidity helps to prevent the template surface from collapsing when the polymer (ex: PDMS) is poured over it for producing stamps. The master templates are fabricated using various techniques such as lithography, chemical methods, e-beam writing, or microcontact printing [Wolfe 2010, Qin 2010]. Photoresist patterned by photolithography, direct laser writing, and

nanosphere lithography are commonly used as master templates [Wolfe 2010]. Apart from the lithographic methods, nonporous materials such as porous alumina or silicon to play as the master template are used.

ii. Stamps

Once producing the master templates, the next step is transferring the patterns from the master template to the stamp. PDMS, an elastomeric polymer, is one of the most widely used materials as the stamp in soft lithography [Lipomi 2012]. It can be cured thermally and it is easy to peel off from the master template after curing. Other than PDMS, polymers such as PMMA and PMMS (poly (3-mercaptopropyl methylsiloxane)) also serve the purpose as stamps in soft lithography.

iii. Embossing (Imprinting)

After obtaining the stamps, the final step is the imprinting of the stamp against the sample surface. This step helps to replicate the pattern from the stamp on to the sample surface. During imprinting a high pressure is always applied to keep the stamp tight to the sample surface and thus to transfer the pattern in the stamp on to the film. Along with this pressure either the sample surface with the stamp will be exposed to light or heat. The mode of treatment depends on the sensitivity of the used materials. This thermal or light treatment helps to produce a firm pattern on the sample surface. Finally the stamp is gently peeled off and thus releases the patterns on to the sample surface.

3.2. Experimental procedures to obtain photomasks and patterning SU-8 surfaces

Using the lithographic techniques such as laser lithography, photolithography and soft lithography, which are explained in section 3.1, we have fabricated photomasks, and various nano- and micro- SU-8 structures. The experimental methods for the fabrication of photomasks and SU-8 structures, and the corresponding results are presented in this section.

Photomasks were fabricated using laser lithography, and photolithography was used for the fabrication of SU-8 macropillars and straight waveguides. In this dissertation, depending on the dimensions (width and height) of the SU-8 pillars produced, they are referred as macropillars, micropillars and nanopillars. SU-8 pillars having dimensions (width and height) above 5 μm are called as macropillars, while SU-8 pillars having a dimension below 3 μm are referred as micropillars. Similarly, those pillars having a dimension below 500 nm are referred as nanopillars. Using soft lithography we have produced SU-8 structures such as SU-8 nanopillars, micropillars, nanopores and micropores. Further, by combining photolithography and soft lithography, we have fabricated SU-8 macropillars patterned decorated with nanopores, micropores, nanopillars and micropillars on its surface.

As mentioned in section 3.1.1, in photolithography the light is projected through the photomask for transferring the patterns to the resist film. In our work, in order to fabricate SU-8 macropillars and straight waveguides using photolithography,

photosmasks with the desired patterns were required. Therefore, prior to the fabrication of SU-8 macropillars and waveguides, photomasks with defined patterns for macropillars and waveguides was produced using laser lithography. The fabrication details and the corresponding results are explained in section 3.2.1.

First part of this section describes on the patterning of photomask and, the second and third part describe on the structuring of SU-8 surfaces using photolithography and soft lithography respectively.

3.2.1. Laser lithography for the patterning of photomask

A photomask is a glass plate coated with an opaque surface. The most common type of photomask used in photolithography is quartz glass plate coated with a chrome layer on one side. For our studies, we have patterned two chromium photomasks, one having designs for the photolithographic fabrication of SU-8 macropillars and another one with the designs for SU-8 waveguide fabrication.

The initial substrate to obtain the photomasks consisted of commercially purchased chromium masks (Nano Film, Westlake Village, CA). The chromium masks were already coated with a positive photoresist, AZ1505 resist when purchased. The thickness of the resist layer on the substrate was 500 nm.

The patterning of chromium masks using laser lithography involves two steps; i) designing the desired pattern, and ii) patterning the defined design on to the photomask using laser lithography.

i. Designing patterns

The designing of the desired patterns were performed using Clewin, layout editor software [PhoeniX Softwares]. Designs can be drawn with any desired dimensions and shapes using this software. For the fabrication of macropillars, two sets of designs having different dimensions were drawn. One set consisted of $6\ \mu\text{m}$ width squares on a square periodic lattice with separation between two nearest neighbors of $6\ \mu\text{m}$.

Similarly, the second set consisted of $8\ \mu\text{m}$ width squares with a separation of $8\ \mu\text{m}$ between two nearest neighbors. Both designs covered a total area of $1\ \text{cm} \times 1\ \text{cm}$. An image that shows how the patterns look when designed using Clewin is shown in figure 3.7.

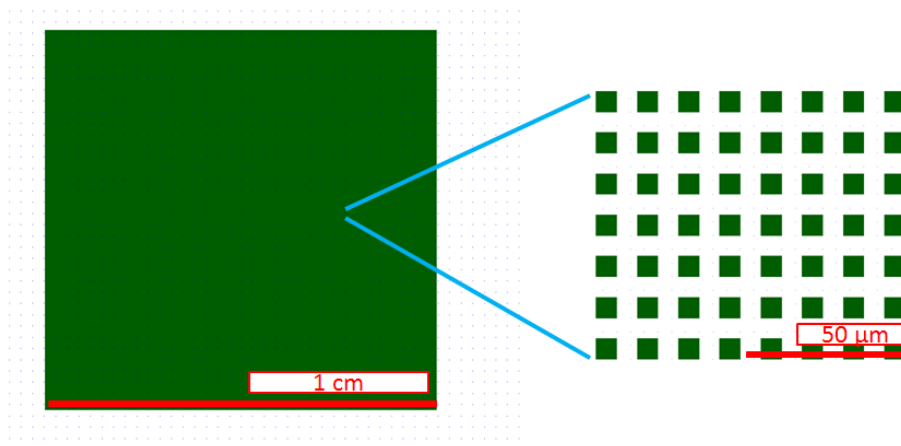


Figure 3.7: Image depicting the square designs drawn using Clewin.

Similarly, the designing of pattern for the patterning of chromium mask for the SU-8 waveguides were done as explained above. The only difference was that, instead of squares, straight lines were drawn for the waveguide fabrication. Two sets of lines having different dimensions were designed. One set had lines having a width of 6 μm and for the other set the lines had a width of 8 μm . In both the cases the length of each line was 5 cm and the separation between each lines were 600 μm .

After designing the patterns, they were transferred to the computer that controls the laser lithographic unit. Once they were transferred, the next step was to pattern these designs on to the chromium using laser lithography. Since the chromium masks we had were already coated with photoresist, no sample preparation was required. They were ready for laser exposure.

ii. Laser lithography for producing photomasks

The laser exposures were performed using a lithographic unit model DWL 66FS, from the company Heidelberg Mikrotechnik GmbH (Heidelberg, Germany), shown in the picture of figure 3.8. The unit is equipped with a diode laser source that emits at a wavelength of 405 nm and the laser power is 50 mW.

As mentioned in section 3.1.2, a very low and a very high exposure power will result in the under-exposure and over-exposure of the patterned structures respectively. Therefore, initially a set of test runs were performed with different filters to optimize the laser power for achieving patterns with high resolution and accurate dimensions on chromium mask. We have used 1%, 3% and 10% neutral filters to find the optimized laser power. The samples drawn with different energies were then checked under

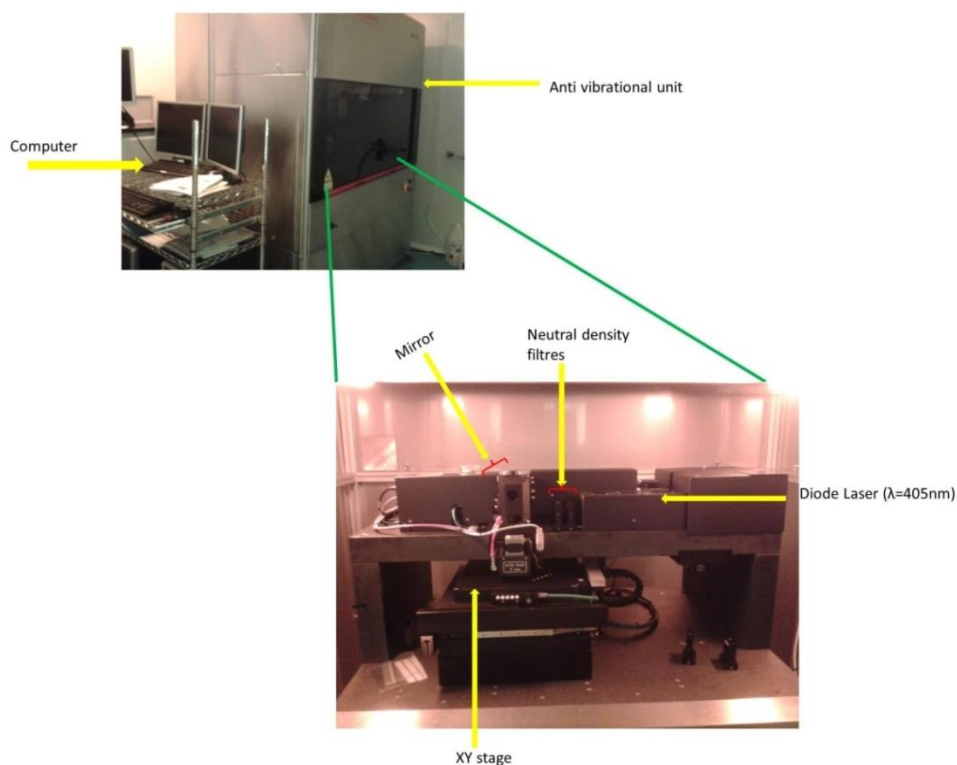


Figure 3.8: Digital photo of the laser lithographic unit.

environmental scanning electron microscope (ESEM) to verify the optimized energy required for patterning the chromium mask. The ESEM results show that for achieving structures with maximum resolution, the laser energy has to be 1 % of the initial laser power. Thus the power used for patterning chromium masks with designs for macropillars and waveguides was 0.5 mW. Figure 3.9 shows the ESEM images of over-exposed and under-exposed SU-8 pattern obtained during power optimization.

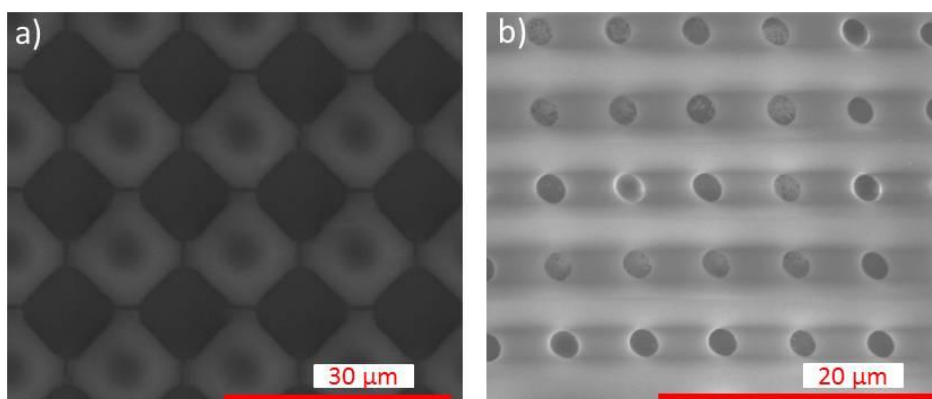


Figure 3.9: (a) Over exposed and (b) under exposed photoresists.

After obtaining the optimized power, the chromium mask was exposed to laser to pattern designs for macropillar fabrication. Once the chromium mask coated with photoresist was exposed, the next step was to develop the exposed mask using a developer solution. Therefore, the chromium masks were developed using AZ725 developer for 1 min. Subsequently, the mask was rinsed with plenty of DI water. Since the photoresist coated on the chromium mask is a positive photoresist, the exposed region was removed during developing.

This chromium mask served as the photomask for the fabrication of SU-8 macropillars. The ESEM images of chromium masks are shown below (figure 3.10). The ESEM images shows that the patterns in the chromium masks have the same dimension as that of the initial designs. One set has squares having a dimension of $6\ \mu\text{m}$ and the center to center distance was $12\ \mu\text{m}$. Similarly, the second set has squares with a dimension of $8\ \mu\text{m}$ and the center to center distance was $16\ \mu\text{m}$.

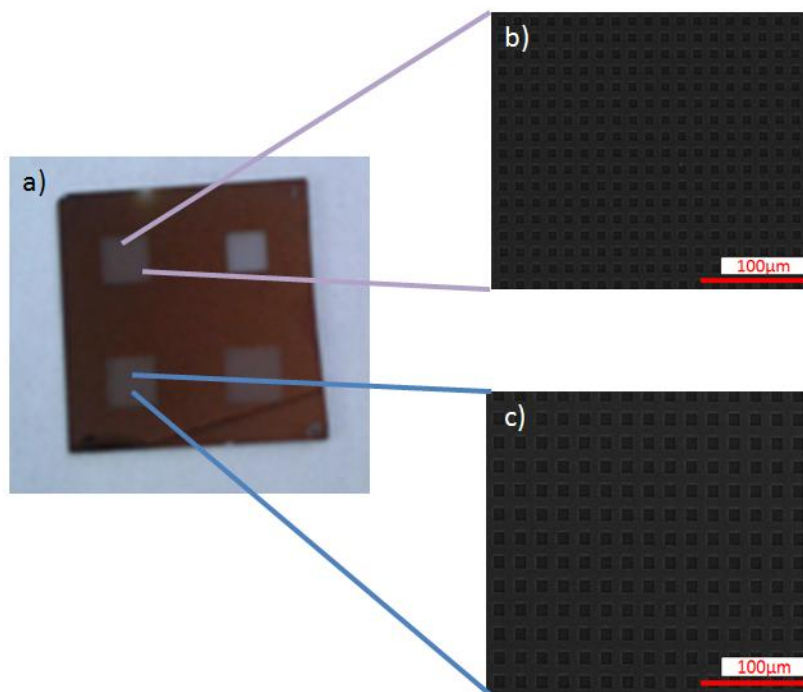


Figure 3.10: Digital photo (a) and the ESEM images of the chromium mask. (b) and (c) represents the ESEM images with squares having a dimension (width and height) of 6 and 8µm respectively.

Similarly, in the case for patterns for waveguides, once the designs were drawn, they were transferred and patterned on to the chromium mask as described in the case of fabrication of mask for macropillars. The designed mask was checked under ESEM and the images show that a line on the chromium mask has a good replication of the initial design. The ESEM image of chromium mask patterned with straight lines is shown in figure 3.11. One set of lines in the chromium mask have a width of 6 µm and the second one has a width of 8 µm.

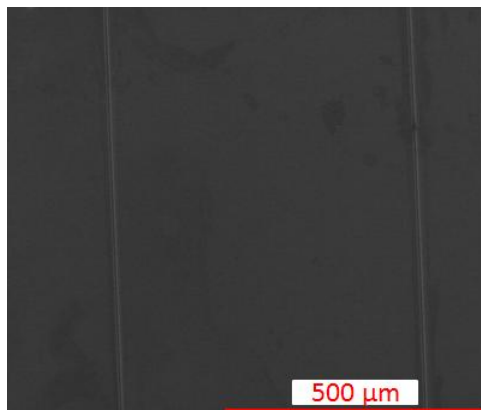


Figure 3.11: ESEM image of the chromium mask with lines having a width of 6 μm .

After fabrication the chromium mask, SU-8 macropillars and waveguides were fabricated using photolithography.

3.2.2. Photolithography for the fabrication of SU-8 microstructures

In our studies we have used SU-8 2005, whose primary solvent is cyclopentanone. SU-8 2005 and the SU-8 developer (1-methoxy-2-propyl-acetate, PGMEA) were obtained from Microchem (Westborough, MA). SU-8 is sensitive to near UV light and thus the structuring of SU-8 is generally performed with light having a wavelength between 350 to 400 nm. This light exposure induces chemical amplifications in SU-8. The UV exposure followed by a cascade of thermal treatments generates highly cross-linked SU-8 structures that have good thermal and chemical stability.

Here we show that SU-8 structures of various dimensions and geometry can be easily patterned and fabricated using photolithography, which has the advantages, such as fast, low-cost and ease of fabrication. Using photolithography we have fabricated SU-8 macropillars and SU-8 waveguides. A description on the parameters used for the fabrication of SU-8 macropillars and waveguides, and the ESEM images of the resulting structures are given below.

a. Fabrication of SU-8 macropillars

SU-8 macropillars were fabricated on two types of substrates, on silicon wafers and on microscopic glass slides. As mentioned in section 3.1.1, the structuring of negative photoresist (SU-8) consisted of five steps; i) substrate preparation, ii) spin coating of SU-8 on to the substrates, iii) soft baking of SU-8 coated substrates, iv) UV exposure of SU-8, v) post exposure bake of exposed SU-8 surfaces, and vi) development of the samples for the removal of the unexposed region.

i. Substrate preparation

Initially both silicon and glass substrates were cleaned using piranha solution. The piranha solution is a mixture of hydrogen peroxide (H_2O_2) and sulfuric acid (H_2SO_4). A 3 to 1 ratio of hydrogen peroxide and sulfuric acid was prepared in a pyrex glass beaker. This was done by adding 30 ml of hydrogen peroxide into a 10 ml solution of concentrated sulfuric acid. Silicon wafers and glass slides were immersed in the prepared solution for 30 min. at $100^\circ C$. In order to make sure that the wafers are clean, the prepared wafers were further cleaned with acetone and isopropanol in an ultrasonic bath for 5 min. each. Subsequently, the substrates were rinsed with plenty of DI H_2O .

Afterwards, to remove the presence of any water content from the substrates, the cleaned silicon wafers and glass slides were kept in a pre-heated oven set at a temperature of 180°C, for 20 min. After drying the substrate were brought out of the oven. The cleaned and dried substrates were then ready for spin coating.

It was observed that the adhesion of SU-8 on substrates was significantly improved after cleaning the substrates with piranha solution, while SU-8 was observed to get removed easily during developing from those substrates that were not cleaned with piranha solution. The improved adhesion of SU-8 on the piranha cleaned substrates could be due to the increased hydrophilicity of the substrates.

ii. Spin coating of SU-8

Initially to obtain the relation between spin coating speed and the thickness of SU-8, 1 ml of SU-8 was spun coated on to the glass and silicon substrates at various spinning speeds. The thickness of the photoresist can be controlled by adjusting the scanning speed (rpm).

A spinning speed ranging from 1000 to 5000 rpm was studied. The spin coated substrates were then soft baked and then examined under ESEM to find the thickness of SU-8. The relationship between the spinning speed and the thickness of the SU-8 is represented in the graph below (figure 3.12)

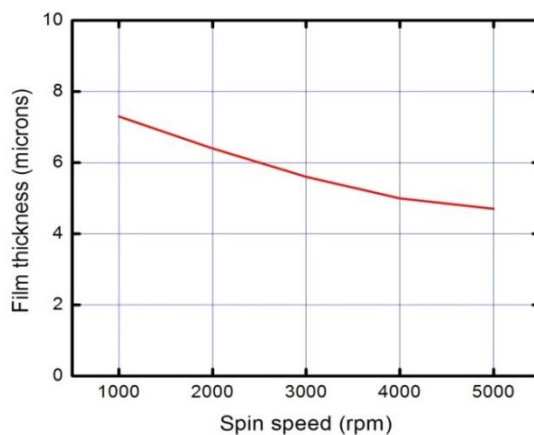


Figure 3.12: Graph representing the relation between spin speed and the thickness of SU-8.

The thickness of SU-8 can vary from 7.7 μm to 4.5 μm by controlling the spin speed from 1000 to 5000 rpm. After obtaining the spinning speed required, 1 ml of SU-8 was dispensed on to the substrate and spin coated at a spinning speed of 1000 rpm for 30 sec. The SU-8 coated substrates were then soft baked.

iii. Soft baking

Since the glass slides used were thicker than silicon wafers, the SU-8 coated glass slides were baked for longer time than silicon wafers. To obtain good results, a gradual increase of temperature during the soft bake is always recommended for SU-8 and therefore, a two-step soft baking was performed for SU-8 solvent evaporation [William 2004, Grist 2010]. To find the soft baking time required for SU-8, the time was varied and from 1 to 10 min. and checked. The optimized soft baking parameters

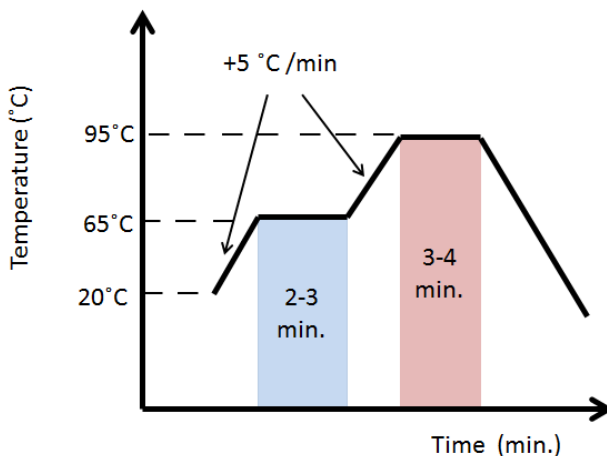


Figure 3.13: Temperature profile during soft baking of SU-8.

for SU-8 having a thickness of 6-7 μm on silicon wafers were observed to be 65°C for 2 min. followed by baking at 95°C for another 3 min. While, SU-8 coated glass slides were soft baked at 65°C for 3 min. then baked for another 4 min at 95°C. The soft baked substrates were then allowed to cool down to room temperature by bringing down the temperature at a ramping rate of 10 °C/min. Figure 3.13 shows a graph that represents the soft baking conditions (time vs temperature) used.

iv. UV exposure

The soft baked samples were then ready for the UV exposure. Since SU-8 is a negative photoresist the exposed parts get polymerized and remain on the substrate, while the unexposed part is removed by the developer. In our studies the UV exposures were performed using a mask aligner MG 1410, Suss MicroTec (Munich, Germany). The aligner is equipped with an Hg lamp with wavelength ranging 365-400 nm and with

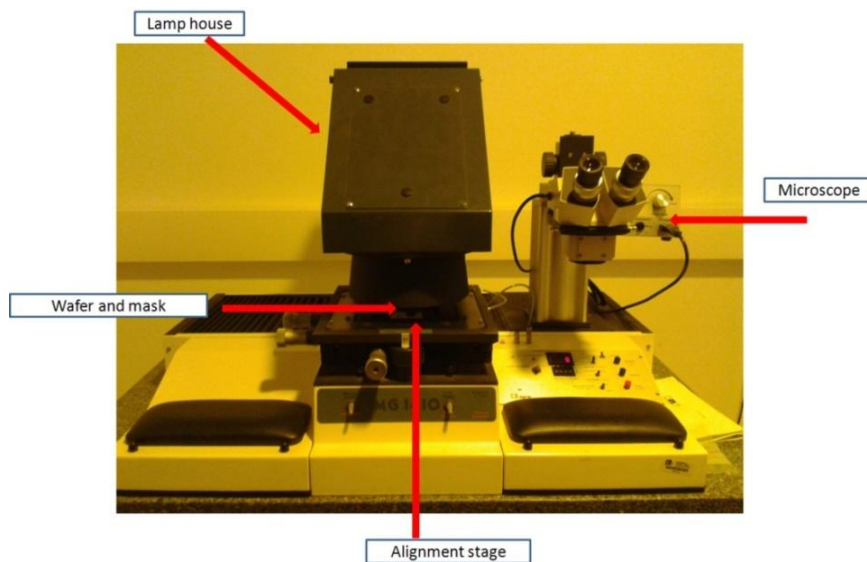


Figure 3.14: Digital photo of the mask aligner.

a power of 350 W. In the mask aligner, both the lamp house and microscope are movable. A digital image of the mask aligner setup we have used is shown in figure 3.14.

The SU-8 coated samples were exposed under the UV light through the prepared chromium mask to transfer the patterns on the mask. To obtain the optimized UV exposure time to produce SU-8 macropillars with maximum resolution, SU-8 coated silicon and glass substrates were exposed with UV light at various exposure time. The exposure time ranged from 1-6 sec. on Si wafer and 3 to 20 sec. on glass slides. Since silicon is more reflective than a glass surface, the exposure time required for a silicon substrate is always less than a glass substrate. It was observed that an exposure time smaller than 3 sec. and 8 sec. on silicon and glass substrates respectively, resulted in the

removal of the photoresist from the substrate during development. The cross-linking of the polymer could not occur with this time due to the under-exposure of SU-8 on substrates. Similarly, a higher exposure dose than 3 sec. and 8 sec. on Si and glass substrates resulted in the formation of overexposed SU-8 macropillars (figure 3.15). However, the degree of over-exposure was different in both substrates. In case of silicon wafer, even a slightly higher exposure time such as 3.3 sec. causes the formation of structures that are over exposed. While, when SU-8 on glass slides was exposed for 9 or 10 sec., the width of the macropillars were observed to be 2 to 3 μm bigger than that of the patterns in chromium mask. Although, on glass when the exposure time was higher than 12 to 14 sec, the structures obtained were over exposed. Thus the optimized UV exposure time in our case to obtain SU-8 macropillars on glass substrate was 8 sec., while for SU-8 coated silicon substrates the exposure time was 3 sec.

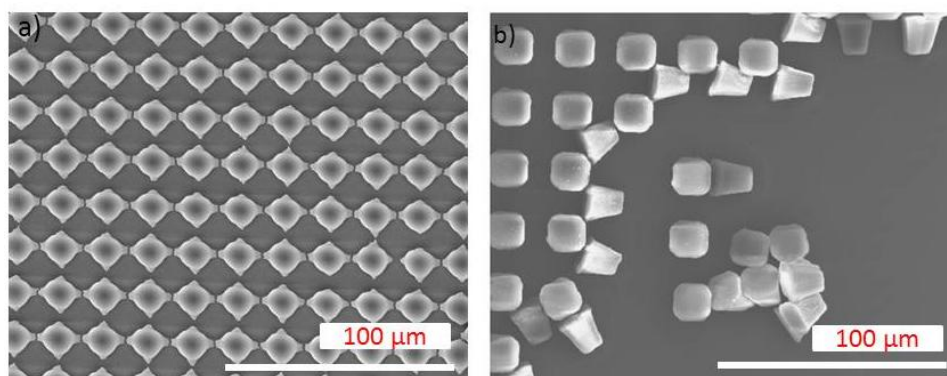


Figure 3.15: ESEM images of over exposed (a) and under exposed (b) SU-8 macropillars.

v. Post exposure bake

Subsequently, to thermally cross-link the exposed region of photoresist, SU-8 coated silicon and glass substrates were post-baked on a hot plate. The conditions of post exposure bake temperature were similar to that of soft baking, except the time. The hot plate having the substrates was initially at room temperature and then the temperature was gradually increased in two steps up to 95°C. Silicon wafers were post baked at 65°C for 2 min. and then the temperature was increased to 95°C and baked for another 2 min. On the other hand, the glass slides were post baked at 65°C for 3 min. then baked for another 3 min at 95°C. The baked substrates were brought down to room temperature by leaving it for another 20 min.

vi. Development

The post-baked samples were then developed using SU-8 developer, PGMEA (1-methoxy-2-propanol acetate) for 1min., followed by rinsing with isopropanol for 10 sec. A development time less than 1 min. was not enough to remove the un-exposed area and a higher development time washed off both the exposed and un-exposed SU-8 from the substrates.

The fabricated SU-8 macropillars on silicon and glass substrates were examined under ESEM. The top view and the cross sectional view of SU-8 macropillars on silicon wafer and glass slide is shown in figure 3.16. The results show that the array of macropillars has good distribution order like in its corresponding chromium mask. Nevertheless, it was observed that during photolithography, the width of the structures increases by 0.3-0.5 μm than the width of the patterns in chromium mask. Thus the fabricated SU-8

macropillars have a width of $6.3\ \mu\text{m}$ with a chromium mask having a $6\ \mu\text{m}$ pattern. Similarly, those macropillars fabricated through patterns with a dimension of $8\ \mu\text{m}$ were observed to have a dimension of $8.4\ \mu\text{m}$. Besides, the images show that the macropillars on glass substrates have a square shape while the macropillars on silicon have a nearly circular shape. This could be due to the difference in reflectivity of the substrates. The macropillars on both the substrates have a width of $6.3\ \mu\text{m}$ and a height of $7.7\ \mu\text{m}$.

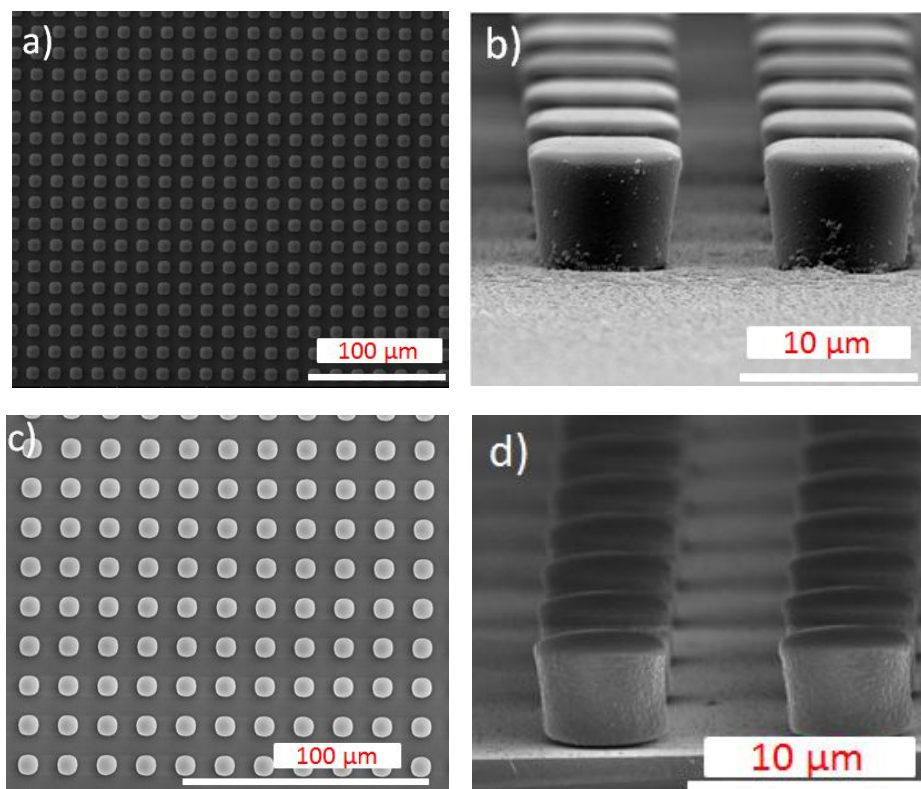


Figure 3.16: ESEM images of SU-8 macropillars (a and b) on glass, and (c and d) on silicon substrates. a and c are the top view, and b and d are the cross-sectional view.

b. Fabrication of SU-8 waveguide

Using photolithography we have fabricated planar SU-8 waveguides on silicon dioxide wafers. A cladding layer with lower refractive index than the core helps to propagate light through the waveguide core by total internal reflection. In our studies, oxidized Si ($n = 1.46$) wafer acts as a lower cladding material and SU-8 acts as the core. SU-8 has a refractive index of 1.58 at a wavelength of 633 nm. Silicon dioxide substrates were accomplished by the thermal oxidation of silicon wafer in a tubular furnace. The fabrication procedures of SU-8 waveguides were similar to that of the fabrication of SU-8 macropillars. The only difference was the substrate preparation in which the silicon wafers were oxidized using thermal oxidation prior to the resist coating.

Before depositing the photoresist the substrates were cleaned using piranha solution as mentioned in the previous section. Cleaned wafers were then dried with air and were ready for thermal oxidation. The oxidation was performed in a tubular furnace. In order to obtain a lower cladding layer (SiO_2) with a low refractive index compared to the core (SU-8), and to provide the surface passivation, the cleaned silicon wafers were oxidized using tubular furnace at a temperature of 1100°C for 10 h. with a homogeneous flow of air. The dry thermal oxidation resulted in the formation of an oxide layer of few micrometers (approximately $< 0.3\mu\text{m}$) on the Si wafers. The oxidized wafer had a slight green color. The oxidized wafers were then cleaned with water and dried in the oven for 30 min. at 180°C . The SiO_2 wafers were then ready for spin coating.

Other than the thermal oxidation, the fabrication procedure of SU-8 waveguides was the same as that of the fabrication of SU-8 macropillars. The optimized conditions of soft

baking, UV exposure parameters, post exposure bake and the development were the same for the fabrication of SU-8 macropillars and waveguides.

The optical waveguides produced were observed under SEM. The results show that during photolithography, the magnitude of the structures increases by around $0.5\ \mu\text{m}$. Thus the SU-8 waveguides produced through a chromium mask having a dimension of $6\ \mu\text{m}$ have a width of $6.2\ \mu\text{m}$. Similarly the structures formed through mask having a width of $8\ \mu\text{m}$ were observed to have a width of $8.3\ \mu\text{m}$. However, this increase in dimension was observed to be repeating in all the structures. The top view of SU-8 waveguides is shown in figure 3.17. The separation between each waveguides was $600\ \mu\text{m}$.

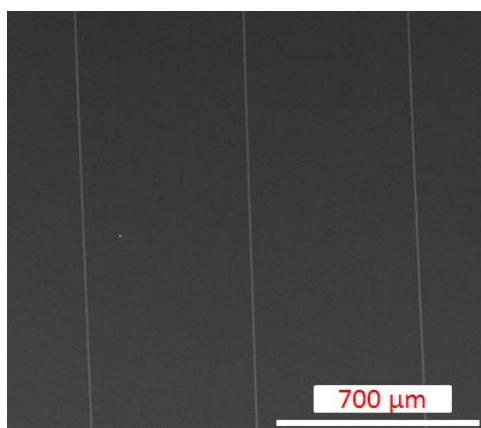


Figure 3.17: SEM images of SU-8 waveguides (top view).

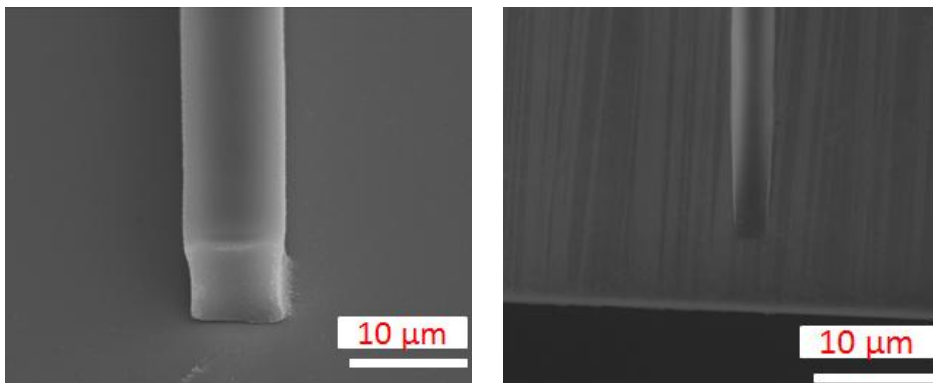


Figure 3.18: SEM images of the a) cross section and b) edge of an SU-8 waveguide.

Besides measuring the width, we have examined a diced piece of wafer in order to check the cross section of the waveguides. The substrate was diced using a diamond cutter, and the analysis was done using SEM. Figure 3.18a shows the obtained result. Similarly the edges of the waveguides were checked under SEM and figure 3.18b shows the results. It was observed that the waveguides do not reach till the edges of the substrates.

3.2.3. Hierarchical structuring of SU-8 with soft lithography and hybrid lithography

In this dissertation the term hierarchical structuring refers to the structuring of surfaces at different features sizes such as in nanometric and micrometric scales, and hierarchical structures are a collective name that defines structures at different scales such as nanometric and micrometric scales. This section describes on the structuring of SU-8

surfaces using two lithographic methods; 1) soft lithography for the patterning of SU-8 surfaces with nanomeric and micromeric pores and pillars, and 2) hybrid lithography for the fabrication of SU-8 macropillars patterned with nanomeric and micromeric pores and pillars on its surface. Here the term hybrid lithography refers to a structuring technique where the structuring is carried out using a combination of two different lithographic techniques; soft lithography and photolithography. In this work, using hybrid lithography we have fabricated SU-8 macropillars patterned with nanomeric and micromeric pores and pillars on its surface.

In this section the first part describes on the fabrication of master templates such as nanoporous alumina and microporous silicon for soft lithographic patterning. Following this the fabrication procedure of PDMS stamps is explained. The last two sections show the soft lithographic and hybrid lithographic patterning of SU-8 surfaces for the fabrication of planar SU-8 surfaces patterned with nanomeric and micromeric pores and pillars, and SU-8 macropillars decorated with nanomeric and micromeric pores and pillars on its surface respectively.

i. Fabrication of master templates

In this work, nanoporous alumina and microporous silicon served as the master templates for patterning PDMS stamps. The ordered nanoporous anodic alumina was fabricated using two-step anodization [Mauda 1995]. Initially, aluminum foils were electropolished for 4 min. at a voltage 20 V in a 1:4 (v/v) mixture of perchloric acid and ethanol. Then to wash away the acid residue, the samples were thoroughly rinsed with water and ethanol followed by drying with air. The first anodization step was carried out in 1% phosphoric acid in ethanol: water mixture (1:4) (v/v) at 194 V and 0°C for 24 h.

Afterwards, the alumina layer with the pores was dissolved through wet chemical etching in a mixture of phosphoric acid 0.4 M and chromic acid 0.2 M (1:1 volume ratio) for 3h. at 70°C. Subsequently, the second step of anodization was performed under the same experimental conditions as those of the first anodization step. The time of anodization was controlled by the charge to obtain layers with 600 nm thickness for NAA. Later, the pore diameter of the as-produced alumina was tuned to obtain the desired dimension using by pore widening in 5 wt.% of phosphoric acid at 30-40 °C. Figure 3.19 shows the digital images of nanoporous alumina produced.

The produced nanoporous alumina was examined using ESEM (figure 3.20). The ESEM results show that the alumina produced has an ordered nanoporous surface. The pores have a diameter of 130 to 140 nm and a depth of 200 nm.



Figure 3.19: Digital image of nanoporous alumina.

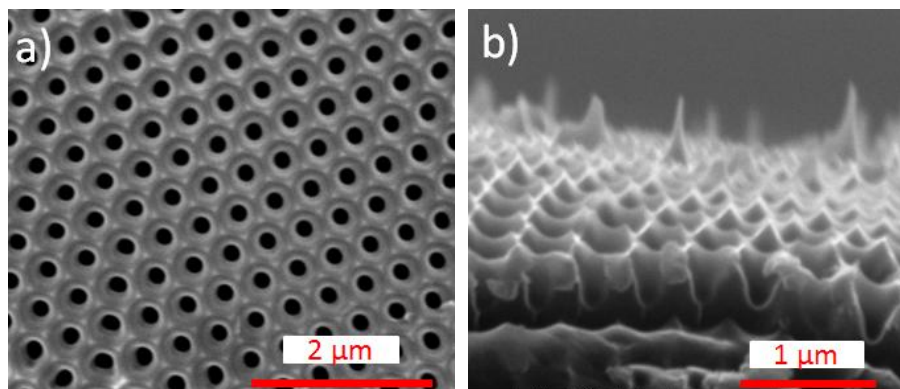


Figure 3.20: ESEM images of nanoporous alumina templates. a) top view and b) cross-sectional view.

Microporous silicon was fabricated by electrochemical anodization of silicon in 40% hydrofluoric acid (HF) solution. This solution acts as the electrolyte and it was prepared by diluting HF (40%) in dimethylformamide solution (DMF). A 10:1 (v/v) proportion of DMF: HF [Vyatkin 2002, Starkov 2003] was used. This porous silicon were produced on p-type silicon wafers with a (1 0 0) orientation and having a resistivity of 10-100 Ωcm . Prior to the etching the silicon wafers were washed with 5% HF, and then rinsed with DI H₂O and dried. The porous silicon was produced with a current density of 5 mA cm^{-2} for 10 min. A custom made Teflon cell with etching area 1,54 cm^2 was used for the fabrication microporous silicon. Figure 3.21 shows the digital images of microporous silicon produced and the ESEM images of microporous silicon produced is shown in figure 3.22. The images show that disordered porous surfaces were produced by this method. The produced micropores had a diameter ranging from 0.8 to 1.1 μm . The depth of the pores varied from 1 to 1.3 μm .



Figure 3.21: Digital image of microporous silicon.

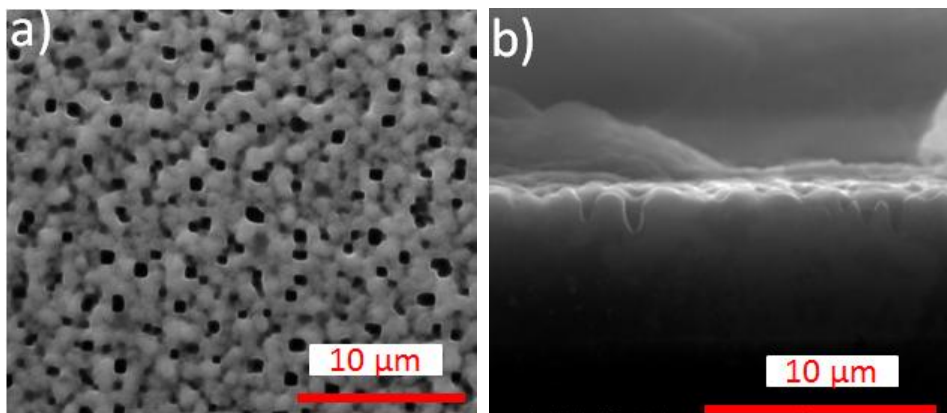


Figure 3.22: ESEM images of microporous silicon templates. a) top view and b) cross-sectional view.

ii. Fabrication of PDMS stamps

Four steps involved in the production of PDMS stamps are; 1) preparation of the polymer, 2) pouring the PDMS over the master templates, 3) curing of PDMS, and finally 4) peeling off the PDMS from the master.

We have fabricated two sets of PDMS stamps: i) PDMS stamps with nanometric and micrometric pillars and ii) stamps with nanometric and micrometric pores on it. PDMS stamps with pillars were produced by single PDMS casting while porous PDMS stamps were obtained by double casting. Generally, in single casting the production of patterned PDMS stamps is achieved using the master template, while in double casting the PDMS stamps prepared using single casting acted as the master templates. In this work, nanoporous and microporous master templates were used for the PDMS stamp production using single casting. While for double casting the PDMS stamps produced by the single casting acted as the master template and thus porous PDMS stamps were obtained. The details of both methods are explained below.

Prior to the production of stamps, the master templates were modified with hexamethyldisilazane vapor to make the PDMS surface hydrophobic [Slavov 2000, Tasaltin 2011]. This surface treatment prevents the PDMS from sticking to the master template surfaces and thus facilitates easy demolding.

Figure 3.23 shows the different steps involved in the fabrication of PDMS stamps. At first, to obtain a soft PDMS mold, a 9:1(v/v) ratio of pre-polymer (sylgard 184) [Down Corning Sylgard 184] and its silicone based curing agent was mixed (figure 3.23a). For that, 9 ml of the pre-polymer was taken and poured into a glass container initially. To

that solution 1ml of the curing agent was then added. In order to have a uniform mixture of pre-polymer and curing agent, the composite was whisked well with a spatula for about 10 min. This mixing process leads to the formation of air bubbles within the prepared mixture. Since the presence of air bubbles can significantly decrease the strength of the produced PDMS stamps, the air bubbles have to be removed from the solution mixture. Moreover these air bubbles can cause irregularities in the PDMS structure produced. Therefore, after the mixing of base and the curing agent, the mixture was degassed under vacuum until all the air bubbles were escaped (figure 3.23b). This mixture was carefully poured on to the master templates (figure 3.23c). Subsequently, it was cured (figure 3.23d) in the oven at 85°C for 1h. and peeled off from the master templates once it was cooled down (figure 3.23e). Thus, PDMS stamps with micropillars and nanopillars were produced (figure 3.23f).

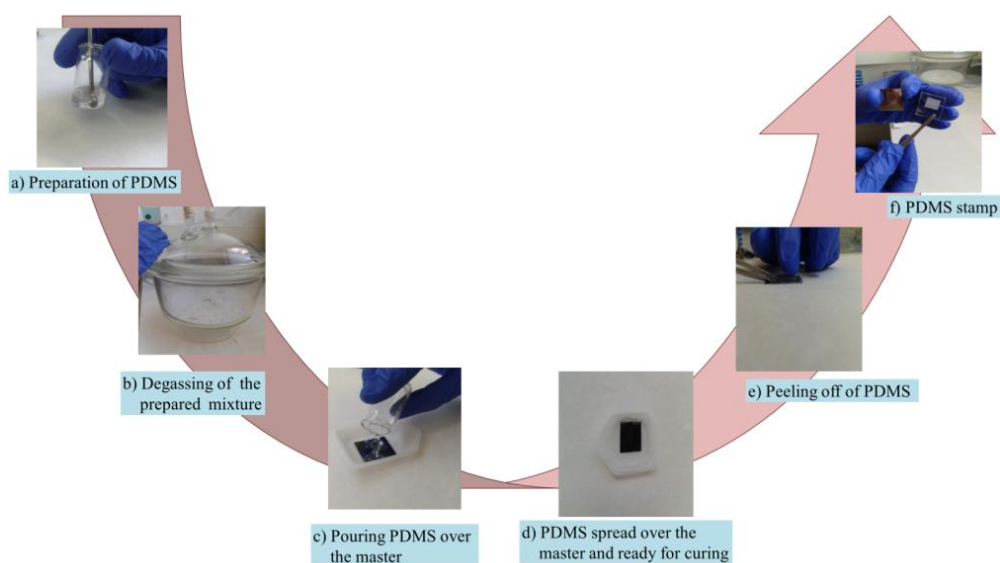


Figure 3.23: Digital images of the fabrication procedure of PDMS stamps.

Once the stamps were produced, they were examined under ESEM. The ESEM images of PDMS stamps with pillars are shown in figure 3.24. The images show that produced PDMS stamps with nanopillars have a pillar diameter of 135-150 nm and height of 200 nm. Similarly, PDMS surface structured with micropillars have a pillar diameter of 0.8-1.2 μm and height of 1-1.2 μm . The digital images of produced PDMS stamps are shown in figure 3.25.

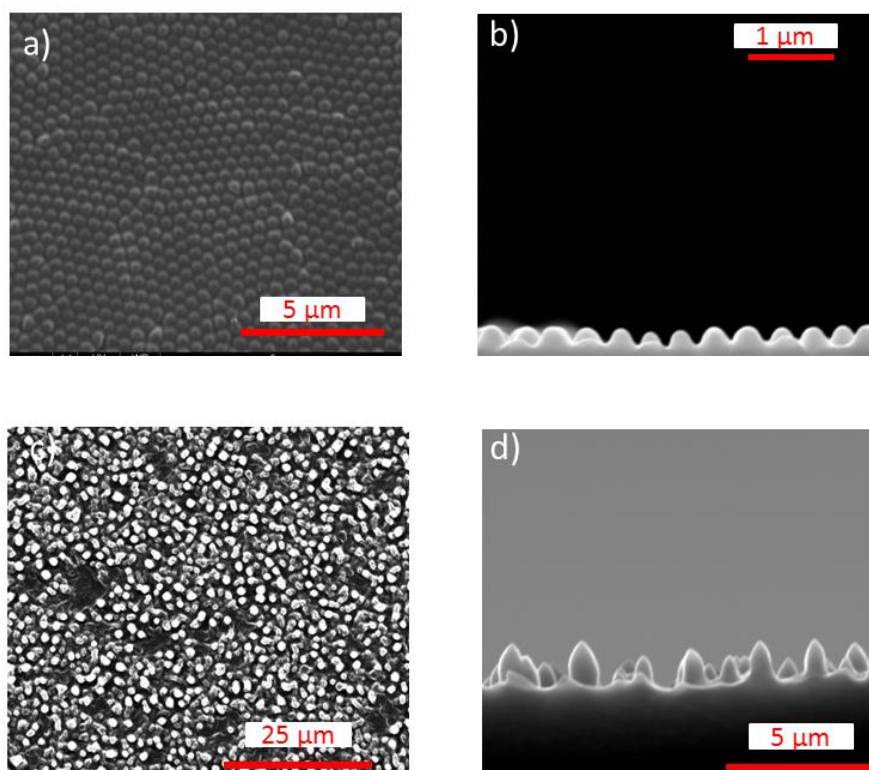


Figure 3.24: ESEM images of PDMS stamps (a and b) nanopillars and (c and d) micropillars.

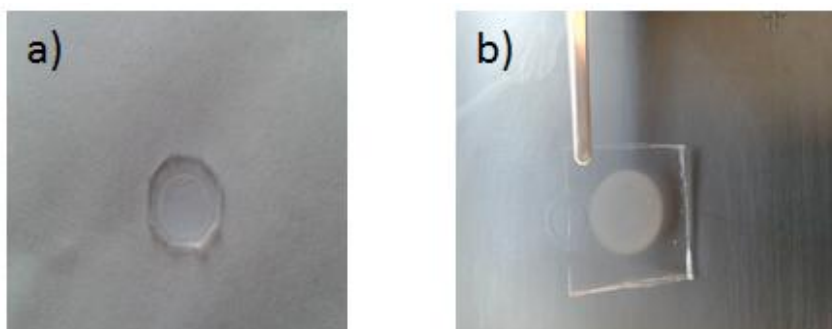


Figure 3.25: Digital images of the (a) nanopillars (b) and micropillars PDMS stamps.

After obtaining PDMS stamps with nanometric and micrometric pillars, the next step was to produce PDMS stamps with micro- and nano-pores by double casting. For the PDMS double casting, initially the obtained first set of PDMS stamps underwent thermal ageing for 48 h. in an air oven at 100°C [Gitlin 2009]. Following the thermal ageing, the stamps were treated with oxygen plasma for 1 min. in environmental plasma to render hydrophilicity of the PDMS surface. This plasma activated the PDMS surfaces which served as the master templates for the second replica molding. The method of fabrication of the second set of PDMS stamps was similar to that of the first set. A 9:1(v/v) ratio of pre-polymer and curing agent was mixed and poured over the activated PDMS templates, followed by degassing and curing in the oven at 85°C for 1h. The second PDMS layer was peeled off from the PDMS template once it cooled down. The obtained PDMS templates were evaluated under ESEM (figure 3.26). The nanopores produced have a depth and a diameter of 200 nm of 135-150 nm, and the micropores have a depth and a diameter of 0.9-1.2 nm and 1.3 µm respectively. The results show that in terms

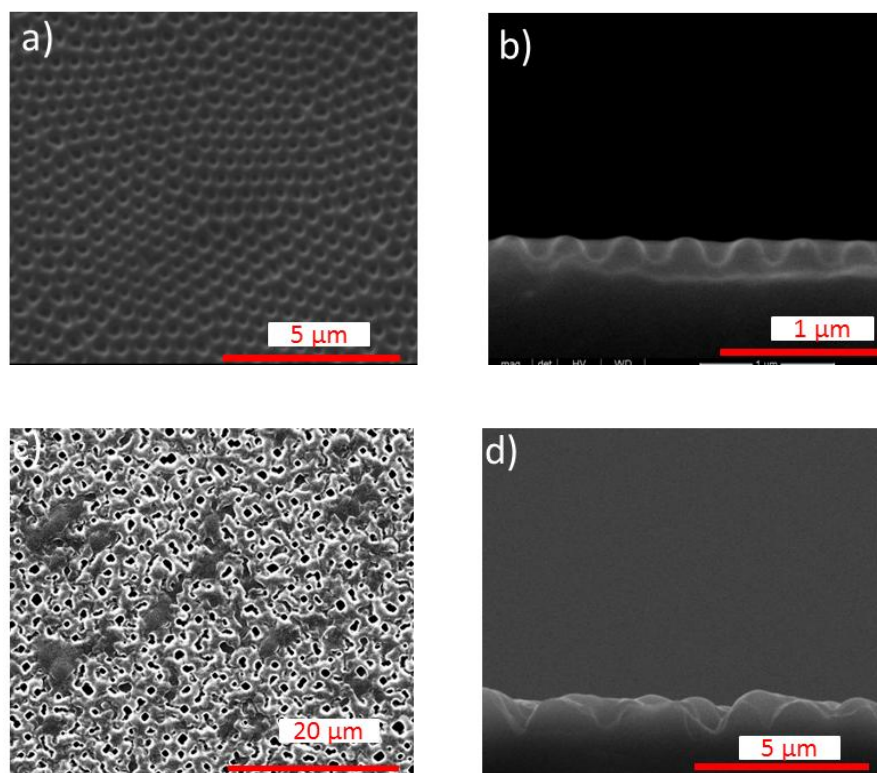


Figure 3.26: ESEM images of PDMS stamps with a) nano pores and b) micro pores.

of the pore diameter and height, the produced PDMS stamps are a good replication of master template used.

iii. Soft lithography of planar SU-8

Nanometric and micrometric structuring of planar SU-8 surfaces was accomplished by embossing the PDMS stamps patterned with pores and pillar on to the SU-8 surfaces.

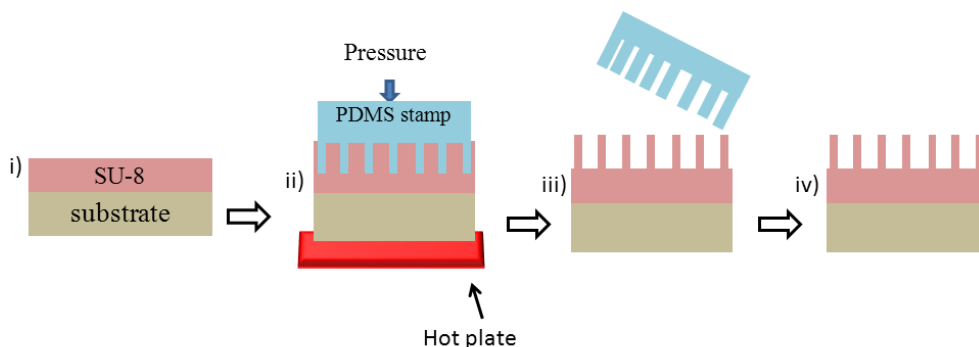


Figure 3.27: Schematic of structuring of planar SU-8 surfaces using PDMS stamp.

Figure 3.27 shows how planar SU-8 surface was structured with pillars and pores using PDMS stamp. At first, using spin coating the cleaned substrates were coated with SU-8 (figure 3.27i). Afterwards, the resist-coated substrate was kept on a hotplate and the PDMS stamp was pressed against the SU-8 surface (figure 3.27ii). Once the SU-8 was baked enough, the substrate removed from the hot plate and the PDMS stamp was peeled off (figure 3.27iii). Hence planar SU-8 surfaces with nanometric and micrometric pores and pillars were achieved (figure 3.27iv).

We have used silicon wafers as the substrate. Initially the substrates were cleaned using piranha solution and then dried at 180 °C for 40 min. Subsequently, 1ml of SU-8 was dispensed on to the cleaned substrates by spin coating. Subsequently, the substrates were kept on the hotplate set at room temperature and then the PDMS stamp with pillars was placed over the SU-8 surface. Simultaneously, to press the PDMS stamp against the SU-8 surfaces well enough, a high pressure was applied on to the PMDS by keeping a metal block of approximately ~1Kg on the top of the stamp. These substrates (with the

metal block on PDMS) were then baked at 65°C for 2 min. followed by baking at 95°C for another 3 min. At a shorter baking time than this, SU-8 solvent was not dried enough to accomplish the structuring, rather it retained in its liquid nature. In such a case, during peeling off of the PDMS stamp SU-8 was stucked on to the stamp surface as it was in liquid form.

After the baking, using a tweezers the PDMS stamp was peeled off from the SU-8 surface to release porous SU-8 surfaces. Afterwards, the obtained SU-8 structures were exposed to UV light so that the polymer surface remains unaltered during further experimental.

Structural characterization of fabricated SU-8 structures was performed using ESEM. The ESEM images of SU-8 nanopores and SU-8 micropores are shown in figure 3.28. The images verify the successful replication of featured patterns of master template on SU-8 surface. The produced SU-8 nanopores have a depth and diameter of 150 and 160 nm respectively. Likewise, the microporous SU-8 surfaces have pores having a depth and diameter of 0.9 and 1.3 μm respectively. In terms of geometry, the results show that the fabricated SU-8 surfaces retained the order, shape, and size of the PDMS stamps without any significant structural deformation.

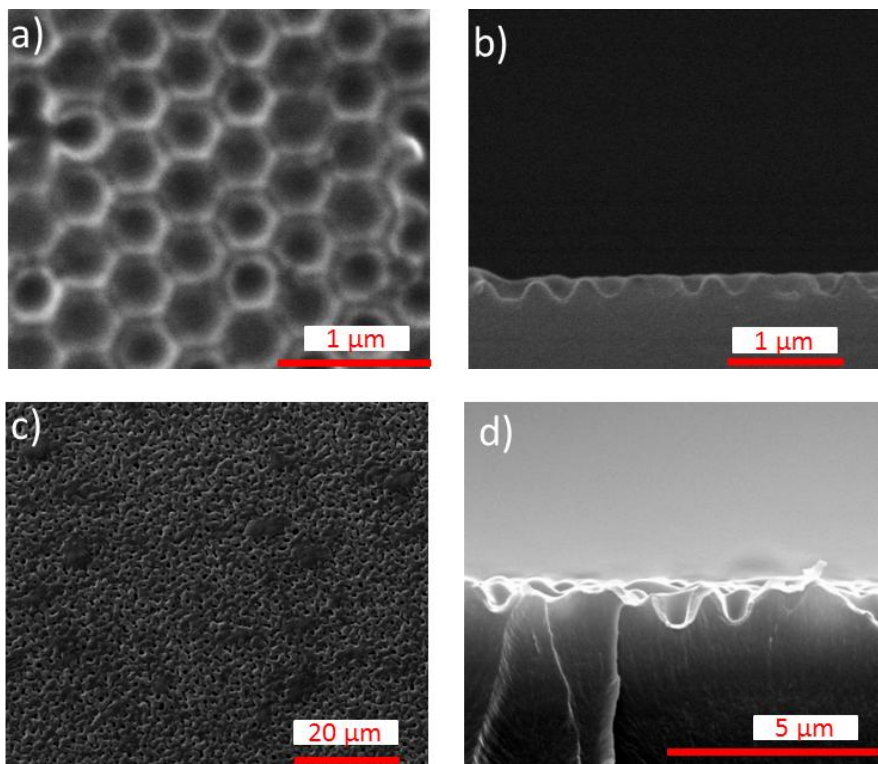


Figure 3.28: ESEM images of SU-8 (a and b) nanopores and (c and d) micropores.

Afterwards, SU-8 surfaces with micropillars and nanopillars were achieved with microporous and nanoporous PDMS stamps respectively. The structuring procedures to obtain SU-8 nano- and micropillar surfaces were same as in the case of structuring of porous SU-8 surfaces. The SU-8 structured obtained were analyzed using ESEM. The ESEM images of SU-8 nanopillars and SU-8 micropillars are shown in figure 3.29.

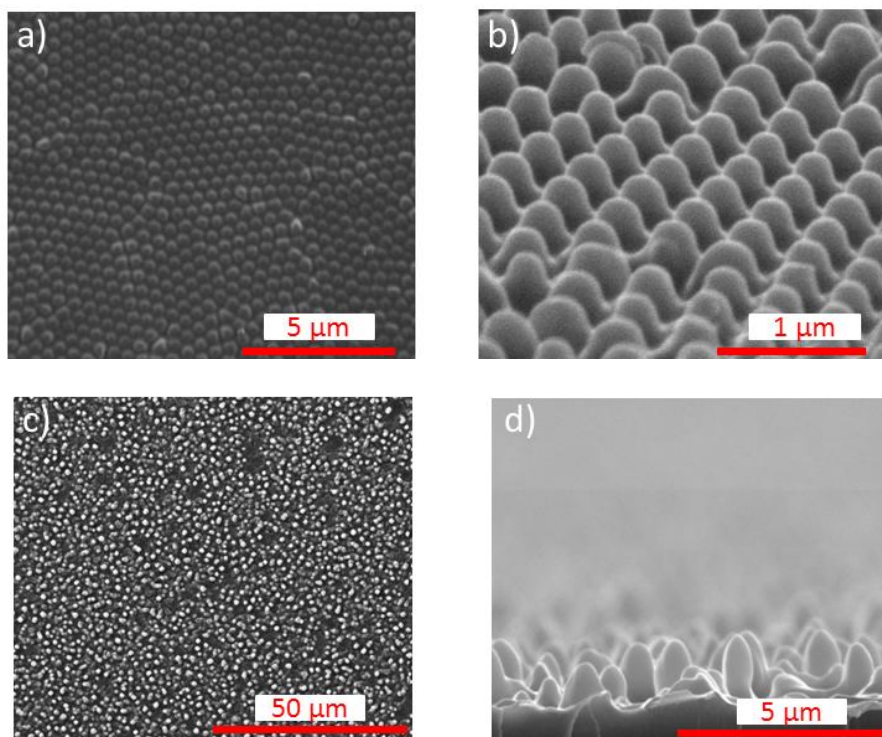


Figure 3.29: ESEM images of SU-8 (a and b) nanopillars and (c and d) micropillars.

As in the case of SU-8 nanoporous and microporous surfaces, here also a successful replication of featured patterns of master template on SU-8 surface was achieved. The nanopillars have a height of 190 nm and a diameter of 150-175 nm. On the other hand the produced micropillars have a height of 1.3 μm and diameter of 0.8-1 μm.

iv. Hybrid lithography of SU-8

Figure 3.31 depicts schematically the procedure to obtain hierarchical SU-8 patterning with hybrid lithography that combine photolithography and soft lithography. The

fabrication of SU-8 macropillars surfaces decorated with porous and pillars comprises of two steps; (figure 3.30i) soft lithography to obtain the porous and pillar pattern on a spin coated SU-8, and (figure 3.30ii) photolithography of the porous and pillar SU-8 surfaces to fabricate SU-8 macropillars. Thus by combining soft lithographic technique with photolithography, the top of the SU-8 macropillar with diameter in the order of 8 μm were decorated with nanometric and micrometric sized pores and pillars are produced (figure 3.30iii).

Initially, the patterning of polymer surface with micropores and nanopores were performed as explained in the section 3.2.3 (iii). Once obtaining the porous SU-8 surfaces, SU-8 macropillars were fabricated using photolithography as described in section 3.2.1. The difference between the fabrication of bare SU-8 macropillars and decorated macropillars is that, unlike in the first case, here the soft baking is performed with a PDMS stamp on the SU-8 surface to produce porous SU-8 surfaces. After the

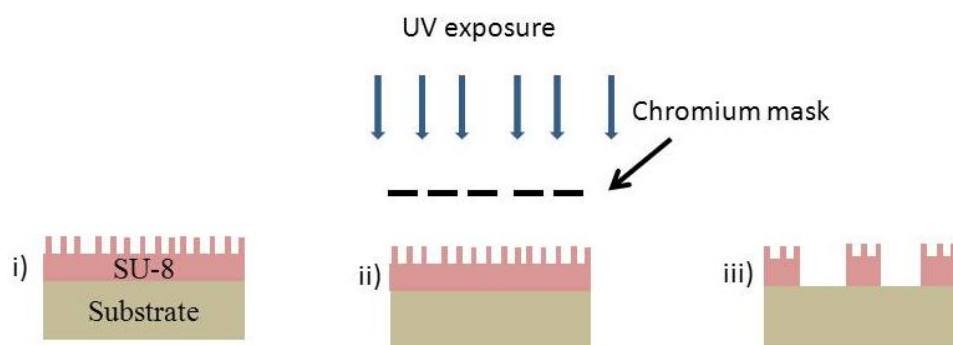


Figure 3.31: Schematic diagram representing the structuring of SU-8 macropillar surfaces with pores and pillars.

soft bake, the stamp was peeled off. Now the SU-8 surface is patterned with pores on it. After peeling off the PDMS stamps, the baked samples were then exposed under UV light through chromium mask. The exposed surfaces were then baked (PEB) and then developed. The conditions and parameters of UV exposure, post exposure bake and development remained the same as for SU-8 macropillar fabrication.

The produced SU-8 surfaces were checked by ESEM (figure 3.31). The images shows that SU-8 macropillars with micrometric and nanometric porous surfaces could be successfully fabricated using a combination of soft lithography and photolithography. But it was observed that the structure of the SU-8 macropillars fabricated on a porous SU-8 surface is different than those SU-8 macropillars produced on planar SU-8 surfaces using photolithography (section 3.2.1). Contrary to the latter case, here the macropillars produced do not have smooth side walls. This could be because; the presence of pores on the SU-8 surfaces might have caused higher diffraction of light during the UV exposure through the chromium mask. Nevertheless, we were able to produce SU-8 macropillars patterned with an ordered distribution of hierarchical pores on the macropillar surfaces.

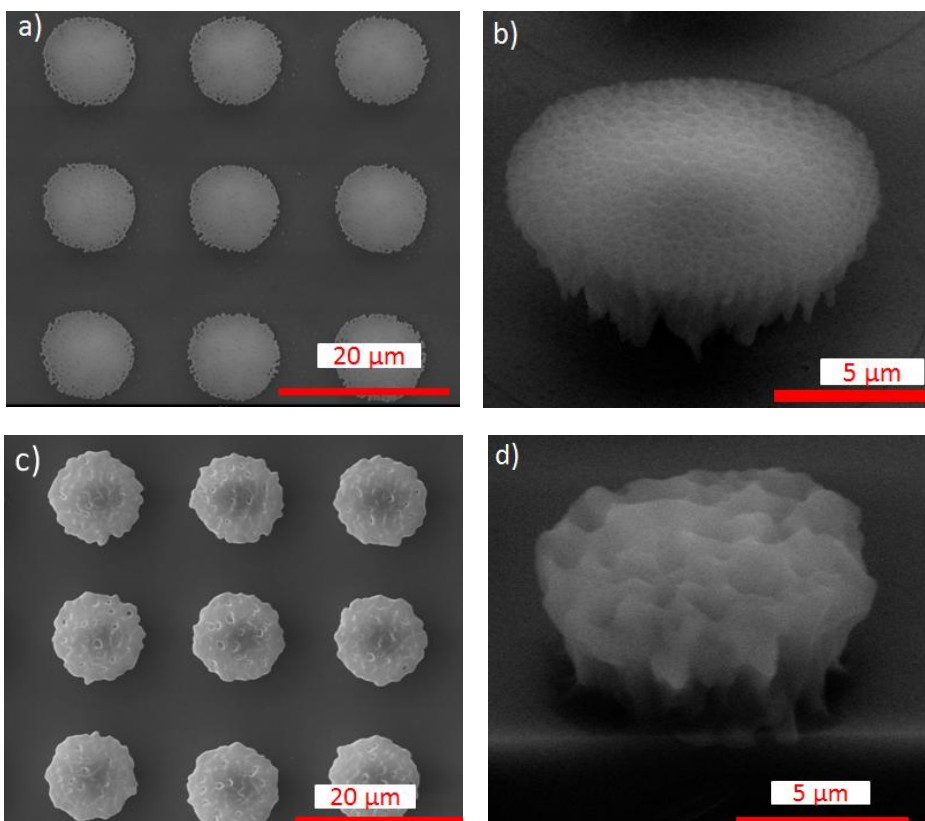


Figure 3.31: ESEM images of SU-8 macropillars with (a and b) nanopores and (c and d) micropores.

Structuring of SU-8 macropillars with nanopillars and micropillars were carried out as explained in the section above. Here we have used nano-porous and micro-porous PDMS stamps to produce hierarchical pillars on the SU-8 surfaces. Other than using different the PDMS stamps, the method of fabrication of SU-8 macropillars patterned with hierarchical pillars remained the same as in the above case. The fabricated SU-8 samples were viewed under ESEM (figure 3.32). The nanopores and micropores have a diameter around 190 nm and 1.2 μm respectively.

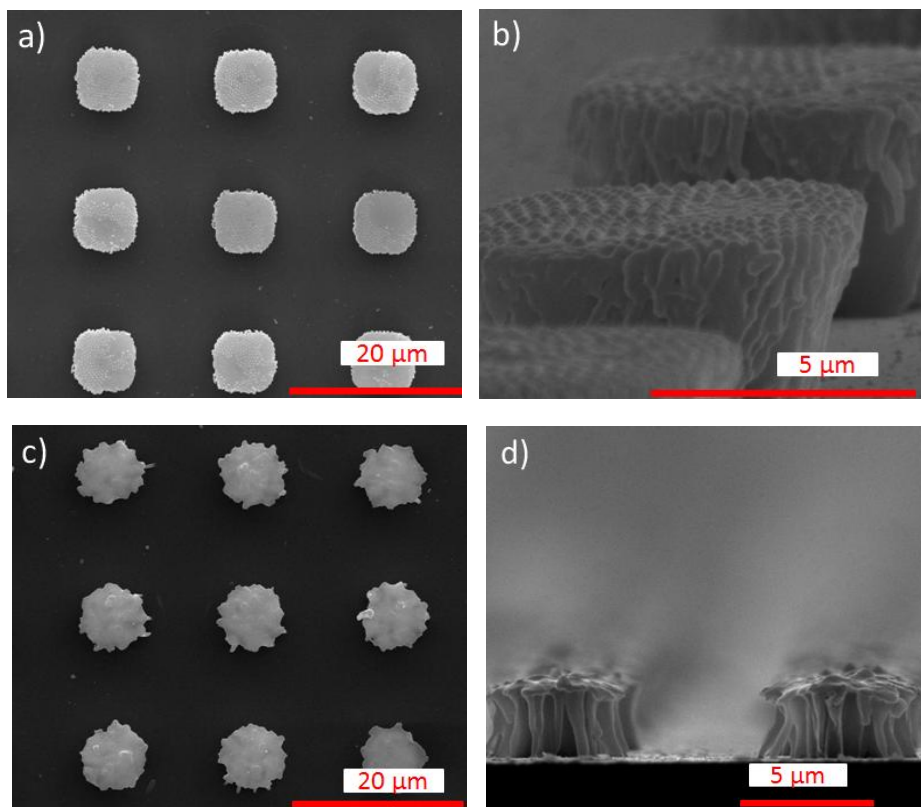


Figure 3.32: ESEM images of SU-8 macropillars with (a and b) nanopillars and (c and d) micropillars.

The results show that using a combination of soft lithography and photolithography, SU-8 macropillars surfaces patterned with nanopillars and micropillars can be achieved. As seen above, the shape of the SU-8 macropillars was observed to be not so smooth. However, the nanopillars and micropillars on the SU-8 macropillar surfaces retained the geometry as that of the corresponding PDMS stamps used. The nanopillars and micropillars have a height about 130-140 nm and 0.7-0.8 μm respectively.

UNIVERSITAT ROVIRA I VIRGILI

LITHOGRAPHIC MICRO- AND NANOSTRUCTURING OF SU-8 FOR BIOTECHNOLOGICAL APPLICATIONS

Pinkie Jacob Eravuchira

Dipòsit Legal: T 773-2015

Chapter 4

Application of Micro- and Nanostructured SU-8 for Immunosensing

The detection and quantification of biomolecules is of great interest in many fields mainly diagnostics, health care monitoring, environmental field monitoring, and drug development. Among bio-detection techniques, an immunosensor is a compact analytical device which utilizes the immunochemical affinity of an antigen for its corresponding antibody. Depending on the detection principle immunosensors can be classified as electrochemical, optical, or electrical.

Although, at present the most widespread bio-detection techniques comprise of labeling of the biomolecules, great effort is being applied to develop label-free bio-detection techniques [Fang 2011, Dong 2010]. Unlike label-free biosensing technique, label-based technique involves time consuming and tedious processing for labeling of samples prior to the measurements [Lichlyter 2003]. Thus the diverse advantages of label-free biosensing techniques such as ease of sample preparation, ease of handling, sensitivity, and cost effectiveness make them preferred over its counterpart, label-based techniques.

Referring to the label-free biosensing methods, a wealth of optical and photonic techniques is available. Surface plasmon resonance [Sipova 2013, Huang 2009], localized SPR [Guo 2012], interferometers [Peter 2011, Kyu-shil 2010], ring resonators [Muhammad 2013, Yuze 2011] and fiber-optic probes [Sai 2010] are couple of the well-known opto-electronic label-free sensing methods whose operating principle is related to the high sensitivity of evanescent waves to the surface changes of the measuring platform.

Recently, studies shows that photoluminescent based biosensors have drawn much attention [Budz 2010, Duplana 2011, Viter 2012]. Although SU-8 finds various applications in biotechnology field, the high photoluminescence it has in the near UV and visible wavelength limits its use in most of the biological applications, especially for studying fluorophore tagged analytes. Lately, studies have reported on the reduction of photoluminescence of SU-8 by coating gold nanoparticles on SU-8 surface [Cao 2012] for biological applications.

In this work we try to exploit the photoluminescence property of SU-8 to fabricate a cost-effective and reliable tool for immunosensing. We study the possibility of using SU-8 as a platform for label-free immunosensing, where the transduction mechanism is the reduction in photoluminescence of SU-8 upon the attachment of an analyte to a functionalized sensing surface. The sensing mechanism is demonstrated using a model antigen-antibody pair (aIgG and IgG from goat serum), where sensor selectively detect IgG. One of the objectives of our work is to prove that the reduction of SU-8 photoluminescence with the binding of analyte on to their ligands immobilized on the SU-8 structure can be a tool for sensing and in particular for immunosensing.

When it comes to the structure of a sensing platform, micrometric or nanometric structuring of the active area of biosensors has proved to be a method that improves the sensing efficiency [venkataramani 2006, Holgado 2010]. The second objective of this work is to evaluate the ability of the various structured SU-8 sensing platforms for IgG sensing. The structures include SU-8 macropillars, micropillars, nanopillars, micropores, nanopores and finally SU-8 macropillars decorated with nanometric and micrometric pillars and pores on its top surface. All these structures were fabricated as described in chapter 3.

The first section of this chapter (4.1) explains on the experimental procedures of functionalization of the SU-8 surfaces with the aminosilanes and glutaraldehyde followed by the immobilization of the antigen-antibody pair on to the functionalized surfaces. Subsequently, section 4.2 present the results on the photoluminescent (PL) measurements carried out on planar and macro-structured SU-8 surfaces. Afterwards, section 4.3 shows the PL measurements performed on hierarchical structured SU-8 surfaces, which includes porous and pillar SU-8 surfaces. Finally, in 4.4 a comparison study on the SU-8 PL reduction on all types of SU-8 surfaces we have studied is presented.

4.1. Surface modification of SU-8 surfaces

As mentioned above, in our study the ability of SU-8 surfaces to function as immunosensors is proved by the selective detection of anti-immunoglobulin G (IgG) by an immunoglobulin G (aIgG) functionalized SU-8 surface. In order to show the ability

of SU-8 to act as an immunosensor, it is necessary to provide binding sites for the analyte (IgG). Consequently, the surface of SU-8 must be first functionalized with the corresponding binding molecule, aIgG. In order to immobilize aIgG on the SU-8 surface, this must be properly functionalized. In this section, this process of functionalization is described and its effect on the PL of the SU-8 is studied.

The immobilization of biomolecules on to any surfaces is promoted by either a physical adsorption or a covalent bonding between the samples and the substrate surfaces. A mere physical adsorption of biomolecules on any surface is easy to break and thus is easy to remove the molecules that are physically adsorbed on to the sample surface. Therefore, due to the increased adhesion stability of biomolecules on to the polymer surface always a covalent bonding is preferred over a physical adsorption. Studies show that a covalent binding of biomolecules on to the SU-8 surface can be obtained by modifying the SU-8 surface to have one of the functional groups, such as CHO, or SH [Deepu 2009, Joshi 2007a, Tao 2008].

Therefore in our work, in order to obtain a covalent bonding between aIgG and SU-8, SU-8 surfaces were functionalized with 3-aminopropyltrimethoxysilane (APTMS) and glutaraldehyde (GTA) before the IgG immobilization.

In this part the first subsection (4.1.1) explains on how the functionalization of SU-8 surfaces with APTMS and GTA was carried out. Following this, in the section 4.1.2, the results of fourier transform infrared spectroscopy measurements are provided, which prove the presence of APTMS and GTA on SU-8 surfaces. The subsequent section (4.1.3) describes on the method of immobilization of aIgG and IgG on to APTMS-GTA functionalized SU-8 surfaces. To observe the distribution of aIgG-IgG over the SU-8

surfaces, fluorophore tagged analyte was immobilized on to SU-8 macropillars and were observed using fluorescent microscope. Section 4.1.4 shows the microscopic image of aIgG-IgG immobilized SU-8 macropillars.

4.1.1. Functionalization of SU-8 surfaces with APTMS and GTA

All the SU-8 surfaces we have used in this work where functionalized with APTMS and GTA as described here. Initially, to promote the adhesion of aminosilane to the epoxy group, SU-8 samples were hydroxylated with 0.1M NaOH and 1M HCl for 30 s. each. The hydroxylation was performed as follows. At first, SU-8 samples were dipped in NaOH for 30 s. followed by dipping it in HCl solution for 30 s. and then washed with DI H₂O and ethanol and then dried with nitrogen. This surface pretreatment modifies the epoxy group and generates hydroxyl groups (-OH) on SU-8 surface.

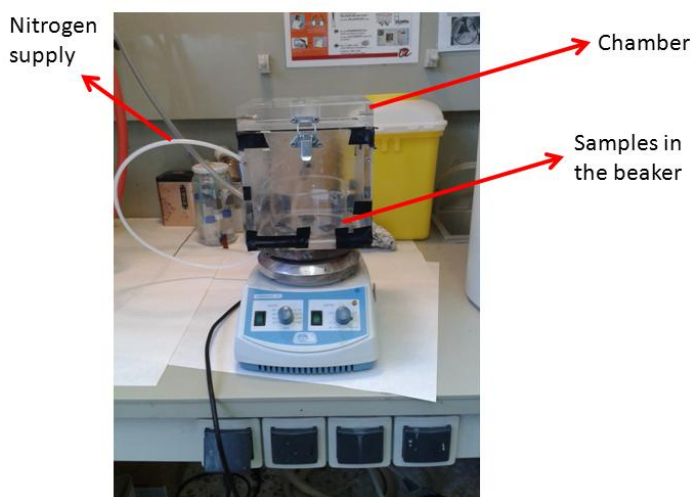


Figure 4.1: Digital image of the set-up used for silanization.

After the hydroxylation, to obtain the amine groups on the SU-8 surfaces, the hydroxylated SU-8 samples were treated with APTMS and GTA [Joshi 2007a]. Initially, silanization of SU-8 was carried out with APTMS for 2 hr. in nitrogen atmosphere. The silanization was performed in an air tight homemade chamber (figure 4.1). The chamber has a lid in the top side, and the middle of this lid is equipped with a rubber stopper having a diameter of approximately 0.5 cm. Apart from the lid, the box is facilitated with a connection tube to which the nitrogen supply can be connected.

After preparing the setup, the hydroxylated SU-8 samples were placed in a glass beaker along with a magnetic stirrer. The beaker was then kept inside the chamber and then the lid was closed tightly. Then, in order to create an inert atmosphere, nitrogen (2 sccm) was allowed flow inside the chamber for 10-12 min.

Afterwards, 20 ml ethanol (99.99%) and 50 μ l APTMS were poured into the beaker containing samples. The samples were then allowed to immerse in 2.5% (v/v of APTMS and ethanol) of silane solution mixture for 2 h. The solution was stirred continuously all through the reaction. This surface treatment renders NH_2 group on the hydroxylated SU-8 surfaces (figure 4.2c).

After 2 h., to remove the unbounded silane molecules on the SU-8 surfaces, the silanized samples were rinsed with ethanol and water for 5 min. each. To remove the moisture content from the cleaned samples, they were then dried at 110 °C for 10 min. in an oven. Finally, to obtain the aldehyde group on the silanized SU-8 surface, the dried APTMS-modified SU-8 samples were treated with 10% GTA (anhydrous 10% in ethanol) for 1 h. at room temperature (figure 4.2d). This was done by immersing the silanized SU-8 surfaces in GTA solution. After 1 h., the excess amount of GTA was

and an aperture size of 3 mm. The spectra were taken in the range of wavenumbers between 800 and 2000 cm^{-1} with a resolution of 4 cm^{-1} .

The ATR spectra of bare SU-8, SU-8 functionalized with APTMA and finally APTMS-GTA modified SU-8 are shown in figure 4.3. The FTIR measurements were performed on SU-8 coated on glass substrate and glass was used as a background for the measurements. The red, blue, and green spectrums represent the ATR spectra of bare SU-8, SU-8 functionalized with APTMS, and finally APTMS-GTA modified SU-8 surface respectively. Many functional groups which are present in SU-8 are also present in the used linkers (APTMS and GTA). However, there are certain functional groups that are specific for SU-8, APTMS and GTA. Therefore it is possible to distinguish the vibrational modes corresponding to APTMS and GTA, and thus confirming the functionalization achieved.

Comparing the spectra of bare SU-8 and SU-8 modified with APTMS helps to notice the additional peaks corresponding to vibrational modes from amine group on the APTMS-SU-8 spectra. The peaks at 1640 and 1560 cm^{-1} are assigned to bending modes vibrations of $-\text{NH}_2$ in APTMS. The vibrational peak from $-\text{C-N-}$ is observed at 1320 cm^{-1} . The presence of APTMS was further confirmed with the vibrational peaks at 3285 and 3350 cm^{-1} which is in the higher wavenumber region. These bands are attributed to $-\text{NH}_2$ vibration. After further modification of APTMS with GTA, changes were appeared in the spectrum. The bending vibrations at 1720 cm^{-1} show the presence of aldehyde group ($-\text{CHO}$) in the GTA modified SU-8 surface. Thus the FTIR-ATR spectra confirm the presence of $-\text{NH}_2$ and $-\text{CHO}$ bands which were obtained with the functionalization of hydrolyzed SU-8 surfaces with APTMS and GTA respectively. Thus using FTIR-

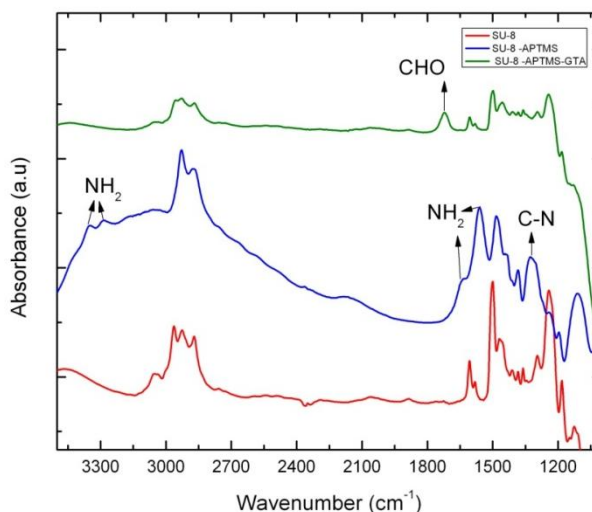


Figure 4.3: ATR spectra of bare SU-8 (red), APTMS (blue) and GTA (green).

ATR the presence of specific chemical groups after functionalization of sample substrates with APTMS and GTA were identified.

4.1.3. Immobilization of aIgG and IgG on surface-modified SU-8

Functionalization of SU-8 with APTMS and GTA was performed to provide a covalent bonding between aIgG and SU-8 surfaces. After the functionalization of SU-8, aIgG was immobilized on to those modified SU-8 surfaces. aIgG functions as the binding site for the analyte, IgG, and the antibody-antigen interaction takes places during the immobilization of IgG on to SU-8 surfaces with aIgG. This aIgG-IgG immobilization step is performed to prove the ability of SU-8 to functions as an immunosensor.

Both antigen and antibody were in liquid form. In order to produce sample (aIgG and IgG) solutions with various concentrations, they were diluted in phosphate buffered saline (PBS, pH 7.4) solution. Once the protein samples were prepared, there were allowed to immobilize on to the APTMA-GTA functionalized SU-8 surfaces. The procedure of aIgG and IgG immobilization on all the SU-8 surfaces (planar and hierarchical SU-8) were the same in our studies.

Initially aIgG was immobilized on to the APTMS-GTA functionalized SU-8 surfaces. The immobilization was achieved by incubating aIgG on SU-8 surfaces for 1 h. in humid atmosphere at room temperature (figure 4.4a). In order to create a humid atmosphere, water wetted tissue papers were spread over in a petri dish. Then the functionalized SU-8 surfaces were placed on the top of the tissues. Subsequently, aIgG was dropped all over the sample surface with the help of a pipette. And finally the petri dish was covered with another dish having water wetted tissues and left it unmoved for an hour.

After incubating the samples with the antigen for 1 h., the unbounded molecules were removed by rinsing the aIgG functionalized SU-8 surfaces with a solution mixture of 5% of Tween 20 in PBS. Following this, the samples were gently rinsed with water and then dried with air.

Once the SU-8 was functionalized with the aIgG, to activate the antigen-antibody interaction the analyte (IgG) was immobilized on to the antigen coated SU-8 surface (figure 4.4b). This immobilization step is where the selective binding of IgG occurs. The immobilization of IgG was carried out in the similar fashion as for the aIgG. It was accomplished by incubating IgG on aIgG coated SU-8 surfaces for 1 h. in humid

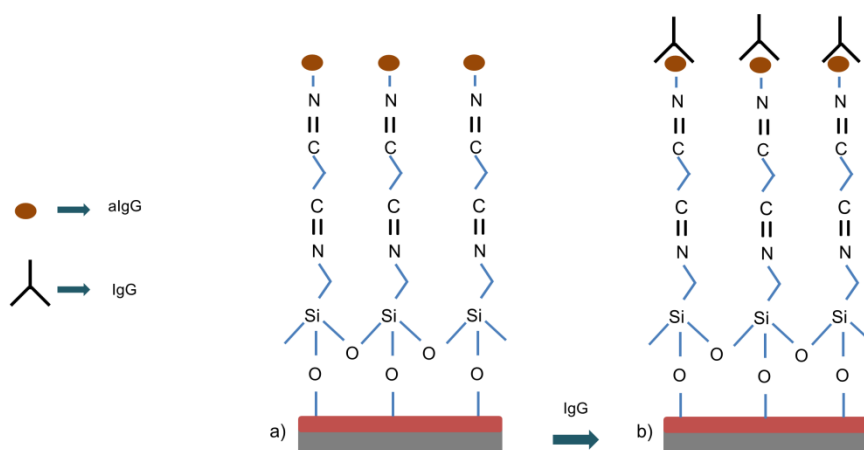


Figure 4.4.: Schematic representation of the immobilization of (a) aIgG, and (b) IgG, on to APTMS-GTA functionalized SU-8 surface.

atmosphere at room temperature. Then the surface was thoroughly rinsed with the solution mixture of PBS and Tween 20, followed by water and then dried with air. Figure 4.4 shows a schematic representation of the immobilization of aIgG and IgG on to SU-8 surface modified with APTMS-GTA.

4.1.4. Labelling of IgG with Rhodamine

Furthermore, to visualize the distribution of biomolecules immobilized on SU-8 surfaces using fluorescence microscopy, rhodamine (rhodamine b isothiocyanate mixed isomers) labeled IgG was immobilized on the SU-8 macropillars. IgG was immobilized on to aIgG coated SU-8 surfaces. Labelling of IgG with rhodamine was performed as follow. Initially a mixture of 5 mg/ml of rhodamine in dimethyl sulfoxide (DMSO) solution was prepared by dissolving 5 mg of rhodamine in 1 ml of DMSO solution. In

order to achieve the complete dissolution of rhodamine in DMSO, the solution mixture was stirred with the help of a magnetic stirrer for 5 min. Subsequently, 1 mg/ml of IgG in PBS was prepared. Then, 100 μ l of fluorophore solution was added drop by drop to 1 ml of IgG solution. Mixture was left to stir until they are miscible. After obtaining the fluorophore labeled IgG solution, they were deployed on to the aIgG functionalized SU-8 surfaces. The immobilization was carried out in humid atmosphere for 1 h at room temperature.

Fluorescence microscopic image were obtained using a NIKON Eclipse TE 2000 (Melville, NY). The images were captured with inverted microscope equipped with a 40x (Nikon Plan Fluor, N.A 1.30) lens. The images were excited with UV filter at a wavelength of 543 nm and the emission was at 550-650 nm for rhodamine labeled protein samples. The images were processed using NIS elements software [Nikon imaging software]. Figure 4.5 depicts the fluorescence image.

The fluorescence images were taken after the immobilization of rhodamine labeled IgG on aIgG functionalized SU-8 macropillars on silicon substrate. The results show that the biomolecules are uniformly distributed over the macropillars without any aggregation. Furthermore the images prove that the molecules are attached on to the SU-8 surfaces and not on the substrates.

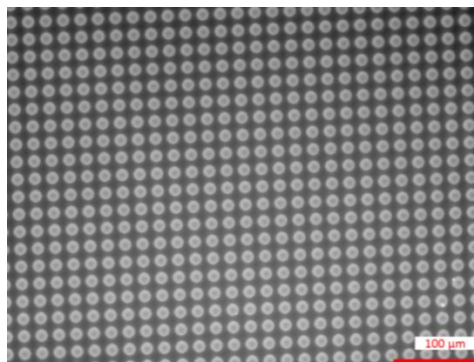


Figure 4.5: Fluorescence image of aIgG-IgG immobilized SU-8 macropillars.

4.2. Immunosensing by reduction of photoluminescence in SU-8 planar and macropillar surfaces

In this section the experiments undertaken to demonstrate the possibility of using the PL of SU-8 as the basis of an immunosensor are described. The main goal of the experiments is to evaluate the decrease in the PL from a SU-8 planar or macrostructured film after each step of functionalization and after the attachment of aIgG to IgG, which is the step in which the sensing is performed. In order to show the ability of the functionalized SU-8 as immunosensor, PL spectra of SU-8 with APTMS-GTA functionalization, with aIgG immobilization and with IgG immobilization were measured. The change in PL of SU-8 with the selective binding of IgG on to aIgG immobilized SU-8 surfaces is the basic principle of this optical immunosensor. The measurements were performed on two types of SU-8 surfaces; planar and macropillars SU-8 surfaces. Initially all the PL measurements were performed on planar SU-8 surfaces, which served as the reference measurements. The study was then extended by

measuring the PL of macro-structured SU-8 sensing platforms. These measurements give an insight to the effect of reduction in PL with 3-D structuring of the sensing platforms.

Apart from studying the effect of structuring of sensing platform, we have compared the dependence of sensor substrate for sensing ability by fabricating SU-8 surfaces on two types of substrates, silicon wafers and glass slides. The fabrication of all the SU-8 structures is explained in section 3.2.

Section 4.2.1 presents the PL measurements on planar and macropillar SU-8 surfaces after the surface modifications. Following this, in 4.2.2 a comparison study on the change in PL of planar and macropillar SU-8 surfaces are presented. Finally section 4.2.3 presents the sensing response of SU-8 macropillar surfaces at various IgG concentrations.

4.2.1. Photoluminescence reduction on planar and macropillar SU-8 surfaces after each surface treatment

The PL measurements were performed using a fluorescence spectrophotometer (Photon Technology International Inc, Spain), which has a Xe lamp as a light source. An excitation slit width of 5 nm and emission slit width 2 nm was used for the measurements. All the measurements were performed at room temperature.

A set of three SU-8 planar and macropillar sample surfaces each on silicon and glass substrates were investigated. The concentration of antigen (aIgG) and antibody (IgG) was 80 $\mu\text{g}/\text{ml}$ in PBS each in both the measurements. In all the cases, the PL

measurements were taken on bare SU-8 surface, APTMS-GTA functionalized SU-8 surface, aIgG immobilized SU-8 surface, and finally on SU-8 surface after the aIgG-IgG interaction.

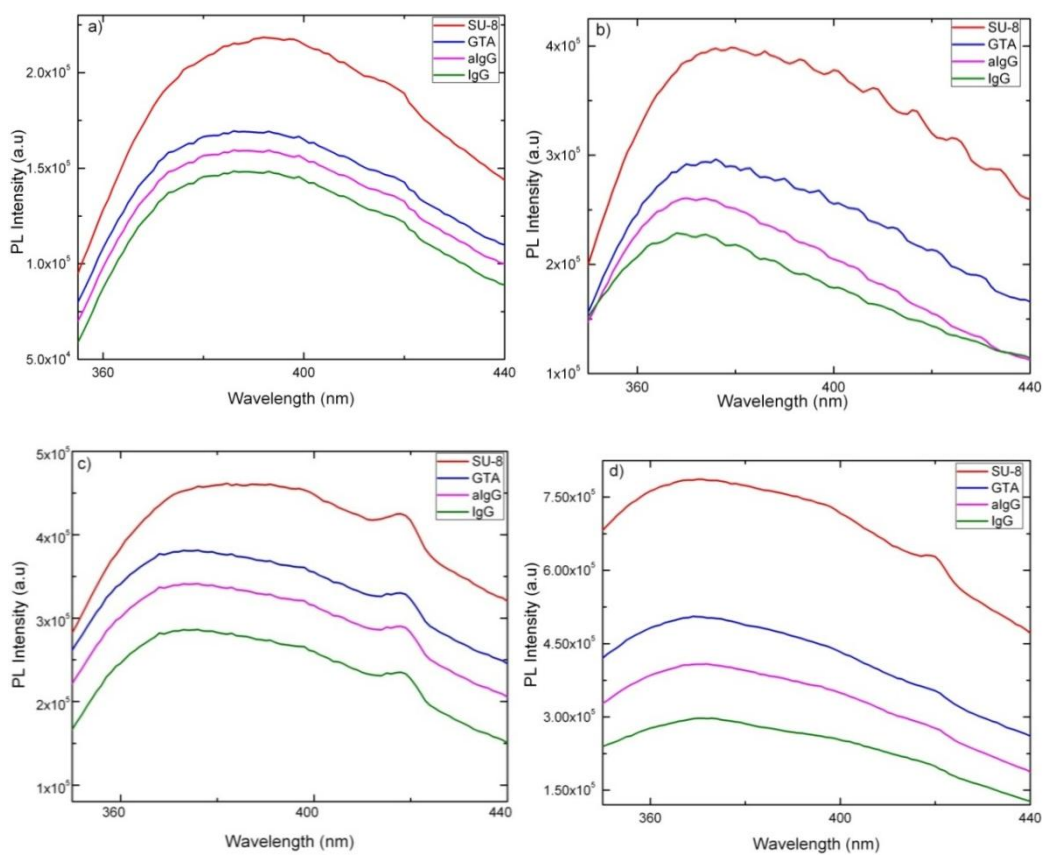


Figure 4.6: PL spectra of planar (a and b) and SU-8 macropillars (c and d) after each surface treatment. (a and c) corresponds to the PL spectra of SU-8 on glass substrates and (b and d) corresponds to those on silicon substrates.

At first, the PL measurements were performed on planar SU-8 surfaces. The PL spectra of planar SU-8 on glass and silicon substrates at various stages of surface modifications are shown in figure 4.6 (a and b). The spectral results show that after each surface modification a gradual decrease in the SU-8 PL occurs.

After obtaining the PL spectra of planar SU-8, to study the dependence of change in PL with the surface structuring of the active area of the sensing platform, further PL measurements were carried out with SU-8 macropillar surfaces. The fluorescence spectra of macro-structured SU-8 surfaces on glass and silicon substrates after each surface modification is shown in figure 4.6 (c and d). The red and blue lines correspond to bare SU-8 surface, and APTMS-GTA modified SU-8 surface modified respectively. The pink and green lines represent the PL spectra of SU-8 surface immobilized with aIgG and IgG respectively.

The results show that at an absorption wavelength of 325 nm, SU-8 shows a peak photoluminescence emission at a wavelength around 380 nm. Besides, from figure 4.6 it can be observed that both planar and macropillar surfaces show a similar fashion of change in PL with each of the surface modification steps. In both cases a gradual decrease in the SU-8 PL is observed.

Besides, the specificity of aIgG was confirmed by measuring the PL spectra of SU-8 surface after immobilizing bovine serum albumin (BSA) on to an aIgG functionalized SU-8 surface. BSA solution of 80 $\mu\text{g}/\text{ml}$ in PBS was incubated on to the SU-8 surface immobilized with aIgG in a humid atmosphere at room temperature for 1 h. The PL intensity of the SU-8 surface before and after immobilizing BSA remained unaltered.

4.2.2. Comparison of photoluminescence of SU-8 planar and macropillar surfaces

Since the observed PL reduction is systematic and appears in all cases, especially in the detection step, permits us to define a metric called R (equation 4.1). The metric R (%) stands for the percentual reduction in the SU-8 PL after the attachment of aIgG to IgG. $I_{\max, aIgG}$ and $I_{\max, IgG}$ represents the maximum PL intensity of SU-8 after aIgG and IgG immobilization respectively.

$$R(\%) = 100 \times \frac{I_{\max, aIgG} - I_{\max, IgG}}{I_{\max, aIgG}} \quad (4.1)$$

The bar graph in figure 4.7 depicts the comparison of PL reduction rate when planar and macro-structured sensing platforms are used. Furthermore, the comparison studies on the dependence of R with the two types of substrates (glass and silicon) used is shown in this bar graph.

PL reduction after the aIgG- IgG interaction on each types of sensing platforms (planar and macropillars on both substrates) are indicated in the graph. The results show that the amount of reduction is different for different substrates (glass and silicon) and different for both planar surfaces and macropillar structures.

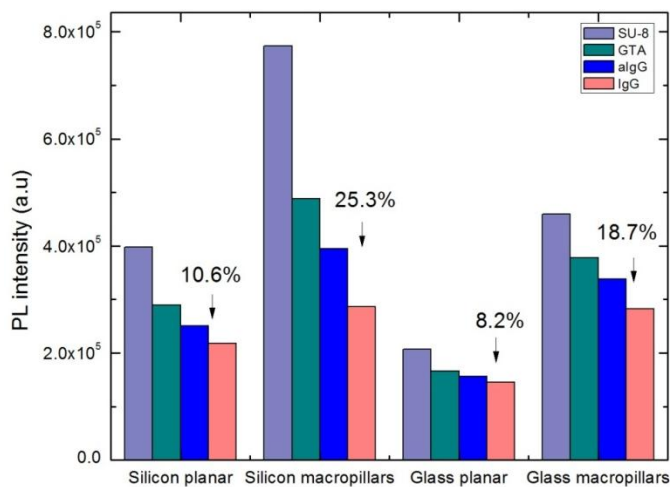


Figure 4.7: Comparison of reduction in photoluminescence of planar and macro-structured SU-8 on both silicon and glass substrates.

Planar SU-8 platforms on glass substrate gives an R value of 8%, while a macro-structured sensing platform on glass substrates shows an R amount of 18%. Similarly, a planar and macro-structure sensing surface on silicon substrate gives an R of 10% and 25% respectively. The above measurements on planar and macro-structured SU-8 surfaces clearly show an increased rate of PL reduction with the macro-structuring of sensing platform. The R is around 50% higher when the sensing platform is patterned with macropillar array than when a planar surface served as the sensing surface. This fashion is observed on both glass and silicon substrates. Thus this study proves the dependence of sensitivity on the total active surface area of an immunosensor, and thus in turn it can be seen that the sensing efficiency can be increased by modifying the

active area by macro-structuring, without increasing the total dimension of the sensing surface.

Furthermore, from the results on both planar and macro-structured SU-8 surfaces on silicon and glass substrates it can be concluded that the R is always higher when a silicon substrate is used. Thus it can be observed that the PL reduction rate is higher when the sensing surface is on silicon substrate than when on glass. This could be attributed to the higher reflection of silicon substrate than a glass substrate. So we can conclude that the use of silicon as a substrate for SU-8 permits a bigger sensitivity than using glass as a substrate.

4.2.3. Sensing response with IgG concentration on SU-8 macropillar surfaces

The dependence of reduction in PL with varying the concentration of IgG on aIgG immobilized SU-8 macropillar surface was also studied. The measurements were done on SU-8 macropillar surfaces on glass and silicon substrates. An aIgG concentration of 80 $\mu\text{g/ml}$ in PBS was kept constant for all the measurements and four different concentrations of IgG such as 10, 20, 40 and 80 $\mu\text{g/ml}$ in PBS were used for the study. Figure 4.8 shows the dependence of R with varying IgG concentration on SU-8 macropillars which are fabricated on silicon and glass substrates. The blue and red lines represent the R when silicon and glass substrates are used respectively.

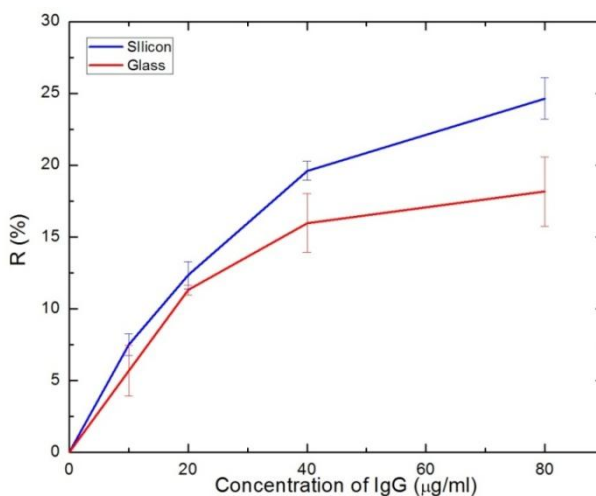


Figure 4.8: Change in photoluminescence reduction with a varying concentration of IgG.

The X-axis represents the concentration of analyte in $\mu\text{g/ml}$ and the Y-axis represents the PL reduction rate in percentage. The results show that the R increases with the increase in IgG concentration. As the IgG concentration increases from 0-80 $\mu\text{g/ml}$, the R was correspondingly varied from 7.5% to 24.7% with an error ranging from 1.44% to 0.67% on silicon substrate. Likewise, when the sensor substrate was glass the R was increased from 5.7% to 18.3 % within an error of 0.35% to 2.41%. Furthermore, it can be observed that both the substrates show a steeper slope at a lower concentration and a tendency to saturate at higher IgG concentrations. This pattern could be due to the unavailability of aIgG binding sites for IgG at higher concentrations.

4.3. Immunosensing by reduction of photoluminescence in SU-8 hierarchical structures.

After demonstrating the possibility of immunosensing by SU-8 PL reduction, we have extended our studies to find the possibility of applying the same sensing principle to more complex SU-8 structures. The structures includes i) planar SU-8 surfaces patterned with nanometric and micrometric pillars, ii) planar SU-8 surfaces patterned with nanometric and micrometric pores, iii) SU-8 macropillars patterned with nanometric and micrometric pillars on it, and iv) SU-8 macropillars patterned with nanometric and micrometric pores on it. Thus this study gives an insight to the effect of reduction in PL with hierarchical 3-D structuring of the sensing platforms. The structuring of all these four types of surfaces were achieved using lithographic technique as introduced in chapter 3.

Except the surface textures of the sensing platforms, the mode of preparation of the samples (functionalization and immobilization) and the experimental procedure remained the same as that of planar and macropillar SU-8 surfaces. This allow us to compare the results of these structures with the previous results (planar and macropillar SU-8).

As an illustration of the PL measurements carried out for such samples, figure 4.9 shows the PL spectra of SU-8 macropillar surfaces decorated with micropillars, and micropores after each surface treatments. The measurements included in figure 4.9 are

representative of all the set of PL spectra measurements, so it would be redundant to include all of them.

At first, the PL spectra of planar SU-8 surfaces patterned with hierarchical pillars and pores were measured. The spectral pattern was similar to that of planar and macropillar SU-8 surfaces. In all the four cases the maximum PL was around 380 nm and PL reduction was observed with each surface treatment.

After studying planar surface patterned with pores and pillars, we have investigated the PL reduction of SU-8 macropillar surfaces structured with nanopores, micropores, nanopillars and micropillars. Interestingly a shift in the PL maximum was observed in the PL spectra of hierarchically structured SU-8 macropillar surface. Instead of 380 nm, the PL maximum was observed at a wavelength around 420 nm. Nevertheless, the spectra show that in all the four cases the PL of SU-8 was decreased with each surface modification.

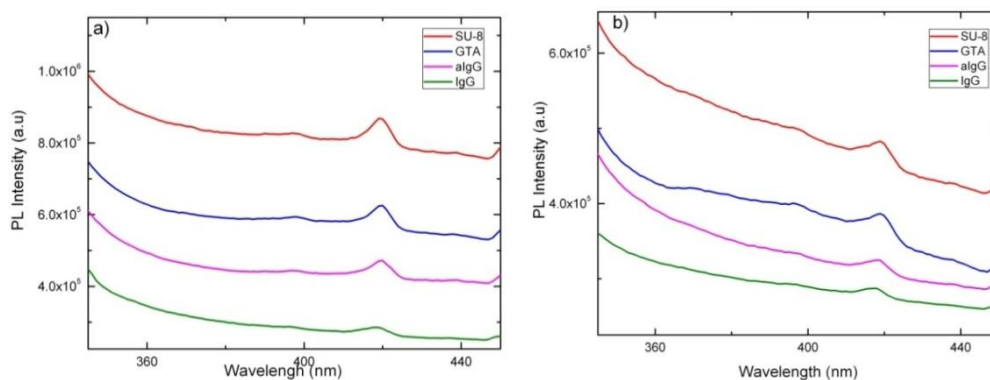


Figure 4.9: Photoluminescence spectra of SU-8 macropillars surfaces patterned with, (a) micropillars, and (b) micropores.

This patterned was observed in both nanometric and micrometric structures. Furthermore, tough not so higher, it was observed that the reduction rate of a microstructures sensing surface is always higher than its nanostructured counterpart. This pattern was the same for both porous and pillar surfaces.

A summary of the PL reduction (R), which is the measure used for IgG detection, with various SU-8 structuring is shown in the figure 4.10. The structures includes planar SU-8, SU-8 macropillars, planar SU-8 patterned with micropillars, nanopillars, micropores, and nanopores, and finally, SU-8 macropillars patterned with micropillars, nanopillars, micropores, and nanopores.

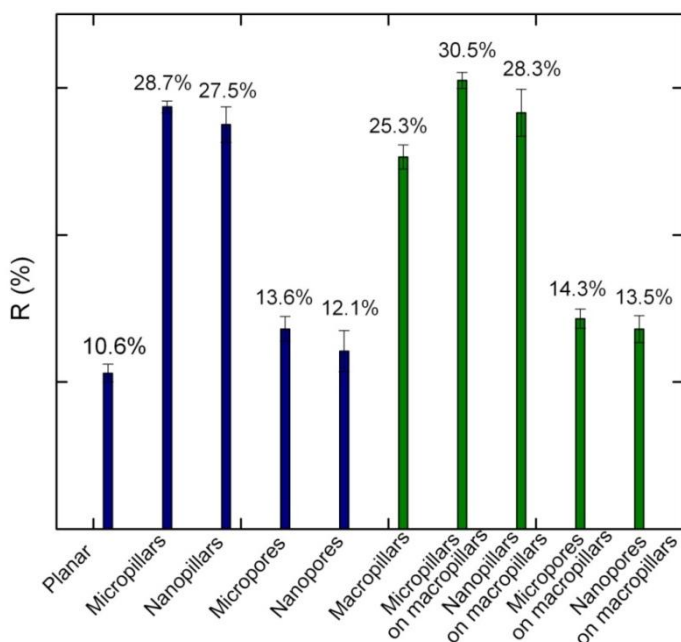


Figure 4.10: Summary of measured PL reduction, R, for the different kinds of SU-8 surfaces.

It can be seen from the graph that in all the cases a structured SU-8 surface gives higher PL reduction than a planar SU-8 surface. The lowest R was given by planar SU-8 surfaces and the highest R was obtained with macropillar SU-8 surfaces patterned with micropillars.

When comparing the macro-structured surfaces, a higher reduction is shown by micropillars patterned with micropillars (30.5%), and the lowest reduction is shown by bare macropillars which is 25.3%.

When it comes to planar SU-8 surfaces structured with pores and pillars, the reduction is bigger for surfaces patterned with pillars than with pores. SU-8 surfaces with nanopillar and micropillars give a reduction rate of 27.5% and 28.7% respectively, while nanoporous and microporous SU-8 surfaces shows an R value of 13.6% and 12.1% respectively.

Further, when comparing all the structured surfaces, SU-8 surfaces patterned with macro-, micro- and nanopillars show a higher PL reduction than a micro- and nanoporous SU-8 surface. This fashion was observed also in the case of SU-8 macropillars patterned with pores and pillars, where the PL reduction is bigger for pillar surfaces than for its counterpart porous surfaces.

SU-8 macropillars with micropillar and nanopillars have an R of 30.5% and 28.3% respectively, and SU-8 macropillars with micropores and nanopores shows an R of 14.3% and 13.51% respectively. Thus from all the above results, it can be observed that the highest R was shown by SU-8 macropillars patterned with micropillars and nanopillars.

All these measurements are a proofs of the concept that R can be used as a sensing transduction parameter for a label-free optical immunosensing. Moreover, the results reported here help also to understand the effects of hierarchical structuring the SU-8 surfaces in their sensing performance.

UNIVERSITAT ROVIRA I VIRGILI

LITHOGRAPHIC MICRO- AND NANOSTRUCTURING OF SU-8 FOR BIOTECHNOLOGICAL APPLICATIONS

Pinkie Jacob Eravuchira

Dipòsit Legal: T 773-2015

Chapter 5

Laser Lithographic Patterning of Silicon Wafers

The works discussed in this chapter were done in collaboration with two of the research groups (Minos and Nephos) among EMaS. The main objective of these works is to investigate on how lithography is a useful tool in different applications developed within the other two groups and EMaS. During the collaboration, we have performed the laser lithographic patterning of silicon wafers to produce various structures such as interdigital electrodes and inverted micropylramid arrays. The produced structures were then modified and used for various applications, such as for gas sensing and in biotechnology. Description on the patterning of silicon wafers and the corresponding applications of the patterned structures are given in this chapter.

2D or 3D structures of silicon, polymer, or alumina find wide range of application in the MEMS, or biotechnology, and so structuring of such patterns with maximum precision is always important. Lithographic structuring (ex: photolithography, e-beam

lithography, or laser lithography) is one of the widely used methods in MEMS and biotechnology. Among this, laser lithography is one of the lithographic techniques which can draw any custom patterns with resolution down to few nanometers.

The structure of this chapter is as follows; the first section (5.1) describes on the fabrication of platinum interdigital electrodes on SiO₂ wafer and their application to gas sensing. The second section (5.2) explains the fabrication of inverted micropylamid arrays using laser lithography followed by electrochemical etching. Following this, a short description on the two applications of the produced micropylamid structures is reported; 1) production of plamonic supercrystal arrays by using inverted micropylamids as a template, and 2) fabrication of silicon dioxide micopillars from inverted micropylamids and their application in biotechnology.

5.1. Fabrication of platinum interdigital electrodes and their application for gas sensing.

The detection of gases, both toxic and non-toxic, is important for monitoring and maintaining a safe and healthy condition in industries and domestic areas, and for the detection of gas leakages. Gas detection is achieved using gas sensors, which detects the gases in its vicinity. A gas sensor interacts with the gases in a particular area and measures the gas concentration. Depending on the mode of detection, there are different types of gas sensor such as resistance based gas sensors, capacitance based and acoustic wave-based gas sensors, optical gas sensors, and electrochemical gas sensors.

Due to the low detection limit, high sensitivity to different gases, compact size and low cost of fabrication, metal-oxides gas sensors are relevant in gas sensing technologies. Among the metal oxides, due to its high sensitivity to gases such as NO_2 , O_3 , H_2 , H_2S , and Ethanol, tungsten trioxide (WO_3) has gained much attraction recently [Stoycheva 2010, Vallejos 2008, Labidi 2005, Hoa 2013, Ahsan 2012].

Referring to the fabrication of electrodes of gas sensors, screen printing is one of the most widely used techniques for electrode fabrication [Annanouch 2013, Murugappan 2011]. However, one of their major difficulties is that, it is not possible to obtain electrodes with smaller widths and a smaller separation between the adjacent electrodes. In this work we show that the laser lithographic technique is a good alternative to pattern high resolution electrodes with smaller dimensions (width and separation). Using this technique we were able to produce interdigital electrodes with a width of 10 μm and a separation (between the adjacent electrodes) of 5 μm on SiO_2 wafers. After patterning the electrodes, using sputtering technique followed by lift-off, we were able to produce platinum interdigital electrodes. Subsequently WO_3 nanoneedles were deposited over platinum interdigital electrodes, and the fabricated sensor was tested for ethanol sensing.

The first part of this section (5.1.1) presents the experimental procedure on the fabrication of platinum interdigital electrodes using laser lithographic and sputtering techniques. The following section (5.1.2) gives a short description on the deposition of WO_3 over the fabricated electrodes and the characterization results of the obtained sensor for ethanol gas sensing. In this collaboration, the fabrication of platinum interdigital electrodes using lithographic patterning followed by sputtering and lift-off

was done in the framework of this Ph.D., and the deposition of WO_3 nanoneedles and gas characterization was carried out by Minos group.

5.1.1. Fabrication of platinum interdigital electrodes

Fabrication of platinum electrodes was accomplished in three steps: i) preparation of SiO_2 substrates by thermal oxidation, ii) patterning the design using laser lithography, and finally iii) the producing platinum electrodes using sputtering followed by lift-off.

i. Substrate preparation

Initially silicon wafers were oxidized using thermal oxidation to produce silicon dioxide wafers. At first the silicon wafers were cleaned with acetone, ethanol, and water for 5 min. each. Then the oxidation of those cleaned wafers was carried out for 10 hours at $1100\text{ }^\circ\text{C}$ in a tubular furnace. Initially the furnace was at room temperature and then the temperature was increased to $1100\text{ }^\circ\text{C}$ with a ramp up rate of $15^\circ\text{C}/\text{min}$. After 10 h. at $1100\text{ }^\circ\text{C}$, the furnace was then brought down to room temperature with a ramp down rate of $20\text{ }^\circ\text{C}/\text{min}$. The oxidized wafers were then prepared for lithographic patterning.

ii. Laser lithographic patterning of interdigital electrodes

As described in section 3.2.1, the patterning of photoresist using laser lithography involves few steps such as the deposition of the photoresist on wafer by spin coating, soft baking of the resist coated wafer, laser exposure of soft baked resist, post exposure bake and finally the development to produce the patterns. The laser lithographic patterning of electrodes was carried out as follows.

Prior to the laser exposure, the substrates were cleaned with acetone, and water for 5 min. each, and then dried for 20 min. at 200°C in an oven. Following this the cleaned wafers were coated with AZ 5214E, a negative photoresist, by spin coating at a spinning speed of 3000 rpm for 25 s. This resulted in the formation of a thin layer of approximately 500 nm of AZ 5214E on the wafer. The resist coated wafer was then placed on a hotplate and soft baked for 1 min. at 100°C.

These baked substrates then underwent laser exposure. As mentioned in section 3.2.1, prior to the laser exposure, the lithographic unit was loaded with the pattern of interdigital electrodes. The designing of the electrodes were achieved using Clewin, layout editor software. An inverse pattern of the required interdigital electrodes were drawn, so that after sputtering followed by lift-off we would be able to produce the desired pattern. The laser exposure was performed using a diode laser that emits a wavelength of 405nm (DWL 66FS, Heidelberg, Mikrotechnik GmbH, Germany). The laser exposure was carried out with a laser power of 5mW.

Subsequently the laser exposed samples were baked (post exposure bake) for 50 s. at 110°C. Then to remove the exposed region of the photoresist the post baked samples were developed for 50 s. using the developer solution AZ725. The wafer was then rinsed with plenty of DI H₂O.

iii. Sputtering and lift-off to produce platinum interdigital electrodes

After patterning the wafers, next step was to deposit platinum over the patterned electrodes, which was accomplished by sputtering technique.

Sputtering is a physical vapor deposition technique to deposit thin film of materials (ex: Ag, Au, Pt, Al, Ti e.t.c) on to substrates such as silicon wafer, glass or more. Sputtering is carried out in a vacuum chamber and during the sputtering this chamber will have a continuous flow of a gas, such as usually argon, oxygen, or nitrogen. The selection of gas depends on the type of material to be deposited. In sputtering the deposition of the material on the substrate is achieved by ejecting the material from its source called the "target". The material gets deposited on the substrate by applying an electrical potential between the cathode (the target) and the anode (the chamber body). This electrical potential causes free electron to accelerate and collide with the gas atom and thus create a positively charged gas ion. These energetic positively charged gas ions hit the target and expel the atoms and thus these atoms drift towards substrate where they condense.

In our work the deposition of platinum was carried out using an ion beam sputtering (AJA sputtering International INC, N.Scituate, MA) system and the sputtering took place in an argon gas atmosphere. Figure 5.1 shows the schematic of the sputtering setup.

The required thickness of the platinum in our case was 150 nm. Since the adhesion of platinum on the SiO₂ wafers is poor, prior to the platinum deposition a thin film of 20 nm of titanium was deposited on to the wafer. After depositing a thin layer of titanium and platinum on the wafers, the next step was to remove the metal layer from the unwanted area of the patterned layer, which was achieved by lift-off.

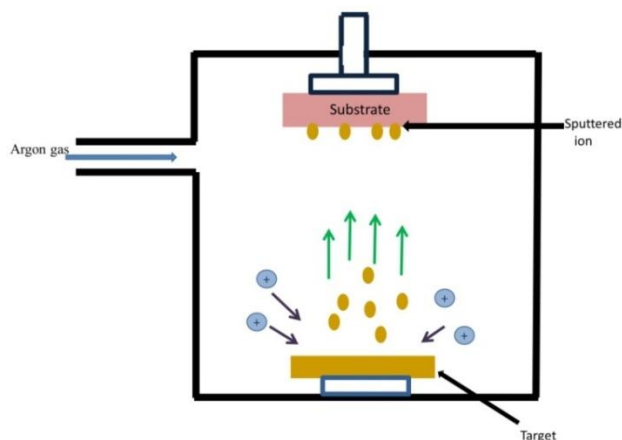


Figure 5.1: Schematic diagram of sputtering.

Lift-off is a method used for creating patterns on any substrate with the support of a sacrificial layer (ex: photoresist). A schematic representation of lit-off process is given in figure 5.2.

Initially the sacrificial layer is deposited and it is patterned using techniques like lithography or etching (figure 5.2b and 5.2c). Afterwards, the required material is deposited over the whole area of the substrate by any material deposition method (in our case, sputtering) (figure 5.2d). Following this, the substrate is washed with solutions that can remove the sacrificial layer (ex: acetone). During this wash the sacrificial layer along with the material on the top of this layer gets lifted-off and removed (figure 5.2e).

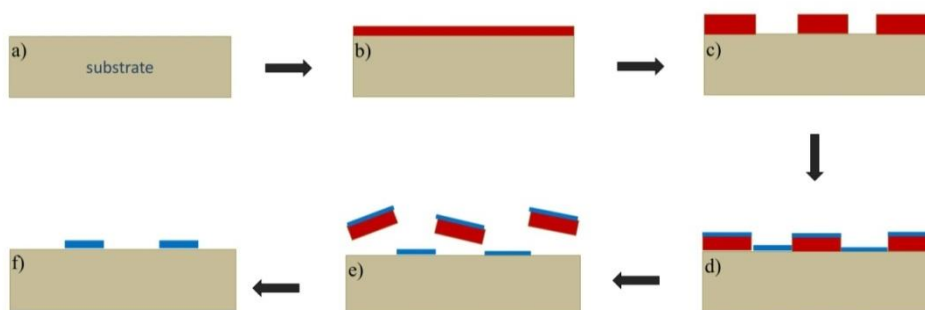


Figure 5.2: Schematic diagram of lift-off process. a) substrate preparation, b) deposition of sacrificial layer, c) patterning of the sacrificial layer, d) deposition of target material, e) removal of the sacrificial layer along with the target material on its surface using lift-off solution, and f) patterned layer of target material.

Thus, after this lift-off the target material remains only in the area where it was in direct contact with the substrate (figure 5.2f).

In our work to remove the platinum from the unwanted area of the wafers and to create the platinum electrodes, lift-off was carried out with acetone solution (99.9%) for 10 s. Subsequently the samples were rinsed with ethanol and DI H₂O for 30 s. each. During lift-off the metal deposited on the photoresist was removed and the desired platinum interdigital electrode pattern was produced. Figure 5.3 shows the SEM images of the produced platinum interdigital electrodes. The electrodes had a width of 10 μm and the separation between the electrodes was 5 μm .

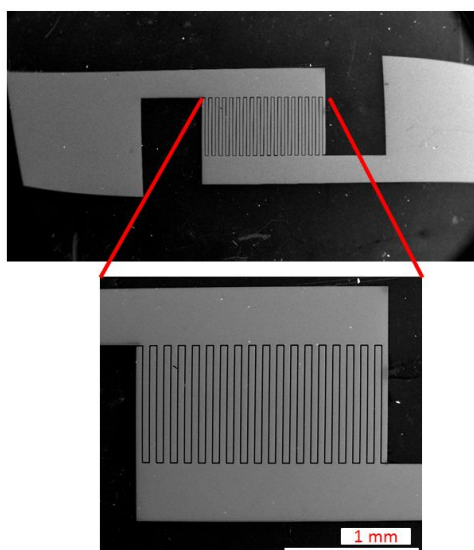


Figure 5.3: SEM image of obtained platinum Interdigital electrodes.

5.1.2. Deposition of WO_3 nanoneedles

After obtaining the platinum interdigital electrodes, WO_3 nanoneedles were deposited over the electrodes, which were achieved by drop coating of WO_3 . In order to obtain an aligned distribution of the nanoneedles across the electrodes, during drop coating a sinusoidal wave with a frequency of 3MHz and amplitude of 14V (peak to peak) was applied to the electrodes using a functional generator. Figure 5.4a shows how the deposition of nanoneedles was carried out, and figure 5.4b shows the SEM images of the distribution of the nanoneedles over the electrodes. The SEM images show that the nanoneedles are bridged across the electrodes and the average lengths of the nanoneedles were around 6 to 10 μm .

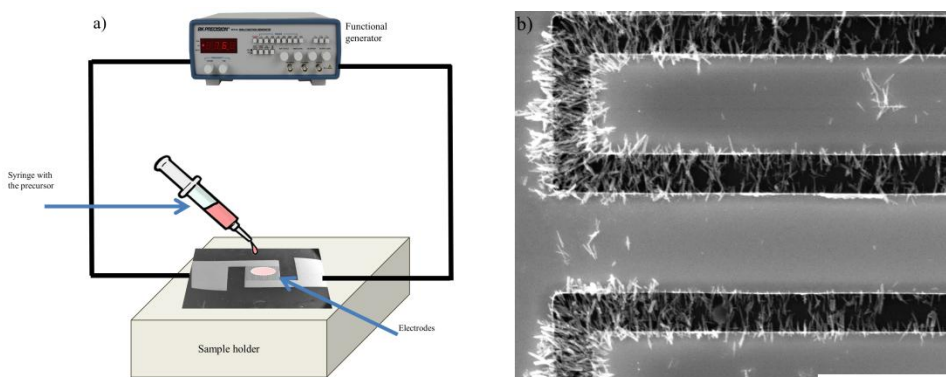


Figure 5.4: (a) Schematic representation of dielectrophoresis for the deposition of WO₃ nanoneedles over the electrodes, and (b) SEM image of WO₃ nanoneedles deposited on the electrodes (scale 10µm).

These electrodes were then tested towards 30 ppm of ethanol at a working temperature of 250°C. The change of resistance of the sensors upon the adsorption of the gas molecules on the metal-oxide is the detection principle of this metal-oxide resistive sensor.

The figure 5.5 represents the resistance as a function of time graph of ethanol sensing. The result shows that the sensor resistance rapidly drops down upon its exposure to the ethanol gas, which in turn confirms the ability of the produced sensor for ethanol sensing. From the graph it can be seen that the response time of this sensor is 96 s. and the recovery time 302 s.

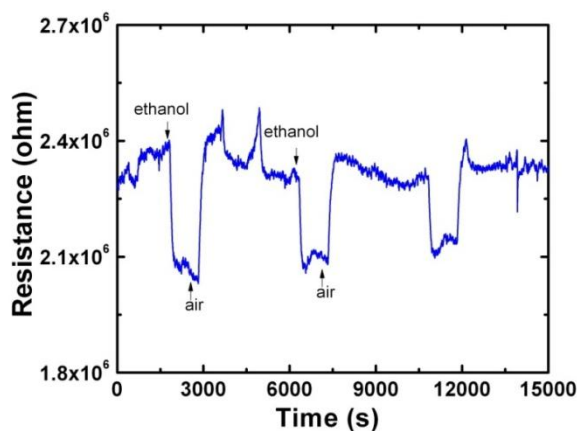


Figure 5.5: The graph depicts the change in sensor resistance with time. The indications corresponding to the introduction of ethanol and of air are indicated.

5.2. Fabrication of silicon inverted micropylramid arrays and their applications in biotechnology.

Due to their high biocompatibility and non toxicity, silicon and silicon dioxide have emerged as a promising material for many studies in biology and biotechnology [Chen 2011, Dhanekar 2013]. Nanostructures and microstructures of Si and SiO₂ in different dimensions have been successfully used in drug delivery, tissue engineering, and cell culture [Spieth 2011, Merlo 2013]. 2D and 3D structures of different materials, especially of silicon, can be fabricated using various techniques such as lithographic techniques (ex: photolithography, soft lithography or laser lithography), followed by wet and dry etching methods (ex: plasma etching, reactive ion etching, or

electrochemical etching) [Choi 2003, Waits 2005]. The possibility of fabricating high resolution silicon structures with various dimensions and shapes make laser lithography a promising structuring tool in biotechnology applications.

This section describes on the fabrication of silicon inverted micropylramid arrays using laser lithography and two applications of the produced inverted pattern. In the work explained here, the lithographic patterning of photoresist on SiO₂ wafers done in the framework of Ph.D. and the rest of the work was performed within Nephos group. Part 5.2.1 explains on the fabrication procedure of inverted micropylramid arrays using a combination of laser lithography and electrochemical etching. Following this, section 5.2.2 describes on the formation of periodic array of pyramidal supercrystals using the inverted micropylramid arrays as the templates. The produced pyramidal surfaces were then tested as an optical sensor for the monitoring of carbon monoxide (CO). Finally, section 5.3.1 explains on the fabrication SiO₂ micropillars and the selective functionalization of external and internal surfaces of the fabricated micropillars with biomolecules.

5.2.1. Fabrication of silicon inverted micropylramid arrays

Silicon micropylramid arrays were fabricated on planar silicon wafers using laser lithography. The fabrication methods were carried out as described in figure 5.6. Initially the silicon wafers were oxidized to grow a thin silicon dioxide layer (figure 5.6a). This oxide layer serves as the mask during the anisotropic alkaline etches. The oxidation was carried out at 1000°C for 15 min. in a tubular furnace and the thickness of the oxide layer formed was around 10-12 nm. The wafers were then cleaned and dried.

Afterwards, a thin layer of a positive photoresist, AZ 1505 was deposited on the wafers by spin coating at a spinning speed of 500 rpm for 30 s. (figure 5.6b). The resist coated wafer was then soft baked at 100°C for 60 s. Following this, square patterns having a width and length of 2 μm each and a separation between the adjacent squares of 2 μm were patterned on to the SiO_2 wafers by laser lithography. The exposures were carried out with a laser power of 5 mW. The exposed wafers were then developed with AZ725 for 50 s. Then the developed wafers rinsed with plenty of DI H_2O .

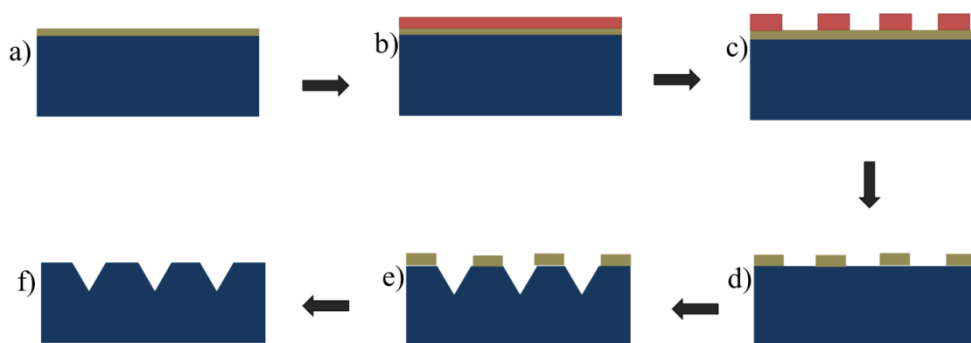


Figure 5.6: Schematic representation of inverted micropyramid arrays fabrication: a) wafer oxidation, b) deposition of photoresist, c) patterning of photoresist by laser lithography, d) selective removal of oxide layer by BHF etch followed by the removal of remaining photoresist, e) formation of inverted pyramids by TMAH etch, and f) dissolution of the residual SiO_2 layer.

To transfer the patterns drawn on the photoresist on to the SiO_2 layer, the wafers were then etched with buffered hydrofluoric acid (BHF) (figure 5.6d). Subsequently, to produce the inverted pyramids on the silicon wafers, the wafer were etched with 8% tetramethylammonium hydroxide (TMAH) solution for 3-6 min. at 80°C (figure 5.6e). The TMAH etches anisotropically the silicon and produces inverted micropylramids on silicon wafers. Finally the oxide layer was dissolved by a quick dip of the wafers in 5% hydrofluoric acid (HF) solution (figure 5.6f).

The as produced inverted micropylramid arrays were examined using SEM and the resulting images of the obtained inverted micropylramid arrays are shown in figure 5.7.

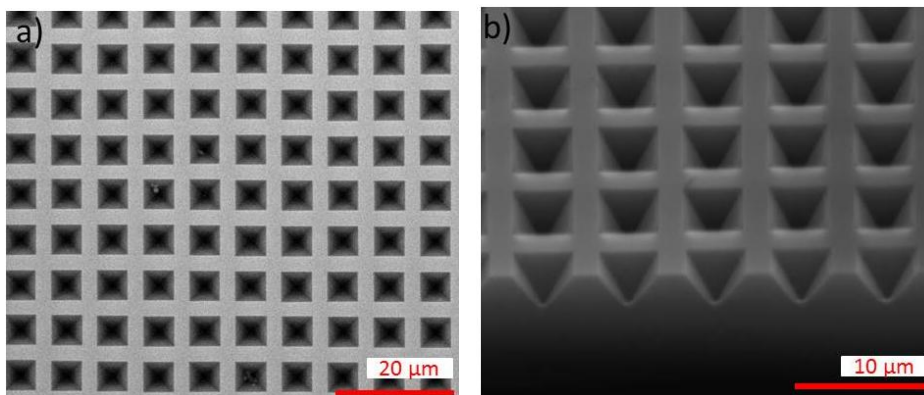


Figure 5.7: SEM pictures of the obtained inverted micropylramid arrays.

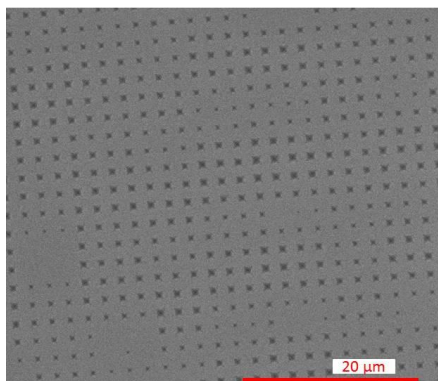


Figure 5.8: SEM images of pattern having a dimension of 1 and 1 μm width and length.

Besides, a couple of tests were also performed to produce micropyramids of lower dimensions (1 μm width, and 1 μm length), but those produced patterned were observed not to have uniformity. Figure 5.8 shows the micropyramid structures having a dimension of 1 μm and 1 μm .

5.2.2. Inverted micropyramids as a template for the formation of macroscale plasmonic substrates for surface enhanced raman scattering.

This section presents a template-assisted method for the fabrication of organized pyramidal supercrystal arrays by stamping the colloidal particles. The produced inverted pyramids served as the templates for the formation of gold nanoparticle pyramid. The produced gold nanoparticle plasmonic platform was then used to produce a handheld portable and reversible surface enhanced raman scattering (SERS) surface for sensing of

carbon monoxide (CO). Using this method a periodic array of plasmonic supercrystals can be produced in a larger area. This work is reported by Alba [Alba 2013].

i. Production of Plasmonic platform

Figure 5.9 depicts the process of obtaining nanoparticle pyramids. The templates were cleaned with oxygen plasma prior to the deposition of nanoparticles. Subsequently, a concentrated solution of gold nanoparticles was casted on the templates and allowed to dry. Thus a periodic array of square pyramids made from a compact packing of plasmonic particles (gold nanoparticles) were formed.

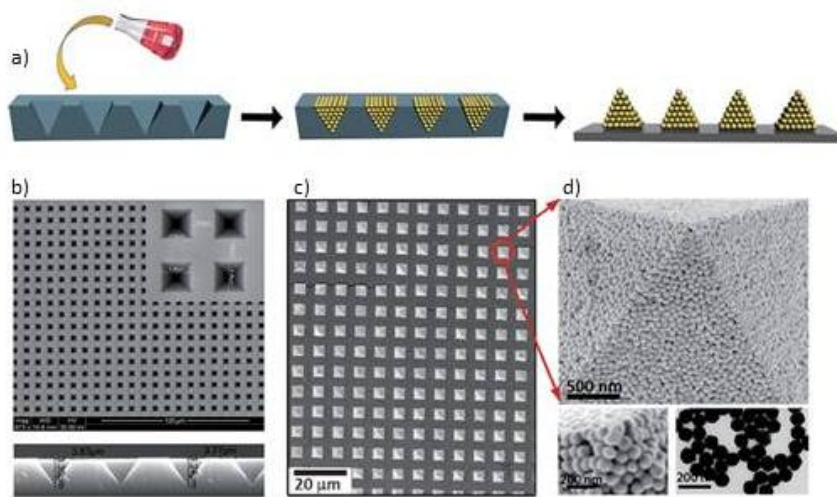


Figure 5.9: a) Schematic representation of the fabrication of the microscale nanostructured film. b) SEM image of the microscale plasmonic film after stamping. c) High-resolution SEM images of the pyramids and d) TEM image of the gold nanoparticle building blocks.

The formed pyramidal structures were then demonstrated as an ultrafast and reversible optical sensor for monitoring CO. The detection was performed using a handheld Raman spectrometer. Prior to the exposure of the analyte to the plasmonic surface, 5-[(triisopropylsilyl)thio]-10,20-diphenylporphyrin(TDPP) complexed with Fe^{II} was allowed to self-assemble on to the gold pyramids. This was done to have to selective and reversible gas (CO) capture on the sensing surface. Subsequently the sensing surfaces were allowed to interact with the analyte (CO) and the vibrational bands were measured. The change in the vibrational bands before and after the interaction of the analyte with the plasmonic pyramid was measured. Figure (5.10) shows the SERS spectra. The vibrational spectra are different before and after the interaction of the analyte with the sensing surface. The new vibrational bands appeared after the interaction of the analyte with the sensing surface are associated with the CO gas. This proves the presence of CO on the sensing platform, and thus shows that plasmonic pyramids with TDPP- Fe^{2+} can serve as an excellent sensing surface for gases such as CO. The SERS measurements were obtained with a handheld Raman macrosystem with an excitation laser wavelength of 785 nm. The acquisition time was 1 s and the laser power at the sample was 1 mW.

The blue, brown and red spectrum corresponds to the raman spectra of TDPP, TDPP- Fe^{2+} , and TDPP- Fe^{2+} -CO respectively. The vibrational bands at 1549, 1490, 1444, 1370, and 1320 cm^{-1} are attributed to the ring stretching, and the bands at 1268 and 1240 are associated with CCN bending. CCH bending (1146 and 1070 cm^{-1}), ring breathing (1026 and 999 cm^{-1}), ring deformation (880 and 857 cm^{-1}), and N-Fe stretching (591 , 569 , 506 , and 420 cm^{-1}). The spectral changes after CO complexation are highlighted by the arrows in the red spectrum.

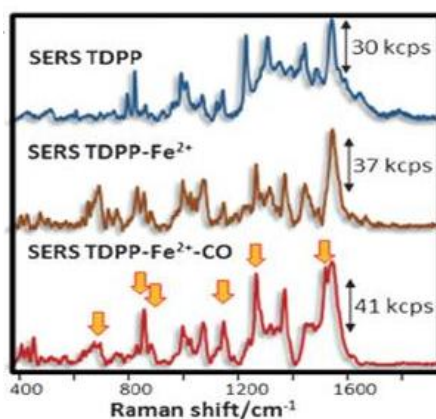


Figure 5.10: SERS spectra of the free porphyrin, the porphyrin coordinated to iron, and the iron porphyrin complexed with CO.

In short, this work shows the possibility of patterning homogeneous macroscale nanoparticle architectures over large areas, and proves that such plasmonic macrosubstrates can be used as a platform for a reversible and portable optical sensor for CO.

5.2.3. Fabrication of SiO₂ hollow micropillar arrays and their application for dual-side functionalization.

This section explains on the fabrication SiO₂ micropillars and the selective functionalization of external and internal surfaces of the fabricated micropillars with biomolecules. After producing the inverted pyramids, an ordered array of SiO₂ micropillars were produced by electrochemical etching from the arrays of inverted

pyramids. The inner and outer surfaces of the produced micropillars were then selectively functionalized with biomolecules without cross-contamination. The inner surfaces were functionalized with mercaptopropyl trimethoxysilane (MPTMS) and the outer surfaces were functionalized with bovine serum albumin (BSA). This work has been published by Alba [Alba 2014].

i. Fabrication of SiO_2 micropillars

The growth of micropores in silicon is not a self-ordering process and by electrochemical etching alone there would not form a periodic arrangement. The resulting pores formed by electrochemical etching alone nucleate at random points on the wafer surface and thus forms an unordered distribution of pores. However, periodically ordered pores can be produced on silicon wafers by combining lithography followed by etching. Lithography is used to define the nucleation sites, that are used as etch pits for the subsequent electrochemical etching. Nevertheless, the pore diameter and shape are defined by the etching condition and the wafer resistivity and not by the size of the pyramidal notch [Trifonov 2004].

In this study, after producing an ordered array of inverted silicon micropyrmaid arrays, an electrochemical etching resulted in the formation of SiO_2 micropillars. The schematic of fabrication of SiO_2 micropillars and the procedure of functionalization of inner and outer surfaces of the micropillars is shown in Figure 5.11.

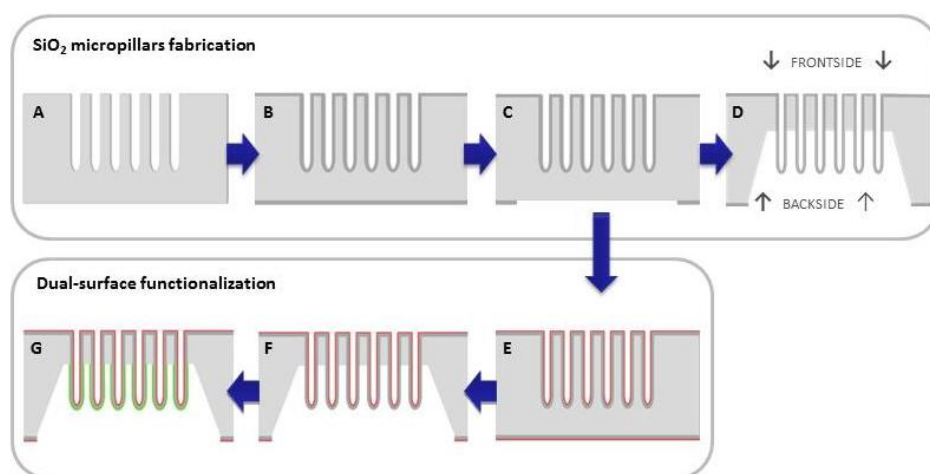


Figure 5.11: Schematic representation of fabrication of SiO₂ micropillars and the dual-side functionalization of the SiO₂ micropillars: A) fabrication of ordered micropores by electrochemical etching (dimethylformamide and 40% hydrofluoric acid solution), B) formation of silicon dioxide by thermal oxidation, C) removal of the oxide layer from the backside of the sample, D) TMAH etching for the formation of SiO₂ micropillars, E) functionalization of the inner side of the micropillars with Rh-MPTMS, (F) backside silicon etching using TMAH and (G) functionalization of the external side of the micropillars with FITC-BSA.

The micropillars were functionalized as follows. Initially the porous structures were exposed to a 5 mM solution of MPTMS-rhodamine in anhydrous toluene for 3 h at 75°C under nitrogen atmosphere (figure 5.11E). After the functionalization of internal surfaces, the micropillars were released by TMAH etch (figure 5.11F) in the back side. TMAH is selective only for silicon that is anisotropic. Then the outer surfaces of the micropillars were functionalized with BSA-FITC (figure 5.11G). This was achieved by incubating the pillars in 100 mg/ml of BSA-FITC in PBS solution for 2h. The

functionalized micropillars were then observed under the fluorescence microscope (figure 5.12). The fluorescence microscopy images show that the inner and outer walls of the micropillars are functionalized with photolabelled MPTMS and BSA respectively.

The results show that a successful dual-side functionalization of SiO_2 micropillars without cross-contamination was achieved. These 3D micropillar arrays of dual-side functionalized micropillars are a promising flexible platform for range of biotechnological applications, such as biosensing, 3D cell culture and drug delivery.

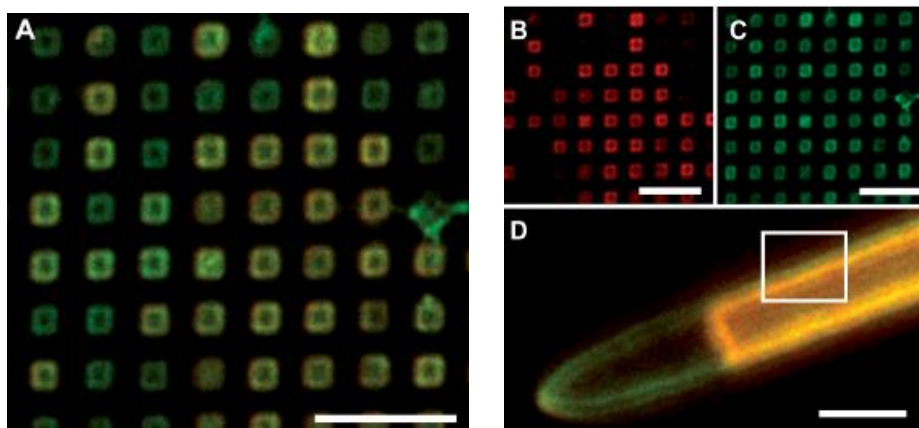


Figure 5.12: Figure 12: Fluorescent images of SiO_2 micropillars after dual-side functionalization with a simultaneous excitation of 488 and 543 nm lasers. Top view images collected through bandpass filters of (A) both 515 ± 15 and 590 ± 30 nm, (B) 590 ± 30 nm and (C) 515 ± 15 nm, and (D) cross-section image of an unattached micropillar collected through both 515 ± 15 and 590 ± 30 nm emission filters. (Scale bar for (A), (B) and (C) is 10 μm ; and for (D) is 2 μm).

UNIVERSITAT ROVIRA I VIRGILI

LITHOGRAPHIC MICRO- AND NANOSTRUCTURING OF SU-8 FOR BIOTECHNOLOGICAL APPLICATIONS

Pinkie Jacob Eravuchira

Dipòsit Legal: T 773-2015

Chapter 6

Conclusions

This Ph.D. Dissertation has focused on three dimensional structuring of SU-8 surfaces in both micrometric and nanometric scales and to utilize the fabricated structures for immunosensing. In this respect, this work has been divided into two sections: initially the structuring of SU-8 surfaces was carried out using lithographic techniques such as photolithography, soft lithography and hybrid lithography, and subsequently the produced SU-8 surfaces were utilized for fabricating photoluminescent-based immunosensors.

The first task of this work was the lithographic structuring of SU-8 surfaces. The structuring of SU-8 surfaces was carried out using photolithography, soft lithography and hybrid lithography. The significant conclusions of this task are:

- Fabrication of SU-8 macropillars on silicon and glass substrates was achieved using photolithography.

- We have demonstrated the fabrication of SU-8 nanometric and micrometric pores and pillars using soft lithographic technique.
- Furthermore, we have developed a technique for the nanometric and micrometric structuring of SU-8 macropillar surfaces. This hierarchical structuring of SU-8 was achieved using hybrid lithographic method, which is a combination of soft lithography and photolithography. Hybrid lithographic patterning of SU-8 surfaces resulted in the production of SU-8 macropillar surfaces decorated with micrometric and nanometric pores and pillars.

The produced SU-8 macropillar, micro- and nano pores and pillars, and macropillars decorated with pores and pillars were utilized as sensing platform for photoluminescent based immunosensing. The most important results obtained from this work are:

- A cost-effective, label-free optical immunosensing based on reduction of photoluminescence of SU-8 sensing platform is presented in this work.
- A reduction of the photoluminescence of SU-8 has been demonstrated with each step of surface modification and especially after the antigen-antibody immobilization. Thus this work proves the possibility of using photoluminescence reduction as a sensing transduction parameter.
- Performing photoluminescence measurements on SU-8 planar and macropillars sensing surfaces proves that a macro-structured SU-8 surface provides higher sensing response to the same analyte concentration.

- Quantitatively evaluation of the sensitivity of the SU-8 platform shows that sensitivity depends strongly on the used substrate.
- This study reveals that an SU-8 sensing surface patterned with pillars (micrometric and nanometric) always gives a higher photoluminescence reduction than porous sensing surfaces.
- Furthermore, this work shows that the SU-8 macropillars patterned with micrometric and nanometric pillars and pores results in a higher sensitivity compared to planar SU-8 surfaces patterned with macropillars, and micrometric and nanometric pores and pillars.

UNIVERSITAT ROVIRA I VIRGILI

LITHOGRAPHIC MICRO- AND NANOSTRUCTURING OF SU-8 FOR BIOTECHNOLOGICAL APPLICATIONS

Pinkie Jacob Eravuchira

Dipòsit Legal: T 773-2015

References

- [Abgrall 2006] P. Abgrall, L. Lattes, V. Conedera, X. Dollat, S. Colin, A. Gue. A novel fabrication method of flexible and monolithic 3D microfluidic structures using lamination of SU-8 films, *J. Micromech. Microeng.*, vol. 16, page 113, 2006.
- [Abgrall 2007] P. Abgrall, V. Conedera, H. Camon, A. M. Gue, N. T. Nguyen. SU-8 as a structural material for labs-on-chips and microelectromechanical systems, *Electrophoresis*, vol. 28(24), page 4539, 2007.
- [Ahsan 2012] M. Ahsan, M.Z. Ahmad, T. Tesfamichael, J. Bell, W. Wlodarski, N. Motta. Lowtemperature response of nanostructured tungsten oxide thin films toward hydrogen and ethanol, *Sens. Actuator. B*, vol. 173, page 789, 2012.
- [Alba 2013] M. Alba, N. Pazos-Perez, B. Vaz, P. Formentin, M. Tebbe, M. A. Correa-Duarte, P. Granero, J. Ferre-Borrull, R. Alvarez, J. Pallares, A. Fery, A. R. Lera, L. F. Marsal, R. A. Alvarez-Puebla. Macroscale Plasmonic Substrates for Highly Sensitive Surface- Enhanced Raman Scattering, *Angew. Chem.*, vol52, page 6459, 2013.
- [Alba 2014] M. Alba, E. Romano, P. Formentin, P. J. Eravuchira, J. Ferre-Borrull, J. Pallares, L. F. Marsal. Selective dual-side functionalization of hollow SiO₂ micropillar arrays for biotechnological applications, *RSC Adv.*, vol. 4, page 11409, 2014.
- [Altuna 2013] A. Altuna, E. Bellistri, E. Cid, P. Aivar, B. Gal, J. Berganzo, G. Gabriel, A. Guimera, R. Villa, L. J. Fernandez, L. M. Prida. SU-8 based microprobes for simultaneous neural depth recording and drug delivery in the brain, *Lab. Chip*, vol. 13, page 1422, 2013.
- [Alvarez 2009] S. D. Alvarez, C. Li, C. E. Chiang, I. K. Schuller, M. J. Sailor, A label-free porous alumina interferometric immunosensor, *ACS Nano*, vol. 3(10), page 3301, 2009.
- [Amato 2012] L. Amato, S. S. Keller, A. Heiskanen, M. Dimaki, J. Ennéus, A. Boisen, M. Tenje. Fabrication of high-aspect ratio SU-8 micropillar arrays, *Microelectron. Eng.*, vol. 98, page 483, 2012.

140 | References

- [Annanouch 2013] F. E. Annanouch, S. Vallejos, T. Stoycheva, C. Balckman, E. Llobet, Aerosol assisted chemical vapour deposition of gas-sensitive nanomaterials, *Thin Solid Film*, vol. 548, page 703, 2013.
- [Barber 2007] R. L. Barber, M. K. Ghantasala, R. Divan, D. C. Mancini, E. C. Harvey, Study of stress and adhesion strength in SU-8 resist layers on silicon substrate with different seed layers, *J. Micro/Nanolith. MEMS MOEMS*, vol. 6(3), page 033006, 2007.
- [Bareil 2010] R. Parenteau-Bareil, R. Gauvin, F. Berthod, Collagen based biomaterials for tissue engineering applications, *Materials*, vol. 3, page 1863, 2010.
- [Beche 2010] B. Beche. Integrated photonics devices on SU8 organic materials, *Int. J. Phy. Sci.*, vol. 5(5), page 612, 2010.
- [Beche 2004] B. Beche, N. Pelletier, E. Gaviot, J. Zyss. Single-mode TE_{00} - TM_{00} optical waveguides on SU-8 polymer, *P Soc. Photo-opt Ins.*, vol. 230, page 91, 2004.
- [Bednorz 2006] M. Bednorz, M. Urbańczyk, T. Pustelny, A. Piotrowska, E. Papis, Z. Sidor, E. Kamińska. Application of SU-8 polymer in waveguide interferometer ammonia sensor, *Mole. Quan. Acoustic*, vol. 27, page 31, 2006.
- [Blagoi 2008] G. Blagoi, S. Keller, A. Johansson, A. Boisen, M. Dufva, Functionalization of SU-8 photoresist surfaces with IgG proteins, *Appl. Surf. Sci.*, vol. 255, page 2896, 2008.
- [Boiragi 2011] I. Boiragi, S. Kundu, R. Makkar, K. Chalapathi, Single mode SU8 polymer based mach-zehnder interferometer for bio-sensing application, *AIP Conf. Proc.*, vol. 327, page 1391, 2011.
- [Boiragi 2009] I. Boiragi, R. Makkar, B. D. Choudhury, A. Mallik, K. Chalapathi. SU8 polymer based waveguide biomedical sensor for medical diagnostic application, *Int. conference on optics and photonics.*, 2009.
- [Brittain 1998] S. Brittain, K. Paul, X. Mei Zhao, G. Whitesides. Soft lithography and microfabrication, *Phys. World*, page 31, 1998.

- [Budz 2010] H.A. Budz, M.M. Ali, Y. Li, R.R. LaPierre, Photoluminescence model for a hybrid aptamer-GaAs optical biosensor, *Journal of Appl. Phy.*, vol. 107 (10), page 104702, 2010.
- [Cao 2012] C. Cao, S. W. Birtwell, J. Hogberg, H. Morgan, A. Wolff, D. D. Bang, Gold nanoparticles-coated SU-8 for sensitive fluorescence-based detections of DNA, *Diagnostics*, vol. 2, page 72, 2012.
- [Campo 2007] A. Campo, C. Greiner. SU-8: a photoresist for high-aspect-ratio and 3D submicron lithography, *J. Micromech. Microeng.*, vol. 17, page 81, 2007.
- [Cannistra 2010] A. T. Cannistra, T. J. Suleski. Characterization of hybrid molding and lithography for SU-8 micro-optical components, *J. Micro/Nanolith.*, vol. 9, page 13025, 2010.
- [Carlier 2004] J. Carlier, S. Arscott, V. Thomy, J. C. Fourier, F. Caron, J. C. Camart, C. Druon, P. Tabourier. Integrated microfluidics based on multi-layered SU-8 for mass spectrometry analysis, *J. Micromech. Microeng.*, vol. 14, page 619, 2004.
- [Cedeno 2002] C. C. Cedeno, J. Seekamp, A.P. Kam, S. Zankovych, T. Hoffmann, C.M. Sotomayor Torres, C. Menozzi, M. Murgia, M. Cavallini, G. Ruani, F. Biscarini, M. Behl, R. Zentel, J. Ahopelto. Nanoimprint lithography for organic electronics. *Microelectron. Eng.*, vol. 61, page 25, 2002.
- [Chen 2011] K. Chen, B. R. Li, Y. Chen. Silicon nanowire field-effect transistor-based biosensors for biomedical diagnosis and cellular recording investigation, *Nano Today*, vol. 6, page 131, 2011.
- [Choi 2003a] K. Choi, T. J. Eom, C. M. LEE, Comparison of the removal efficiency for organic contaminants on silicon wafers stored in plastic boxes between UV/O₃ and ECR oxygen plasma cleaning methods, *Thin Solid Films*, vol. 435, page 227, 2003.
- [Choi 2003b] K. Choi, S. Ghosh, J. Lim, C.M. Lee, Removal efficiency of organic contaminants on Si wafer by dry cleaning using UV/O₃ and ECR plasma, *Appl. Surf. Sci.*, vol 206, page 355, 2003.

[Chuang 2003] Y. Chuang, F. Tseng, J. Cheng, W. Lin. A novel fabrication method of embedded micro channels by using SU-8 thick-film photoresist, *Sens. Actuators. A*, vol. 103, page, 64, 2003.

[Chung 2013] S. Chung, S. Park. Effects of temperature on mechanical properties of SU-8 photoresist material, *J. Mech. Sci. Tech.*, vol 27(9), page 2701, 2013.

[Conradie 2002] E. H Conradie, D. F. Moore. SU-8 thick photoresist processing as a functional material for MEMS applications *J. Micromech. Microeng.*, vol. 12, page 368, 2002.

[Cui 2000] L. Cui, H. Morgan. Design and fabrication of travelling wave dielectrophoresis structures, *J. Micromech. Microeng.*, 10, page 72, 2000.

[Cui 2002] L. Cui, H Morgan. Optical particle detection integrated in a dielectrophoretic lab-on-a-chip, *J. Micromech. Microeng.*, vol. 12, page 7, 2002.

[Choi 2010] S. Choi, J. K. Park. Two-step photolithography to fabricate multilevel microchannels, *Biomicrofluidics*, vol. 10(4), page 46503, 2010.

[Dai 2005] W. Dai, K. Lian, W. Wang. A quantitative study on the adhesion property of cured SU-8 on various metallic surfaces, *Microsyst. Technol.*, vol. 11, page 526, 2005.

[Deepu 2009] A. Deepu, V. V. R. Sai, S. Mukherji, Simple surface modification techniques for immobilization of biomolecules on SU-8, *J. Mater. Sci: Mater. Med.*, vol. 20, page 25, 2009.

[Dentinger 2002] P. M. Dentinger, K. L. Krafcik, K. L. Simison, R. P. Janek, J. Hachman. High aspect ratio patterning with a proximity ultraviolet source, *Microelectron. Eng.*, vol. 61, page 1001, 2002.

[Dhanekar 2013] S. Dhanekar, S. Jain. Porous silicon biosensor: Current status *Biosens. Bioelectron.*, vol. 41, Pages 54, 2013.

[Dongliang 2010] F. Dongliang, L. Lain-Jong, Label-free electrical detection of DNA hybridization using carbon nanotubes and grapheme, *Nano Rev.*, vol. 1:5354, page 1, 2010.

- [Duplana 2011] V. Duplana, E. Frost, J. J. Dubowski, A photoluminescence-based quantum semiconductor biosensor for rapid in situ detection of Escherichia coli, *Sensors Actuat. B-Chem.*, vol. 160, page 46, 2011.
- [Duarte 2011] R. M. Duarte, M. J. Madou. SU-8 photolithography and its impact on microfluidics, *Microfluidics and nanofluidics handbook*, page 231, 2011.
- [Duarte 2011] J.P. Esquivel, T. Senn, P. Hernández-Fernández, J. Santander, M. Lorgen, S. Rojas, B. Löchel, C. Cané, N. Sabate. Towards a compact SU-8 micro-direct methanol fuel cell, *J. Power Sources*, vol. 195, page 8110, 2010.
- [Erkan 2007] Y. Erkan, I. Czolkos, A. Jesorka, L. M. Wilhelmsson, O. Orwar. Direct immobilization of cholesteryl-TEG-modified oligonucleotides on to hydrophobic SU-8 surfaces, *Langmuir*, vol. 23, page 5259, 2007.
- [Fang 2011] Y. Fang, Lbel-free biosensors for cell biology, *Int. J. Electro. Chem.*, vol., page 1, 2011.
- [Fernandez 2007] L. J. Fernandez, M. Tijero, R. Vilares, J. Berganzo, K. Mayora, F. J. Blanco, SU-8 based microneedle for drug delivery in nanomedicine application with integrated electrodes, *Eleventh International Conference on Miniaturized Systems for Chemistry and Life Sciences*, 2007.
- [Gates 2004] B. D. Gates, Q. Xu, J. C. Love, D. B. Wolfe, G. M. Whitesides. Unconventional nanofabrication, *Ann. Rev. Mater. Res.*, vol 354, page 339, 2004.
- [Gelorme 1989] J. D. Gelorme, R. J. Cox, S. A. R. Gutierrez. Photoresist composition and printed circuit boards and packages made therewith. Patent 4882245. November 21, 1989.
- [Genolet 2001] G. Genolet, G New photoplastic fabrication techniques and devices based on high aspect ratio photoresist. Ph.D. Thesis, *Ecole Polytechnique Federale de Lausanne (EPFL)*, Lausanne, 2001.
- [Ghodssi 2010] R. Ghodssi, P. Lin. *MEMS materials and processes handbook*, page 193, 2010.

- [Glowacki 2008] J. Glowacki, S. Mizuno, Collagen scaffolds for tissue engineering, vol. 89(5), page 338, 2008.
- [Gitlin 2009] L. Gitlin, P. Schulze, D. Belder. Rapid replication of master structures by double casting with PDMS. *Lab Chip*, vol. 9, page 3000, 2009.
- [Guo 2012] X. Guo, Surface plasmon resonance based biosensor technique: A review, *J. Biophotonics*, vol 5(7), page 483, 2012.
- [Guerin 1997] L. Guerin, M. Bossel, M. Demierre, S. Calmes, P. Renaud. Simple and low cost fabrication of embedded microchannels by using a new thick-film photoplastic, *Proc. Transducers*, vol. 97, page 1419, 1997.
- [Guerin 1997] L. Guerin, M. Bossel, M. Demierre, S. Calmes, P. Renaud. Simple and low cost fabrication of embedded microchannels by using a new thick-film photoplastic, *Proc. Transducers*, vol. 97, page 1419, 1997.
- [Grist 2010] S. Grist, J. N. Patel, M. Haq, B. L. Gray, B. Kaminska. Effect of surface treatments/coatings and soft bake profile on surface uniformity and adhesion of SU-8 on a glass substrate, *Proceedings of the SPIE, Volume 7593*, 2010.
- [Han 2004] M. Han, W. Lee, S. Lee, S. S. Lee. 3D microfabrication with inclined/rotated UV lithography, *Sensor. Actuators A*, vol. 111, page 14, 2004.
- [Hoa 2013] N.D. Hoa, N.V. Duy, N.V. Hieu, Crystalline mesoporous tungsten oxide nanoplate monoliths synthesized by directed soft template method for highly sensitive NO₂ gas sensor applications, *Mater. Res. Bull.*, vol. 48, page 440, 2013.
- [Holgado 2010] M. Holgado, C.A. Barrios, F.J. Ortega, F.J. Sanza, R. Casquel, M.F. Laguna, M.J. Banuls, D. López-Romero, R. Puchades, A. Maquieir, Label-free biosensing by means of periodic lattices of high aspect ratio SU-8 nano-pillars, *Biosens. Bioelectron.*, vol. 25, page 2553, 2010.

- [Hostis 2000] E. Hostis, P. Michael, G. Fiaccabrino, D. Strike, N. Rooij, M. Koudelka-Hep. Microreactor and electrochemical detectors fabricated using EPON SU-8, *Sens. Actuators. B*, vol. 64, page 156, 2000.
- [Huang 2009] H. Huang, C. Tang, Y. Zeng, X. Yu, B. Liao, X. Xia, P. Yi, P. K. Chu, Label-free optical biosensor based on localized surface plasmon resonance of immobilized gold nanorods, *Colloid. Surface. B.*, vol. 71, page 96, 2009.
- [Hu 2006] W. Hu, B. Yang, C. Peng, S. W. Pang. Three-dimensional SU-8 structures by reversal UV imprint, *J. Vac. Sci. Technol. B*, vol. 24(5), page 2225, 2006.
- [Jeon 2007] S. Jeon, D. J. Shir, Y. S. Nam, R. Nidetz, M. Highland, D. G. Cahill, J. A. Rogers, M. F. Su, I. F. El-Kady, C. G. Christodoulou, G. R. Bogart. Molded transparent photopolymers and phase shift optics for fabricating three dimensional nanostructures, *Optic. Express*, vol. 15(10), page 6358, 2007.
- [Jenkins 2013] G. Jenkins. Rapid prototyping of PDMS devices using SU-8 lithography, *Methods Mol. Bio.*, vol. 949, page 153, 2013.
- [Jianlin 2013] L. Jianlin, M. J. Sailor, Synthesis and characterization of a stable, label-free optical biosensor from TiO₂-coated porous silicon, *Biosens Bioelectron.* vol. 55(C), page 372, 2013.
- [Joshi 2007a] M. Joshi, R. Pinto, V. R. Rao, S. Mukherji, Silanization and antibody immobilization on SU-8, *Appl. Surf. Sci.*, vol. 253, page 3127, 2007.
- [Joshi 2007b] M. Joshi, N. Kale, R. Lal, V. R. Rao, S. Mukherji, A novel dry method for surface modification of SU-8 for immobilization of biomolecules in Bio-MEMS, *Biosens Bioelectron.* vol 22 (11), page 2429, 2007.
- [Johari 2014] S. Johari, N. Tamilchelvan, M. Nuzaihan, M. M. Ramli, B. N. Taib, M. Mazalan, Y. Waha, The effect of softbaking temperature on SU-8 photoresist performance, *IEEE-ICSE2014 Proc*, page 467, 2014.

146 | References

- [Keller 2010] S. Keller, D. Haefliger, A. Boisen. Fabrication of thin SU-8 cantilevers: initial bending, release and time stability, *J. Micromech. Microeng.*, vol. 20, page 1, 2010.
- [Kim 2006] D. Kim, P. Kim, I. Song, J. M. Cha, S. H. Lee, B. Kim, K. Y. Suh, Guided three-dimensional growth of functional cardiomyocytes on polyethylene glycol nanostructures, *Langmuir*. vol 6;22 (12), page 5419, 2006.
- [Kotzar 2002] G. Kotzar, M. Freas, P. Abel, A. Fleischman, S. Roy, C. Zorman, J. M. Moran, J. Melzak. Evaluation of MEMS materials of construction for implantable medical devices, *Biomaterials*, vol. 23(13), page 2737, 2002.
- [Kumeria 2014] T. Kumeria, M. M. Rahman, A. Santos, J. Ferre-Borrull, L. F. Marsal, D. Losic, Structural and optical nanoengineering of nanoporous anodic alumina rugate filters for real-time and label-free biosensing applications, *Anal. Chem.*, vol. 86, page 1837, 2014.
- [Kyu-Shik 2010] M. Kyu-Shik, D. A. Sara, C. Won-Youl, J. S. Michael, A Stable Label-free Optical Interferometric Biosensor Based on TiO₂ Nanotube Arrays, *ACS Nano*, vol. 4(4), page.2070, 2010.
- [Labidi 2005] A. Labidi, C. Jacolin, M. Bendahan, A. Abdelghani, G.J.K. Aguir, M. Maaref. Impedance spectroscopy on WO₃ gas sensor, *Sens. Actuator. B*, vol. 106, page 713, 2005.
- [Lee 2001] C. H. Lee, A. Singla, Y. Lee, Biomedical applications of collagen, *Int. J. Pharm.*, vol. 19, page 1, 2001.
- [Lee 2003] G. Lee, C. Lin, G. Chang, Micro flow cytometers with buried SU-8/SOG optical waveguides, *Sensor Actuator A*, vol. 103, page 164, 2003.
- [Lee 2005] D. S: Lee, H. Yang, K. H. Chung, H. B. Pyo. Wafer-scale fabrication of polymer-based microdevices via injection molding and photolithographic micropatterning protocols. *Anal. Chem.*, vol. 77(16), page 5414, 2005.
- [Lee 1995] K. Y. Lee, N. LaBianca, S. A. Rishton, S. Zolgharnain, J. D. Gelorme, w, T. H. P. Chang, Micromachining applications of a high resolution ultrathick photoresist, *J. Vac. Sci. Technol.*, vol 13, page 3012, 1995.

- [Leinse 2004] A. Leinse, M.B.J. Diemeer, A. Driessen. High speed electro optic polymer micro-ring resonator, Proceedings Symposium IEEE/LEOS Benelux Chapter, Ghent, 2004.
- [Lipomi 2012] D. J. Lipomi, R. V. Martinez, L. Cademartiri, G. M. Whitesides. Soft Lithographic approaches to nanofabrication. *Polym. Sci.*, vol. 7, page 211, 2012.
- [Lichlyter 2003] D. J. Lichlyter, S. A. Grant, O. Soykan, Development of a novel FRET immunosensor technique, *Biosensors Biot.*, vol.19, page 219, 2003.
- [Liu 2007] C. Liu. Recent developments in polymer MEMS, *Adv. Mater.*, vol. 17, page 3783, 2007.
- [Liu 2004] J. Liu, B. Cai, J. Zhu, G. Ding, X. Zhao, C. Yang, D. Chen. Process research of high aspect ratio microstructure using SU-8 resist, *Microsyst. Technol.* Vol. 10, page 265, 2005.
- [Lin 2002] C. Lin, G. Lee, B. Chang, G. Chang. A new fabrication process for ultra-thick microfluidic microstructures utilizing SU-8 photoresist, *J. Micromech. Microeng.*, vol. 12, page 590, 2002.
- [Liu 2014] J. Liu, D. Song, G. Zong, P. Yin, X. Zhang, Z. Xu, L. Du, C. Liu, L. Wang, Fabrication of SU-8 moulds on glass substrates by using a common thin negative photoresist as an adhesive layer, *J. Micromech. Microeng.*, vol.24(3), page ,2014.
- [Lipomi 2007] D. J. Lipomi, R. V. Martinez, L. Cademartiri, G. M. Whitesides. Soft Lithographic Approaches to Nanofabrication, *Polym. Sci. A*, vol. 7, page 211, 2007.
- [Loechel 2000] B. Loechel. Thick-layer resists for surface micromachining, *J. Micromech. Microeng.*, vol. 10, page 108, 2000.
- [Lopez 2006] J. M. R. Lopez, M. Aguirregabiria, M. Tijero, M. T. Arroyo, J. Elizalde, J. Berganzo, I. Aranburu, F. J. Blanco, K. Mayora, A new SU-8 process to integrate buried waveguides and sealed microchannels for a Lab-on-a-Chip, *Sensor Actuator B*, vol. 114, page 542, 2006.

[Maltman 2010] D. J. Maltman, S. A. Przyborski, Developments in three-dimensional cell culture technology aimed at improving the accuracy of in vitro analyses, *Biochem. Soc. Trans.*, vol. 38(4), page 1072, 2010.

[Merlo 2011] S. Merlo, F. Carpignano, G. Silva, F. Aredia, A. Scovassi, G. Mazzini, S. Surdo, G. Barillaro. Label-free optical detection of cells grown in 3D silicon microstructures, *Lab Chip.*, vol. 13(16), page 3284, 2013.

[Murugappan 2011] K. Murugappan, J. Lee, D. Silvester, Comparative study of screen printed electrodes for ammonia gas ionic liquids, *Electrochem. Commun.*, vol. 13, page 1435, 2011.

[Marie 2006] R. Marie, S. Schmid, A. Johansson, L. Ejsing, M. Nordstroem, D. Haefliger, C.B.V. Christensen, A. Boisen, M. Dufva, Immobilisation of DNA to polymerized SU-8 photoresist, *Biosens. Bioelectron.*, vol. 21, page 1326, 2006.

[Masuda 1995] H. Masuda, K. Fukuda, Ordered metal nanohole arrays made by a two-step replication of honeycomb structures of anodic alumina, *Science*, vol. 268, page 1466, 1995.

[Matschegewski 2010] C. Matschegewski, S. Staehlke, R. Loeffler, R. Lange, F. Chai, D. P. Kern, U. Beck, B. J. Nebe. Cell architecture cell function dependencies on titanium arrays with regular geometry, *Biomaterial*, vol. 31, page 5729, 2010.

[Moona 2005] J. H. Moona, A. Smallb, G. Yic, S. Leea, W. Changd, D. J. Pineb, S. Yang. Patterned polymer photonic crystals using soft lithography and holographic lithography, *Synthetic Met.*, vol. 148, page 99, 2005.

[Morikaku 2013] T. Morikaku, Y. Kaibara, M. Inoue, T. Miura, T. Suzuki, F. Oohira, S. Inoue, T. Namazu. Influences of pretreatment and hard baking on the mechanical reliability of SU-8 microstructures, *J. Micromech. Microeng.*, vol. 23, page 105016, 2013.

[Muhammad 2013] H. M. S. Muhammad, G. Andrew, S. Marc, R. Julien, M. C. Jonathan, Polymer dual ring resonators for label-free optical biosensing using microfluidics, *Chem. Commun.*, vol. 49, page 3095, 2013.

- [Natarajan 2008] S. Natarajan, D. A. Chang-Yen, B. K. Gale. Large-area, high-aspect-ratio SU-8 molds for the fabrication of PDMS microfluidic devices, *J. Micromech. Microeng.*, vol. 18(4), 2008.
- [Nguyen 2002] N. Nguyen, S. T. Wereley. *Fundamentals and Applications of Microfluidics*, chapter 3, 2002.
- [Nordstrom 2006] M. Nordstrom, J. Hubner, A. Boisen, Sloped side walls in SU-8 structures with ‘Step-and-Flash’ processing, *Microelectro. Eng.*, vol. 83, page 1269, 2006.
- [Nordstrom 2007] M. Nordstrom, D. A. Zauner, A. Boisen, J. Hubner. Single-Mode Waveguides With SU-8 Polymer Core and Cladding for MOEMS Applications, *J. Lightwave Technol.*, vol. 25 (5), page 1284, 2007.
- [Nordstrom 2008] M. Nordstrom, S. Keller, M. Lillemose, A. Johansson, S. Dohn, D. Haefliger, G. Blagoi, M. Jakobsen, A. Boisen. SU-8 cantilevers for bio/chemical sensing; fabrication, characterisation and development of novel read-out methods, *Sensor*, vol. 8, page 1595, 2008.
- [O'Brien 2001] J O'Brien, P J Hughes, M Brunet, B O'Neill, J Alderman, B Lane, A O'Riordan, C O'Driscoll. Advanced photoresist technologies for microsystems *J. Micromech. Microeng.*, vol. 11, page 353, 2001.
- [Patel 2008] J. N. Patel, B. Kaminska, B. L. Gray, B. D. Gates. PDMS as a sacrificial substrate for SU-8-based biomedical and microfluidic applications, *J. Micromech. Microeng.*, vol. 18, page 1, 2008.
- [Padgen 2009] M. R. Padgen, A. Gracias, N. Tokranova, N. Cady, J. Castracane. SU-8 microfluidic channels with porous sidewalls for biological applications, *Microfluidic BioMEMS Medical Microsys.*, vol. 7207, page 720707, 2009
- [Parida 2009] O. P. Parida, N. Bhat, Characterization of optical properties of SU-8 and fabrication of optical components, *Int. Conf. Optic. Photonic.*, 2009.

- [Passeraub 2003] P. A. Passeraub, A. C. Almeida, N. V. Takor. Design, microfabrication and analysis of a microfluidic chamber for the perfusion of brain tissue slices, *Biomed. Microdevice*, vol. 5(2), page 147, 2003.
- [Pai 2007] J. Pai, Y. Wang, G. T. Salazar, C. E. Sims, M. Bachman, G. P. Li, N. L. Allbritton. Photoresist with low fluorescence for bioanalytical applications. *Anal. Chem.*, vol. 79, page 8774, 2007.
- [Parl 2002] S.W. Park, Y.I. Kim, K.H. Chung. Covalent immobilization of GL-7-ACA acylase on silica gel through silanization, *React. Funct. Polym.*, vol. 51, page 79, 2002.
- [Pelletier 2007] N. Pelletier, B. Beche, N. Tahani, J. Zyss, L. Camberlein, E. Gaviot. SU-8 waveguidinginterferometric micro-sensor for gage pressure measurement, *Sensor. Actuator. A*, vol. 135, page 179, 2007.
- [Pelletier 2006] N. Pelletier, B. Bêche, E. Gaviot, L. Camberlein, N. Grossard, F. Polet, and J. Zyss. Single-mode rib optical waveguides on SOG/SU-8 polymer and integrated mach-zehnder for designing thermal sensors, *J. IEEE Sensor. J.*, vol. 6(3) page 565, 2006.
- [Peter 2011] K. Peter, H. András, K. Sándor, C. Kaspar, H. Robert, Grating coupled optical waveguide interferometer for label-free biosensing, *Sensor Actuator B*, vol. 155, page 446, 2011.
- [Poon 2004] J. K. S. Poon. Soft lithography replica molding of critically coupled polymer microring resonators, *IEEE Photonics Tech. Lett.*, vo. 16(11), page 2496, 2004.
- [Pramanick 2013] B. Pramanick, P. K. Dey, S. Das, T. K. Bhattacharyya. Design and development of a PDMS membrane based SU-8 micropump for drug delivery system, *J. ISSS*, vol. 2(1), page 1, 2013.
- [Qin 2010] D. Qin, Y. Xia, G. M. Whitesides. Soft lithography for micro- and nanoscale patterning, *nat. protoc.*, vol. 5(3), page 491, 2010.
- [Qin 1998] D. Qin, Y. Xia, J. A. Rogers, R. J. Jackman, X. Zhao, G. M. Whitesides. Microfabrication, microstructures and microsystem. *Top. Curr. chem.*, vol. 194, page 2, 1998.

- [Qin 2010] D. Qin, Y. Xia, G.M. Whitesieds, Soft lithography for micro- and nanoscale patterning, *nature protocols*, vol.5 (3), page 491, 2010.
- [Ribeiro 2005] J.C. Ribeiro, G. Minas, P. Turmezei, R.F. Wolffenbuttel, J.H. Correi. A SU-8 fluidic microsystem for biological fluids analysis, *Sensor Actuator A*, vol. 123, page 77, 2005.
- [Saha 2009] A. A. Saha, S. K. Mitra, M. Tweedie, S. Roy, J. McLaughlin. Experimental and numerical investigation of capillary flow in SU8 and PDMS microchannels with integrated pillars, *Microfluid. Nanofluid.*, vol. 7, page 451, 2009.
- [Salleh 2013] M. H. M. Salleh, A. Glidle, M. Sorel, J. Reboud, J. M. Cooper. Polymer dual ring resonators for label-free optical biosensing using microfluidics, *Chem. Commun.*, vol. 49, page 3095, 2013.
- [Sato 2004] H. Sato, Y. Houshi, S. Shoji. Three-dimensional micro-structures consisting of high aspect ratio inclined micro-pillars fabricated by simple photolithography, *Microsyst.Technol.* 10 440–3, 2004.
- [Sai 2010] V.V.R. Sai, T. Kundu, C. Deshmukh, S. Titus, P. Kumar, S. Mukherji, Label-free fiber optic biosensor based on evanescent wave absorbance at 280 nm, *Sensor Actuators B*, vol. 143, page 724, 2010.
- [Sethi 2010] D. Sethi, A. Kumar, R. P. Gandhi, P. Kumar, P. K. C. Gupta. New protocol for oligonucleotide microarray fabrication using SU-8-coated glass microslides. *Bioconjug. Chem.*, vol. 21, page 1703, 2010.
- [Serra 2007] S. G. Serra, A. Schneider, K. Malecki, S. E. Huq, W. Brenner. A simple bonding process of SU-8 to glass to seal a microfluidic device, *4M 2007 Conference*, Borovets, Bulgaria, 3-5 October, 2007.
- [Shew 2008] B.Y. Shew, Y.C. Cheng, Y.H. Tsai. Monolithic SU-8 micro-interferometer for biochemical detections, *Sensor Actuator A*, vol. 141, page 299, 2008.
- [Shew 2005] B.Y. Shew, C.H. Kuo, Y.C. Huang, Y.H. Tsai. UV-LIGA interferometer biosensor based on the SU-8 optical waveguide, *Sensor Actuator A*, vol. 120, page 383, 2005.

152 | References

- [Shameli 2011] S. M. Shameli, C. Elbuken, J. Ou, C. L. Ren, J. Pawliszyn. Fully integrated PDMS/SU-8/quartz microfluidic chip with a novel macroporous poly dimethylsiloxane (PDMS) membrane for isoelectric focusing of proteins using whole-channel imaging detection, *Electrophoresis*, vol. 32, page 333, 2011.
- [Shew 2006] B.Y. Shew, Y. H. Tsai, C.H. Kuo, Ultra-sensitive biosensor based on SU-8 planar interferometer, *Solid-State Sensors, Actuators and Microsystems*, vol. 2, page 1784, 2006.
- [Sipova 2013] H. Sipova, J. Homola, Surface plasmon resonance sensing of nucleic acids: A review, *Anal. Chim. Acta*, vol. 773, page 9, 2013.
- [Sikanen 2006] T. Sikanen, S. Tuomikoski, R. Ketola, R. Kostianen, S. Franssila, T. Kotiaho. SU-8 microchips for biomolecule analysis using free zone electrophoresis, *Microtas*, Tokyo, page 380, 2006.
- [Slavov 2000] S. V. Slavov, A. R. Sanger, K. T. Chuang. Mechanism of silation of silica with hexamethyldisilazane. *J. Phys. Chem. B*, vol. 104, page 983, 2000.
- [Spieth 2011] S. Spieth, O. Brett, K. Seidl, A. A. A. Aarts, M. A. Erismis, S. Herwik, F. Trenkle, S. Tätzner, J. Auber, M. Daub, H. P. Neves, R. Puers, O. Paul, P. Ruther, R. Zengerle. A floating 3D silicon microprobe array for neural drug delivery compatible with electrical recording, *J. Micromech. Microeng.*, vol. 21(12), 1250001, 2011.
- [Stevenson 1986] J. T. M. Stevenson, A. M. Gundlach. The application of photolithography to the fabrication of microcircuits. *J. Phys. E: SCI. Instrum.*, vol. 19, page 654, 1986.
- [Stanciu 2012] I. Stanciu. Dispersion of SU-8 photolithography process for fabrication of microfluidics devices, *U.P.B. Sci. Bull., series C*, vol. 74(2), page 127, 2012.
- [Starkov 2003] V.V. Starkov, Ordered macropore formation in silicon, *Phys. Stat. Sol. (a)*, vol. 197, page 22, 2003.
- [Stoycheva 2010] T. Stoycheva, S.Vallejos, J.Calderer, I.Parkin, C. Blackman, X. Correig. Characterization and gas sensing properties of intrinsic and Au-doped WO₃ nanostructures deposited by AACVD technique, *Procedia Engineering*, vol. 5, page 131, 2010.

- [Svasek 2004] P. Svasek, E. Svasek, B. Lendl, M. Vellekoop. Fabrication of miniaturized fluidic devices using SU-8 based lithography and low temperature wafer bonding, *Sens. Actuators. A*, vol. 115, page 591, 2004
- [Tao 2008] S. L. Tao, K. C. Papat, J. J. Norman, T. A. Desai, Surface modification of SU-8 for enhanced biofunctionality and nonfouling Properties, *Langmuir* vol. 24, page 2631, 2008.
- [Tao 2006] S.L. Tao, k. Papat, T. A. Desai. Off-wafer fabrication and surface modification of asymmetric 3D SU-8 microparticles. *Nat. Protoc.*, vol. 1, page 3153, 2006.
- [Tasaltin 2011] N. Tasaltin, D. Sanli, A. Jonas, A. Kiraz, C.Erkey. Preparation and characterization of superhydrophobic surfaces based on hexamethyldisilazane-modified nanoporous alumina. *Nanoscale Res. Lett.*, vol. 6, page 487, 2011.
- [Tatte 2003] T. Tatte, K. Saal, I. Kink, A. Kurg, R. Lohmus, U. Ma'eorg, M. Rahi, A. Rincken, A. Lohmus. Preparation of smooth siloxane surfaces for AFM visualization of immobilized biomolecules, *Surf. Sci.*, vol 532, page 1085, 2003.
- [Toh 2007] Y. Toh, C. Zhang, J. Zhang, Y. M. Khong, S. Chang, V. D. Samper, D. van Noort, D. W. Hutmacher, H. Yu, A novel 3D mammalian cell perfusion-culture system in microfluidic channels, *Lab Chip*, vol. 7(3), page 302, 2007.
- [The 2005] W. H. The. Effect of low numerical-aperture femtosecond two-photon absorption on SU-8 resist for ultrahigh-aspect-ratio microstereolithography, *J. Appl. Phys.*, vol. 97, page 054907, 2005.
- [Torres 2003] C. M. S. Torres, S. Zankovych, J. Seekamp, A.P. Kam, C. Clavijo Cedeno, T. Hoffmann, J. Ahopelto, F. Reuther, K. Pfeiffer, G. Bleidiessel, M.V. Maximov, B. Heidari. Nanoimprint lithography: an alternative nanofabrication approach. *Mater. Sci. Eng. C*, vol. 23, page 23, 2003.
- [Trifonov 2004] T. Trifonov, L. F. Marsal, A. Rodriguez. Photonic bandgap analysis and fabrication of macroporous silicon by electrochemical etching, 2004.

154 | References

[Tseng 2012] C. Tseng, Y. Chou, T. Hsieh, M. Wang, Y. Shu, M. Ger. Interdigitated electrode fabricated by integration of ink-jet printing with electroless plating and its application in gas sensor, *Colloid. Surface. A*, vol. 402, page 45, 2012.

[Tuomikoski 2005a] S. Tuomikoski, S. Franssila. Free-standing SU-8 microfluidic chips by adhesive bonding and release etching, *Sensor Actuator A*, vol. 120, page 408, 2005.

[Tuomikoski 2005b] S. Tuomikoski, T. Sikanen, R. A. Ketola, R. Kostianen, T. Kotiaho, S. Franssila. Fabrication of enclosed SU-8 tips for electrospray ionization-mass spectrometry, *Electrophoresis*, vol. 26, page 4691, 2005.

[Vallejos 2008] S. Vallejos, V. Khatko, J. Calderer, I. Gracia, C. Canè, E. Llobet, X. Correig. Micro-machined WO₃-based sensors selective to oxidizing gases, *Sens. Actuator. B*, vol. 132, page 209, 2008.

[Venkataramani 2006] L. Venkataramani, L. R. Yeswanth, Z. Guigen, Nanopillar array structures for enhancing biosensing performance, *International J of Nanomed.*, vol. 1(1), page 73, 2006.

[Vernekar 2008] N. V. Vernekar, D. K. Cullen, N. Fogleman, Y. Choi, A. J. Garcia, M. G. Allen, G. J. Brewer, M. C. LaPlaca. SU-8 2000 rendered cytocompatible for neuronal bioMEMS applications, *J. Biomed. Mater. Res. A*, page 139, 2008.

[Viter 2012] R. Viter, V. Smyntyna, N. Starodub, ZnO nanrods room temperature photoluminescence biosensor for salmonella detection, 2012.

[Voskerician 2003] G. Voskerician, M. Shive, R. Shawgo, H. Recum, J. Anderson, M. Cima, R. Langer. Biocompatibility and biofouling of MEMS drug delivery devices, *Biomaterial.*, vol. 24, page 1959, 2003.

[Wang 2006] Y. Wang, M. Bachman, C.E. Sims, G. P. Li, N. L. Allbritton, Simple Photografting Method to chemically modify and micropattern the surface of SU-8 photoresist, *Langmuir*, vol. 22, page 2719, 2006. [Wolfe 2010] D. B. Wolfe, D. Qin, G. M. Whitesides. Rapid prototyping of microstructures by soft lithography for biotechnology. *Meth. Mol. Biol.*, page 81, 2010.

- [Wang 2011] H. Wang, M. Witek, D. Park, J. Huang, F. Barany, S. A. Soper. Novel 3D lithographically-prepared solid-phase surfaces made from Su-8 for next generation sequencing, 15th Int. Conf. Miniaturized Systems for Chemistry and Life Sciences, page 73, 2011.
- [Walther 2007] F. Walther, M. Hennemeyer, S. Kerstan, P. Davidovskaya, K. Schürzinger, A. M. Gigler, S. Massberg, R. W. Stark. Enhancement of cell growth on SU-8 by O₂ Plasma activation, *European Cells and Materials*, vol. 14 (3), page 1473, 2007.
- [Weisenberg 2002] B. A. Weisenberg, D. L. Mooradian, Hemocompatibility of materials used in microelectromechanical systems: Platelet adhesion and morphology in vitro. *J. Biomed Mate. Res.*, vol. 60(2), page 283, 2002.
- [Wei 2000] Z.W. Wei, C. Wang, C.F. Zhu. Study on single-bond interaction between amino-terminated organosilane self-assembled monolayer by atomic force microscopy, *Surf. Sci.*, vol. 459, page 401, 2000.
- [Williams 2004] J. D. Williams, W. Wang, Study on the post baking process and the effects on UV lithography of high aspect ratio SU-8 microstructures, *Photo Opti. Inst. Eng.*, vol. 3(4), page 563, 2004.
- [Wolfe 2010] D. B. Wolfe, D. Qin, G.M. Whitesides. Rapid prototyping of microstructures by soft lithography for biotechnology, *Microengineering in biotechnology, methods in molecular biology*, chapter 3, page 81, 2010.
- [Wouters 2012] K. Wouters, R. Puers. Characterization of the adhesion of SU-8 and Epoclad, *J. Micromech. Microeng.*, vol. 22(9), 2012.
- [Xiang 2013] Z. Xiang, H. Wang, A. Pant, G. Pastorin, C. Lee. Development of vertical SU-8 microneedles for transdermal drug delivery by double drawing lithography technology, *Biomicrofluidics*, vol. 7, page 066501, 2013.
- [Xia 2010] Y. Xia, and G. M. Whitesides. Soft lithography. *Angew. Chem. Int. Ed. Engl.*, vol. 37, page 551, 1998.

[Xia 1998] Y. Xia, G. M. Whitesides. Soft lithography. *Annu. Rev. Mater. Sci.*, vol. 28, page 153, 1998.

[Yanga 2010] A. H. J. Yanga, D. Erickson. Optofluidic ring resonator switch for optical particle transport, *Lab Chip*, vol. 10, page 769, 2010.

[Yang 2005] R. Yang, W. Wang, A numerical and experimental study on gap compensation and wavelength selection in UV-lithography of ultra-high aspect ratio SU-8 microstructures, *Sensor. Actuator B: Chem.*, vol. 110(2), page 279, 2005.

[Youn 2008] S. Youn, A. Ueno, M. Takahashi, R. Maeda. Microstructuring of SU-8 photoresist by UV-assisted thermal imprinting with non-transparent mold, *Microelectron. Eng.*, vol. 85, page 1924, 2008.

[Yuze 2011] S. Yuze, F. Xudong, Optical ring resonators for biochemical and chemical sensing, *Anal. Bioanal. Chem.*, vol. 399, page 205, 2011.

[Zhang 2001] J. Zhang, K. L. Tan, G. D. Hong, L. J. Yang, H. Q. Gong. Polymerization optimization of SU-8 photoresist and its applications in microfluidic systems and MEMS, *J. Micromech. Microeng.*, vol. 11, page 20, 2001.

[Zhang 2011] X. Zhang, L. Du, Y. Zhu, C. Liu. Investigation of adhesion properties between SU-8 photoresist and stainless steel substrate, *Micro Nano Letters*, vol. 6(6), page 397, 2011.

[Zhang 2005] J. Zhang, W. X. Zhou, M. B. Chan-park. Argon plasma modification of SU-8 for very high aspect ratio and dense copper electroforming, *J. Electrochem. Soc.*, vol. 152, page 716, 2005.

UNIVERSITAT ROVIRA I VIRGILI

LITHOGRAPHIC MICRO- AND NANOSTRUCTURING OF SU-8 FOR BIOTECHNOLOGICAL APPLICATIONS

Pinkie Jacob Eravuchira

Dipòsit Legal: T 773-2015